Kinematics and Energetics of Swimming Zooplankton

by

Lalith N. Wickramarathna

from Sri Lanka

Accepted Dissertation thesis for the partial fulfillment of the requirements for a

Doctor of Natural Sciences

Fachbereich 7: Natur- und Umweltwissenschaften

Universität Koblenz-Landau

Thesis examiners:

Prof. Dr. Andreas Lorke, University of Koblenz-Landau

Dr.-Ing. Christian Noß, University of Koblenz-Landau

Date of the oral examination: 22.07.2016

Declaration

I herewith declare that this PhD dissertation entitled "Kinematics and Energetics of Swimming Zooplankton" is the result of my original research work carried out at the University of Koblenz-Landau, Landau, Germany. The dissertation contains no materials previously published or written by another person, or substantial proportions of material which have been accepted for the award of any other degree at the University of Koblenz-Landau or any other educational institution, except where due acknowledgement is made in the thesis. Any contribution made to the research by others, with whom I have worked at the University of Koblenz-Landau or elsewhere, is explicitly acknowledged in the thesis. I also declare that the intellectual content of this thesis is the product of my own work, except to the extent that assistance from others in the project's design and conception or in style, presentation and linguistic expression is acknowledged.

Lalith N. Wickramarathna
Landau in der Pfalz
02nd June 2016

Acknowledgements

FIRST and the foremost, I would like to thank late Anula Mawilmadage (mother) and Roy Wickramarathna (father) for empowering me with the best possible education in shaping up my early academic career which many others in the context of then-Sri Lanka were not privileged of and for having stood by my side during the most testing of times. Though they both have not been lucky enough to see the fruits that they sew, their sacrifices inspired me to reach this new high.

I also thank my little daughter, Nitzanah, for getting me involved with her daily tasks which smothered the stress and strain of research and at the same time for allowing me to take some time out of her playing sessions and focus on my research. Your laughters turned a lemon into a lemonade! And, I greatly admire the support provided by Nirosha (wife), and I am ever thankful for her reluctance to go overboard about discussing scientific themes, thereby, showing the life beyond the research domain. I also appreciate my only sibling, Nishantha (brother), for showing immense serenity and tranquillity in the wakes of troublesome waters.

I would like to thank Andreas Lorke for his supervision, specially, his willingness and availability to discuss about research questions at any time. Moreover, to his credit he was quickly able to comprehend conditions in which I would thrive and excel in research. That is the freedom to work on my own thoughts without engaging in over-supervision. Therefore, I have not worked under anyone who provided me that much freedom and support to work on my own ideas. A special thank goes out to Christian Noss for his intensive discussions and valuable inputs during our weekly progress meetings. Also, I have had the pleasure to work with the former technician of the institute of environmental physics group, Sebastian Geissler, who was eager to provide the initial technical support in setting up the experiments.

I would like to thank Angelika Horderle for the support provided to negate the burdens of bureaucracy without which I would have struggled. Finally, all my colleagues of the environmental physics group helped to make this research project successful. And, my sincere thanks go out to all those whose names are not mentioned here yet supported this work.

Summary

THE work presented in this thesis investigated interactions of selected biophysical processes that affect zooplankton ecology at smaller scales. In this endeavour, the extent of changes in swimming behaviour and fluid disturbances produced by swimming *Daphnia* in response to changing physical environments were quantified. In the first research question addressed within this context, size and energetics of hydrodynamic trails produced by *Daphnia* swimming in non-stratified still waters were characterized and quantified as a function of organisms' size and their swimming patterns. The results revealed that neither size nor the swimming pattern of *Daphnia* affects the width of induced trails or dissipation rates. Nevertheless, as the size and swimming velocity of the organisms increased, trail volume increased in proportional to the cubic power of Reynolds number, and the biggest trail volume was about 500 times the body volume of the largest daphnids. Larger spatial extent of fluid perturbation and prolonged period to decay caused by bigger trail volumes would play a significant role in zooplankton ecology, e.g. increasing the risk of predation. The study also found that increased trail volume brought about significantly enhanced total dissipated power at higher Reynolds number, and the magnitudes of total dissipated power observed varied in the range of $(1.3\text{-}10)\times10^{-9}$ W. Furthermore, this study provided strong evidence that swimming speed of *Daphnia* and total dissipated power in *Daphnia* trails exceeded those of some other selected zooplankton species.

In recognizing turbulence as an intrinsic environmental perturbation in aquatic habitats, this thesis also examined the response of *Daphnia* to a range of turbulence flows, which correspond to turbulence levels that zooplankton generally encounter in their habitats. Results indicated that within the range of turbulent intensities to which the *Daphnia* are likely to be exposed in their natural habitats, increasing turbulence compelled the organisms to enhance their swimming activity and swimming speed. However, as the turbulence increased to extremely high values (10^{-4} m^{2}s^{-3}), *Daphnia* began to withdraw from their active swimming behaviour. Findings of this work also demonstrated that the threshold level of turbulence at which animals start to alleviate from largely active swimming is about 10^{-6} m^{2}s^{-3}. The study further illustrated that during the intermediate range of turbulence; 10^{-7} - 10^{-6} m^{2}s^{-3}, kinetic energy dissipation rates in the vicinity of the organisms is consistently one order of magnitude higher than that of the background turbulent flow.

Swarming, a common conspicuous behavioural trait observed in many zooplankton species, is considered to play a significant role in defining freshwater ecology of their habitats from food exploitation, mate encountering to avoiding predators through hydrodynamic flow structures produced

by them, therefore, this thesis also investigated implications of *Daphnia* swarms at varied abundance & swarm densities on their swimming kinematics and induced flow field. The results showed that *Daphnia* aggregated in swarms with swarm densities of $(1.1\text{-}2.3)\times10^3$ L^{-1}, which exceeded the abundance densities by two orders of magnitude (i.e. 1.7 - 6.7 L^{-1}). The estimated swarm volume decreased from 52 cm^3 to 6.5 cm^3, and the mean neighbouring distance dropped from 9.9 to 6.4 body lengths. The findings of this work also showed that mean swimming trajectories were primarily horizontal concentric circles around the light source. Mean flow speeds found to be one order of magnitude lower than the corresponding swimming speeds of *Daphnia*. Furthermore, this study provided evidences that the flow fields produced by swarming *Daphnia* differed considerably between unidirectional vortex swarming and bidirectional swimming at low and high abundances respectively.

Contents

Original contributions

1. Wickramarathna LN, Noss C, Lorke A (2014) Hydrodynamic trails produced by *Daphnia*: size and energetics. PLoS ONE 9(3): e92383. Doi: 10.1371/journal.pone.0092383

2. Wickramarathna LN, Noss C, Lorke A (2016) *Daphnia* pushed to the limits: kinematics and energetics of swimming in turbulence. Limnologica. Revised submission under review.

3. Wickramarathna LN, Noss C, Lorke A (2016) The kinematics and energetics of *Daphnia* swarms. Hydrobiologia. Original submission under review.

Author contributions

Article I Hydrodynamic trails produced by *Daphnia*: size and energetics

AUTHORS   Wickramarathna, L. N. (LNW), Noss, C. (CN) and Lorke, A. (AL)

STATUS   Published in 2014 in PLoS ONE 9(3): e92383

CONTRIBUTIONS   Conceived and designed the experiments: CN AL LNW (75%). Performed the experiments: LNW (80%) CN. Analysed the data: LNW. Contributed reagents/materials/analysis tools: CN. Wrote the paper: LNW. Editorial support in writing the manuscript: AL CN. Interpretation of the results: AL LNW CN.

Article II *Daphnia* pushed to the limits: kinematics and energetics of swimming in turbulence

AUTHORS   Wickramarathna, L. N. (LNW), Noss, C. (CN) and Lorke, A. (AL)

STATUS   Limnologica. Revised submission (06.05.2016) under review.

CONTRIBUTIONS   Conceived and designed the experiments: LNW (90%) CN AL. Performed the experiments: LNW. Analysed the data: LNW. Contributed analysis tools: CN. Interpretation of the results: LNW. Wrote the paper: LNW. Editorial support in writing the manuscript: AL CN.

Article III The kinematics and energetics of *Daphnia* swarms

AUTHORS   Wickramarathna, L. N. (LNW), Noss, C. (CN) and Lorke, A. (AL)

STATUS   Hydrobiologia. Original submission (24.04.2016) under review.

CONTRIBUTIONS   Conceived and designed the experiments: LNW (80%) CN AL. Performed the experiments: LNW. Analysed the data: LNW. Contributed analysis tools: CN. Interpretation of the results: LNW. Wrote the paper: LNW. Editorial support in writing the manuscript: AL CN.

List of Figures

List of Tables

This thesis is dedicated to the memory of my late parents,

Anula Mawilmadage (mother) and *Roy Wickramarathna* (father),

whose words of inspiration and encouragement in pursuit of excellence, still linger on.

Chapter 1

Introduction

1.1 Background

IN stratified marine or freshwater environments, the degree of turbulent vertical mixing can define its chemical, nutrition, hydrodynamic characteristics of the environment. For instance, the turbulent vertical mixing has shown to determine the distribution of dissolved substances (Boehrer and Schultze, 2008), affect the exchange of gasses and solutes at interfaces (Lorke and Peeters, 2006), and control carbon and nutrient cycling (Denman and Gargett, 1995). While it has attributed to oceanic circulation on a global scale profoundly affecting earth's climate (Wunsch and Ferrari, 2004), on smaller scales it influences the underwater light climate (Macintyre, 1993), phytoplankton and bacterial growths rates (Bergstedt et al., 2004; Peeters et al., 2007) and predator-prey interactions in zooplankton and fish (Kiørboe and Mackenzie, 1995; Pitchford et al., 2003).

Even if the implications of turbulent vertical mixing on aquatic environments at different scales are significant, the underlined mechanisms of mixing are not fully understood (Ivey et al., 2008). The discrepancy of diffusivity estimates in lakes and ocean basins being about one order of magnitude higher than locally measured values (Wüest and Lorke, 2003; Wunsch and Ferrari, 2004) suggests that breaking internal waves could be one of the mechanisms (Garrett, 2003; Goudsmit et al., 1997). Turbulence and vertical mixing induced by swimming of aquatic animals (i.e. biomixing) has also been suggested as another mechanism attributing to the discrepancy in diffusivity estimates. Also, turbulent kinetic energy produced by marine species have shown to generate kinetic energy at a rate of about 10^{-5} Wkg^{-1} (Huntley and Zhou, 2004), which exceeds dissipation rates typically observed in stratified lakes by about two orders of magnitude (Ivey et al., 2008; Wüest and Lorke, 2003) indicating that animal-induced turbulence is comparable in magnitude to rates of turbulent energy dissipation that result from major storms. The total biosphere contribution to the aphotic ocean mechanical energy estimated (≈ 1 TW), also affirms comparable dissipation rates in magnitudes to that of wind and tides (Dewar et al., 2006).

Besides the scarcity of experimental evidence for biomixing, a few observations have indicated the existence of biologically-induced velocity fluctuations in stratified waters. For instance, diel

vertical migration of krill swarms in the coastal ocean strongly increased levels of turbulence (Kunze et al., 2006), patches of small fish in Monterey Bay contributed to enhance turbulent dissipation rates (Gregg and Horne, 2009), and abundance of fish around an artificial reef in Lake Constance and measured rates of turbulent kinetic energy dissipation were found to be correlated (Lorke and Probst, 2010).

However, the contribution of aquatic organisms to vertical mixing is not confined to the generation of turbulence and corresponding velocity fluctuations. It has estimated that fluid transport within the viscous boundary layer surrounding swimming animals can provide an amount of energy comparable in magnitude to major winds and tides on a global scale (Katija and Dabiri, 2009). Successive interactions of zooplankton organisms with parcel of fluid have also shown to vertically displace the fluid parcels over distances much larger than the individual body size (Dabiri, 2010).

Fluid disturbance and mixing induced by swimming zooplankton at small-scale have also shown to be significant for the organisms themselves. Fluid disturbance can affect feeding strategies and success of suspension feeders (Garcia et al., 2007; Visser et al., 2009), the reception of chemical cues, the encounter with contaminants (Lovern et al., 2007), and the detection of prey and by predators (Visser, 2001).

Despite the important role that swimming zooplankton play in the aquatic environment, less is known about their behaviour and induced flow field. Studies based on numerical simulation have oversimplified with assumptions requiring experimental justification (Dabiri, 2010; Jiang and Strickler, 2007) while studies based on direct observations using imaging techniques (Van Duren and Videler, 2003; Jiang and Strickler, 2007; Michalec et al., 2015) have used either tethered organisms or conducted in small enclosures in comparison to the number of animals (thereby interfering with swimming behaviour and flow field is influenced by boundary effects). Zooplankton are one of smallest propelling organisms in aquatic ecosystems, however, as they are often found in relatively high densities and many of zooplankton perform a diel vertical migration (Cohen and Forward, 2009), their contribution to flow disturbance can expect to be significant.

1.2 *Daphnia* swimming in still-water

As it was pointed out in the previous section, swimming zooplankton may play a significant role in their ecological environment at organism and population scale. From feeding success (Kiørboe, 2011), sensing chemical or hydrodynamic cues (Lombard et al., 2013; Visser, 2001) to detecting predators (Kiørboe et al., 2010) are affected by small-scale flow perturbations produced by swimming zooplankton. It was previously shown that swimming of zooplankton significantly contributed to vertical mixing of stratified waters (Dewar et al., 2006; Huntley and Zhou, 2004), which later rebuked considering the spatial scales that zooplankton perturbations occur (Kunze, 2011; Visser, 2007).

Numerical simulations (Jiang et al., 2002b) and theoretical analysis (Jiang et al., 2002a) have shown that flow produced by appendages and swimming legs in the vicinity of zooplankton (re-

gions 1 and region 2 in Fig. 1.1) is offset by viscosity, and fluctuations take place at small-scales than viscous length scale ($\sqrt{\nu/\omega}$; where ν and ω are kinematic viscosity and angular frequency of beating appendages respectively). Another flow field is developed at a spatial scale larger than the organism's size (region 3 in Fig. 1.1) depending on whether inertia of displaced fluid exceeds viscous forces (Re > 1). Thus, Reynolds number provides a measure of relative trail length as it indicates the ratio of length scale over which hydrodynamic disturbances dissipate to organism size (Lauga and Powers, 2009). However, this does not allow to visualize the complete picture of the size of zooplankton traces.

Furthermore, the most of existing studies analysing hydrodynamic traces of zooplankton have largely considered copepods (Jiang and Osborn, 2004; Kiørboe et al., 2010). However, it is worth understanding if freshwater zooplankton of similar size with different swimming pattern or foraging strategy may leave different traces (Kiørboe, 2011). A common freshwater zooplankton, *Daphnia* (also known as water fleas), are propelled by extending their appendages and erected hairs and folded appendages and collapsed hairs during recovery stroke (Walker, 2002). Beating of second antenna at frequencies of 3-5 Hz generates forward thrust which translates them a distance of about one body length (Gries et al., 1999). *Daphnia* typically swim in a Reynolds number range of 10-100 (Kohlhage, 1994) which is comparable to that of copepods (Morris et al., 1990; Walker, 2002). Size of *Daphnia* trails observed in density-stratified waters by means of laboratory experiments have indicated wake volumes much larger than organisms (Gries et al., 1999). However, large density gradients required for optical Schlieren method used in their measurements strongly affected the trails length. Freely swimming *Daphnia* in weakly density-stratified waters have indicated an enhanced dissipation rate in their trails on spatial scales exceeding the size of the organism by two orders of magnitude (Noss and Lorke, 2012).

1.3 *Daphnia* swimming in turbulence

The limits of zooplankton tolerance are often tested (Carrasco et al., 2013) by changing environmental conditions at a broad spatial and temporal scales (Kiørboe, 2011), and turbulence is one such physical environment present in all aquatic ecosystems (Wüest and Lorke, 2003).

The response of zooplankton to turbulence has been investigated by conducting laboratory experiments (Alcaraz et al., 1994; Saiz et al., 2003; Fuchs et al., 2013), field measurements (Visser and Stips, 2002; Maar et al., 2003), and numerical simulations (Mackenzie et al., 1994; Zhan et al., 2014). Many of these former studies have focused on understanding effects of turbulence in swimming behaviour (Haury et al., 1992; Prairie et al., 2012), predator-prey encounter rates (Rothschild and Osborn, 1988; Mackenzie et al., 1994), feeding patterns (Saiz and Kiørboe, 1998), metabolism (Saiz and Alcaraz, 1992; Alcaraz et al., 1994), and growth rates (Alcaraz et al., 1988; Saiz et al., 1992), however, these have not produced consistent results.

For various freshwater zooplankton species, these inconsistencies have provoked regarding the threshold level of avoiding turbulence or due to unquantified level of turbulence used (Oviatt, 1981; Alcaraz et al., 1988). Several other studies have suggested threshold levels for the dissipation rate
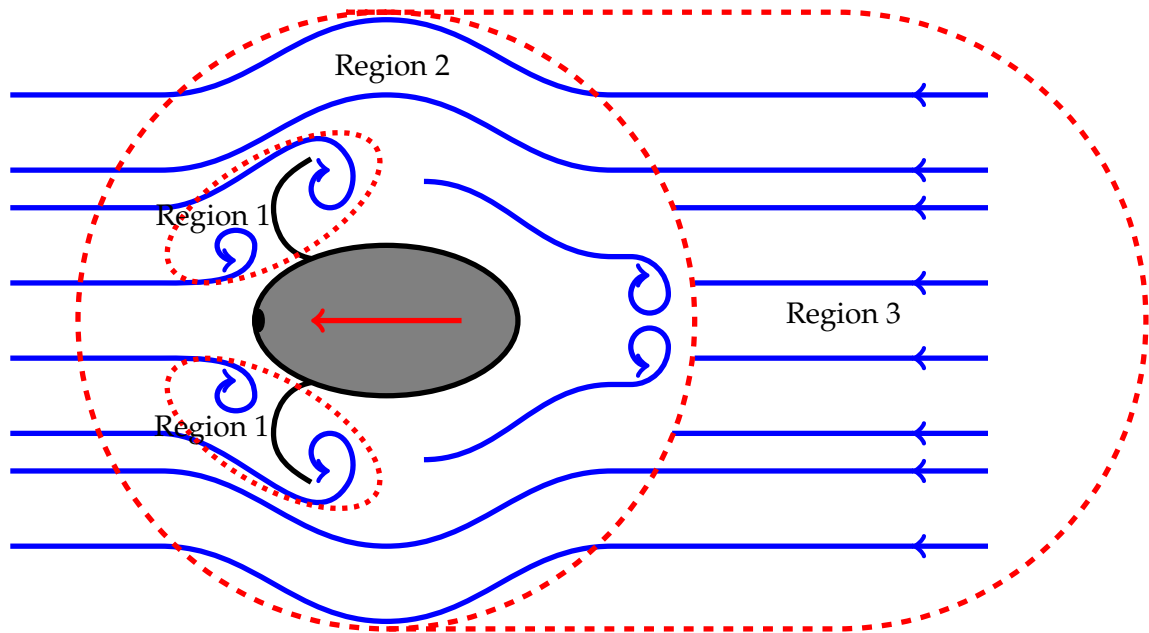
Figure 1.1: *A conceptual sketch of the flow fields around a swimming Daphnia (grey ellipsoid). The red arrow indicates the swimming direction and black curves represent antennas. The three distinct spatial scales of the flow field (blue stream lines) generated by the swimming organisms are indicated by red dashed lines.*

of turbulent kinetic energy at which copepods begin to avoid turbulence ($10^{-6.5}$ m^{2}s^{-3} (Incze et al., 2001), 10^{-7} m^{2}s^{-3} (Pringle, 2007)). In another study (Yen et al., 2008), it was shown that copepods could withstand low turbulence intensities by controlling their position and movements whereas at higher turbulence intensity they were passively displaced. The transition occurred at a dissipation rate of 9×10^{-7} m^{2}s^{-3}. Further suggesting that zooplankton have an optimum fitness level under turbulent conditions, a dome-shaped correlation between swimming and turbulence intensity have been observed (Visser et al., 2009) while the optimum occurred at a turbulence level about 10^{-4} m^{2}s^{-3}. They also asserted that this dome-shaped relationship may affect the vertical distribution of organisms. Also, the response to turbulence has shown to vary among species within the same zooplakton type. For instance, two copepod species exposed to two turbulence levels (9×10^{-7} m^{2}s^{-3} and 9.6×10^{-6} m^{2}s^{-3}) showed (Webster et al., 2015) that Acartia tonsa did not significantly respond to the lower turbulence level but significantly altered their swimming behaviour in the higher turbulence level by increasing the relative speed of swimming. In contrast, T. longicornis did not indicate a behavioural response to both levels. Another study conducted recently also showed that active swimming contributed substantially to the swimming velocity of copepods even when turbulence is significant (Michalec et al., 2015).

In addition to zooplankton, meroplankton (mainly marine vertebrate larvae) have been reported

to trigger changes in larval swimming behaviour actively or passively in response to turbulence (Roy et al., 2012). However, like with copepods, findings are not consistent. Fast swimming larvae crab zoea observed to actively change their swimming speeds (Welch and Forward, 2001) while barnacle cyprids opposed downwelling currents by swimming upwards (DiBacco et al., 2011). Moderately fast swimming oyster larvae has shown to sink (Fuchs et al., 2013) or swim upward (Wheeler et al., 2013; Fuchs et al., 2015; Wheeler et al., 2015) in high turbulence. At turbulence intensity equivalent to the kinetic energy dissipation rate of 10^{-6} m^{2}s^{-3}, an active upward swimming of sand dollar and a passively stable swimming of purple sea urchin have been observed (McDonald, 2012). Sea urchin exposed to two levels of turbulent dissipation rates (9×10^{-9} or 4×10^{-7} m^{2}s^{-3}) showed that under no flow and low turbulence conditions, animals moved towards the water surface whereas in high turbulence, larvae were passively transported with the flow (Roy et al., 2012).

Less is known about how turbulent flows affect the swimming and energetics of freshwater zooplankton. *Daphnia* as only a few studies have focused on understanding behavioural changes of *Daphnia* in the presence of turbulence (Brooks, 1947; Alcaraz et al., 1994; Laforsch and Tollrian, 2004). (Spitael, 2007) observed that D. magna tolerated higher levels of turbulence to remain in the oxygen-rich surface zone. (Seuront et al., 2004) investigated swimming speed and behaviour of Daphnia pulicaria for a range of turbulent dissipation rates (3.8×10^{-8}- 1.1×10^{-4} m^{2}s^{-3}) and found increased escape responses with increasing turbulence.

Therefore, the extent of adaptation or avoidance of turbulence among zooplankton types and species still remain ambiguous. This vagueness may have derived due to the fact that the experimental approach has underscored organisms behaviour and overlooking the significance of observing flow fields. To date, studies deployed simultaneous measurements of behaviour and flow field are scarce (Yen et al., 2008; Adhikari et al., 2015; Michalec et al., 2015).

The results corresponding to previous work of this thesis conducted in still-water indicated that *Daphnia* exhibited higher swimming speeds among zooplankton species (Wickramarathna et al., 2014), and *Daphnia* showed to enhance metabolism in turbulence as indicated by 14.3% increase in heart rate compared to calm water conditions (Alcaraz et al., 1994). These findings suggest that *Daphnia* may be more resilient and can potentially enhance their swimming activity in response to turbulence. Therefore, we hypothesize that *Daphnia* intensify their swimming activity in response to increasing turbulence up to a threshold, beyond which, the animals gradually withdraw from active swimming.

1.4   Swarming of *Daphnia*

Aggregation of animal is common among mammals, flying animals as well as among aquatic organisms. Unlike schooling of animals, a swarm is defined as a dense patch of organism within which organism are not aligned in parallel to each other in their movements (Leising and Yen, 1997) or they are not a completely random set of movements (Banas et al., 2007).

Depending on the dominant component of physical and biological processes, a swarm can be

either an active or a passive process. For instance, passive swarms may be formed as a result of dominant physical characteristics of water (e.g. eddies, fronts) (Huber et al., 2011) or active swarms are formed by resisting dispersion without orienting (Banas et al., 2007). Both passive and active swarming affect predator-prey encounter rates (Pijanowska Kowalczewski, 1997; Lorke et al., 2008), food capturing success (Davis et al., 1991), and encountering mates (Hebert et al., 1980; Gendron, 1992).

Cues that triggers active swarms can be due to either social or non-social interactions (Banas et al., 2007). Socially interactive swarms are driven by density-dependent responses of individual organisms to their neighbours (Flierl et al., 1999). zooplankton aggregations induced by long-distance interactions along neighbours' scent trails (Weissburg et al., 1998), attempting to improve probability of encounter (Gerritsen, 1980) or attempting to enhance mating among conspecific adults (Ambler et al., 1996) are some of typical examples for socially interactive swarms.

In contrast to social aggregations formed as a result of individual organisms to their neighbours, non-social zooplankton swarms are formed as a result of external cues such as light, food, or predators (Van Gool and Ringelberg, 1997; Cohen and Forward, 2009). Among these external cues, presence of predators has been extensively studied as a cue inducing non-social zooplanton aggregations (Kvam et al., 1995; Buskey et al., 1996; Kleiven et al., 1996; Pijanowska Kowalczewski, 1997).

Phototactic behaviour of *Daphnia* is well known and use as a model organism for mechanistic explanations of diel vertical migration (Ringelberg, 1999). However, non-social swarms formed as a result of spatial gradients in light intensity have largely understudied. And, being unable to form an image with their eyes (Buchanan and Goldberg, 1981) and make long-range communication between *Daphnia* (Larsson and Dodson, 1993) to trigger social interactions, aligned synchronization of swimming has not been detected among *Daphnia* (Okubo and Levin, 2001). However, numerical simulations have suggested that short-ranged hydrodynamic interactions can induce aligned swimming directions in high-density *Daphnia* swarms (Ordemann et al., 2003; Mach and Schweitzer, 2007). They further suggest that unidirectional vortex swarming can be expected if swarm the density exceeds a critical value.

Daphnia have exhibited the largest total dissipated power in their trails, higher swimming speeds than those of copepods and krill, and trail volumes of several folds bigger than the size of organisms (Wickramarathna et al., 2014). Also, despite important physiological and ecological consequences of flow field produced by zooplankton at organism and population scale such as feeding success (Kiørboe, 2011), sensing chemical and hydrodynamic cues (Lombard et al., 2013; Visser, 2001) detecting prey or predators (Kiørboe et al., 2010), the flow field induced by swarming zooplankton has rarely been observed in former studies.

1.5   Goals and specific objectives

In this study, swimming behaviour and corresponding flow structures produced by the propulsion of *Daphnia* are characterized and quantified under selected environmental conditions established in laboratory. In view of this, this dissertation is aimed at the general objectives of (i) characterizing flow disturbances in the wakes of singular *Daphnia* swimming in still water, (ii) understanding the interactions of swimming *Daphnia* in turbulent flows, and (iii) characterizing swimming behaviour and the flow field produced by *Daphnia* swarms.

There exists no consensus agreement regarding the extent of flow perturbation that swimming of zooplaton are produced. Although Reynolds number provides a clue of relative trail length, it does not indicate actual volume of hydrodynamic traces which is important to understand ecological consequences of induced trails. Furthermore, footprints produced by swimming *Daphnia* are largely understudied, thus, there exists a gap of knowledge regarding their behaviour and flow field. Therefore, as the first major goal of this study, trajectories and hydrodynamic footprints produced by freely swimming *Daphnia* of different sizes in the absence of density stratification and background flow were analysed. The specific objectives of this study were;

- Are *Daphnia* swimming in calm water capable of producing large scale flow structures ?

- How the size and energetics of these hydrodynamic trails are affected by the organism age (size) and swimming patterns ?

As it was described in Section 1.2, the scientific debate regarding how zooplanton respond to turbulence has so far yielded inconsistent results possibly due to the lack of flow field observations along with organisms' swimming behaviour. In addition to inconsistencies among marine zooplankton and meroplankton, the current knowledge of how *Daphnia* may respond to turbulence is clearly insufficient. Therefore, in the second objective of this study, laboratory observations of *Daphnia* swimming in turbulent flows of different intensities were analysed. The measurements resolve both behavioural changes in animals' motility and the corresponding characteristics of the turbulent and animal-induced flow fields. The specific objectives of this study were;

- Are zooplankton, *Daphnia* in particular resilient enough to overcome turbulence or do they avoid turbulence ?

- Is there a threshold of turbulence intensity that they make a transition from overcoming to avoidance?

Large trail volumes produced by individual *Daphnia* swimming in still water (Wickramarathna et al., 2014) suggest a strong potential to instigate large scale flow structures by *Daphnia* swarms. Also, *Daphnia* is known for its phototactic behaviour, light-induced *Daphnia* swarms have been understudied. Futhermore, while flow field induced by zooplankton swarms has rarely been reported, laboratory experiments and numerical simulations have led to contradictory results regarding aligned synchronization of *Daphnia* swarms. To address these unresolved issues, swarming behaviour of *Daphnia* in combination with measurements of the swarm-induced flow fields were analysed as the third goal of this work. The specific objectives of the study were;

- Do *Daphnia* swarms instigate large scale flow structures ?

- If hydrodynamic interactions can cause an alignment of swimming directions in dense swarms

- How abundance and swarm densities in aggregations affect their behaviour and induced flow?

These questions are answered by means of laboratory experiments, which deploy a novel approach of simultaneously capturing information of induced flow field and organisms' behaviour using particle image velocimetry method and organism tracking respectively.

1.6   Outline of the thesis

The thesis is divided into five chapters, and is comprised of three original research articles that address the research questions stated above, which are presented in Chapters 2 - 4. After this introductory Chapter where the research questions were formulated, size and energetics of hydrodynamic trails produced by individual *Daphnia* swimming in non-stratified still waters are characterized and quantified as a function of organisms' size, their swimming patterns (Chapter 2). The work outlined in Chapter 3, the response of *Daphnia* to a range of turbulence flows, which correspond to turbulence levels that zooplankton generally encounter in their habitats, is discussed in great details with respect to their behavioural changes and induced flow field.In the work presented in Chapter 4, implications of *Daphnia* swarms at varied abundance & swarm densities on their swimming kinematics and induced flow field are discussed. The last Chapter (5) synthesizes the results and outlines an overall outlook pertaining to the three topics covered in this Ph.D. work and a brief overview of their environmental relevance.

Hydrodynamic trails produced by *Daphnia*: size and energetics

Lalith N. Wickramarathna, Christian Noss, and Andreas Lorke

Institute for Environmental Sciences, University of Koblenz-Landau, Landau, Germany.

Abstract

This study focuses on quantifying hydrodynamic trails produced by freely swimming zooplankton. We combined volumetric tracking of swimming trajectories with planar observations of the flow field induced by *Daphnia* of different size and swimming in different patterns. Spatial extension of the planar flow field along the trajectories was used to interrogate the dimensions (length and volume) and energetics (dissipation rate of kinetic energy and total dissipated power) of the trails. Our findings demonstrate that neither swimming pattern nor size of the organisms affect the trail width or the dissipation rate. However, we found that the trail volume increases with increasing organism size and swimming velocity, more precisely the trail volume is proportional to the third power of Reynolds number. This increase furthermore results in significantly enhanced total dissipated power at higher Reynolds number. The biggest trail volume observed corresponds to about 500 times the body volume of the largest daphnids. Trail-averaged viscous dissipation rate of the swimming daphnids vary in the range of 1.8×10^{-6} W/kg to 3.4×10^{-6} W/kg and the observed magnitudes of total dissipated power between 1.3×10^{-9} W and 1×10^{-8} W, respectively. Among other zooplankton species, daphnids display the highest total dissipated power in their trails. These findings are discussed in the context of fluid mixing and transport by organisms swimming at intermediate Reynolds numbers.

2.1   Introduction

Small-scale fluid motion and mixing induced by swimming zooplankton in aquatic ecosystems have important physiological and ecological consequences at organism and population scale. The flow field around the organisms affects feeding strategies and feeding success (Kiørboe, 2011; Visser et al., 2009) as well as the reception and dispersal of chemical (Lombard et al., 2013; Pijanowska Kowalczewski, 1997) and hydro-mechanical cues (Visser, 2001), which allow for detecting prey or predators (Kiørboe et al., 2010). Fluid transport and mixing by swimming zooplankton also has been considered as a potentially significant energy source for vertical mixing in density-stratified waters on global scales (Dabiri, 2010; Dewar et al., 2006; Huntley and Zhou, 2004). The extent to which zooplankton-generated flow can contribute to vertical mixing, however, was argued to be insignificant due to the small spatial scales at which currents are produced (Kunze, 2011; Visser, 2007).

Theoretical analysis (Jiang et al., 2002a) and numerical simulations (Jiang et al., 2002b) on copepods suggest that the highly fluctuating flow field around their beating feeding appendages and swimming legs is damped by viscosity and high-frequency temporal fluctuations are restricted to spatial scales, which are smaller than the viscous length scale $\sqrt{\nu/\omega}$ (with ω and ν being the angular frequency of the beating appendages and the kinematic viscosity respectively). Beyond this length scale, a steady flow field develops, which depends on organism Reynolds number (Re). If $Re > 1$, i.e. if inertia of the displaced fluid surpasses viscous forces, an increasing fraction of total power is dissipated at spatial scales exceeding the size of the organism. In fact, Re can be considered as a relative trail length because it scales with the ratio of length scale over which hydrodynamic disturbances dissipate to organism size (Lauga and Powers, 2009). However, energy dissipation provides only one possible measure of the size of the footprint of swimming zooplankton. Because the molecular diffusivities of dissolved substances are much smaller than the diffusivity of momentum, which is described by the kinematic viscosity, the corresponding concentration fluctuations are more persistent and are dissipated at much larger spatial scales (Noss and Lorke, 2014).

Existing laboratory and numerical studies on the size and the structure of hydrodynamic footprints of swimming zooplankton have mainly focused on copepods (Jiang and Osborn, 2004; Kiørboe et al., 2010; Videler et al., 2002). The different feeding strategy and resulting swimming patterns of other highly abundant zooplankton species of similar size, such as *Daphnia*, can, however, be expected to result in different hydrodynamic footprints (Kiørboe, 2011).

Locomotion of the filter-feeding daphnids is attained by a pair of extended appendages (second antennae) and erected swimming hairs during the downward directed power stroke that generates more drag than folded appendage and collapsed swimming hairs during the upward recovery stroke (Walker, 2002). Beating of the second antennae with typical frequencies of 3-5 Hz (Arana et al., 2007; Gries et al., 1999) produces the thrust required to propel the 0.2-5 mm sized organism forward. This length scale is about 0.2 mm for a beating antenna of a *Daphnia*.

The typical organism (body) Reynolds number of *Daphnia* is about $O \propto 10^1$ to 10^2 (Kohlhage, 1994; Walker, 2002) and similar to those of copepods (Morris et al., 1985, 1990; Walker, 2002). The

size of the hydrodynamic trails of swimming *Daphnia* has been investigated in laboratory experiments by Gries et al. (1999) as a function of density stratification. They observed that the volume of the wakes is much larger than the organism itself. The optical Schlieren technique applied in their measurements, however, required very large density gradients, which were demonstrated to strongly affect trail length. In weak density stratification, Noss and Lorke (2012) have recently observed enhanced dissipation rates of kinetic energy in the trail of a freely swimming daphnid on spatial scales exceeding the size of the organism by two orders of magnitude.

In this study we analyze a series of laboratory measurements of the trajectories and hydrodynamic footprints produced by freely swimming *Daphnia* of different sizes in the absence of density stratification and background flow. By quantifying the spatial dimensions of enhanced kinetic energy dissipation rates in the trail of the swimming organism, we provide experimental evidence for the ubiquitous existence and Re dependence of highly-energetic flow structures exceeding the size of the organism swimming at intermediate Re. The intermediate Re in our study refers to $Re > 1$ (viscous flow), but not fully turbulent (i. e. not $Re >> 1$).

2.2 Materials and Methods

2.2.1 Organisms and Measurements

All test organisms of species *Daphnia magna* were cultured following standard regulatory requirements (OECD, 2004). For the measurements, groups of 5-20 organisms of the same age (5, 20, and 25 days old, respectively) were inserted into the test aquarium and allowed to sufficiently adapt to the test environment. For each age group, the core body length l_D (head to the proximal end of the caudal spine (Ranta et al., 1993)) was estimated for 5-10 different organisms from selected images. The average growth rate estimated for the culture was 0.072 mm/day, and can be considered as typical for *D. magna* (Ranta et al., 1993).

The test aquarium with a cross-sectional area of 17.5 cm $\times$ 11 cm and a height of 16 cm was submerged in a larger temperature-controlled aquarium to prevent the generation of convective currents due to slight fluctuations of room temperature. The aquarium was illuminated from above with a dimmable natural white LED-panel, while light intensity was adjusted (568 lm) so that it provides sufficient illumination for organism tracking. Swimming behavior of organisms was not affected by the white light because, given the size of the aquarium in our system, white light was homogenously distributed with negligible attenuation. As previously reported (Ringelberg, 1999; Ringelberg et al., 1997; Van Gool and Ringelberg, 1997), the swimming behavior depends on the rate of change in light intensity but not on the magnitude of light intensity itself.

We deployed two cameras for tracking in combination with two stereoscopic PIV (Particle Image Velocimetry) cameras for three-dimensional velocity measurements. Swimming trajectories of all daphnids were tracked using two orthogonally arranged CCD-cameras (FlowSense4M, Dantec Dynamics, four-megapixel, 8 bit greyscale resolution) mounted on bi-telecentric lenses (TC 4M, Opto Eng.) having a focal depth of 5.6 cm (Figure 2.1). The usage of bi-telecentric lenses pro-
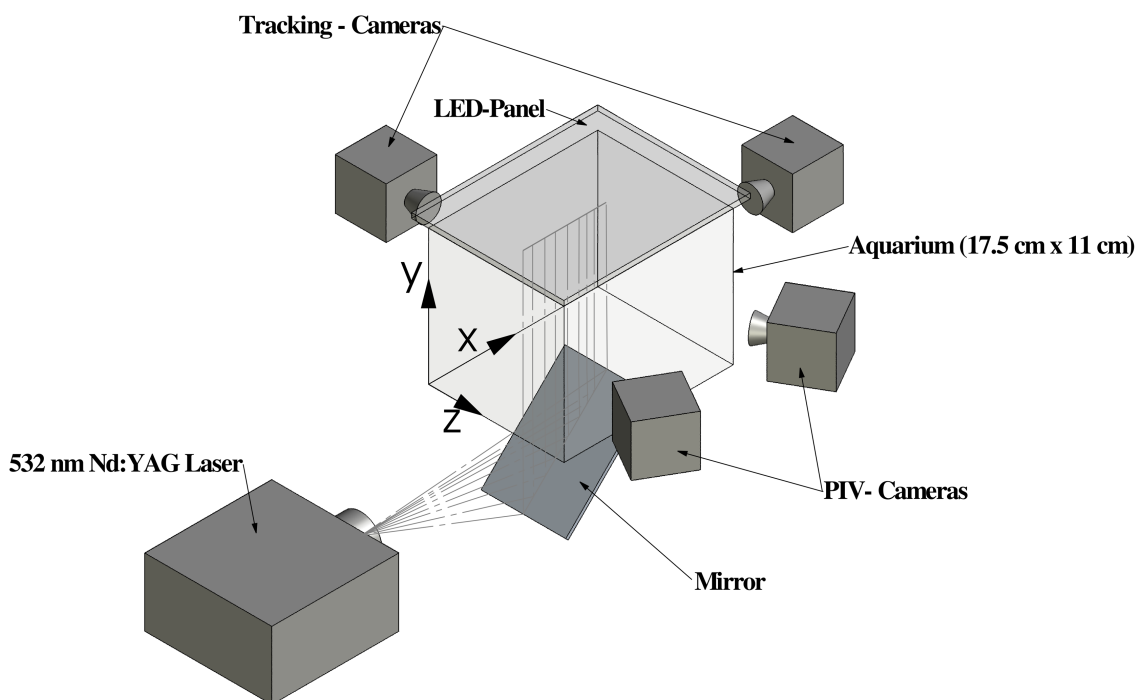
Figure 2.1: *A three-dimensional depiction of the experimental set-up. Temperature fluctuations potentially causing convective currents in the test aquarium were suppressed by placing it into an outer aquarium of constant temperature, which is not shown here.*

vided a pixel resolution of about 19.5 pixels mm^{-1}, which is independent of location within the sampling volume. The spatial resolution of each camera-lens combination was measured using a custom-made calibration target.

Three-dimensional current velocities were measured within a vertical plane located in the center of the test aquarium using stereoscopic PIV. The plane was illuminated by short laser pulses (Litron Nano L 200-15 PIV double pulse laser, wavelength: 532 nm, pulse duration: 4×10^{-9} s), and the displacement of seeding particles ($50 \, \mu$m diameter Polyamide particles, Dantec Dynamics) was observed from two different perspectives (Figure 2.1). The laser light sheet had a thickness of ≈ 5 mm, and it should be noted that the swimming behavior was not affected by the green laser light (Table A.1 provided in the supporting information). A four-megapixel greyscale CCD-camera (FlowSense4M, Dantec Dynamics) and a two-megapixel greyscale PCO camera (HiSense 610, Dantec Dynamics) were used for the PIV measurements. Video A.1 (provided in the supplementary information) exemplifies a sequence of raw images showing particle displacements by freely swimming daphnids of different sizes.

The timing of laser pulses and image acquisition of all four cameras were controlled using *Dantec Dynamicstudio* software (version 3.20). The two stereoscopic PIV cameras captured images during the exposure with the laser light sheet, while two tracking cameras captured images during the time window in which the laser light sheet was off. Images from all four cameras were recorded

at 14.8 Hz for 5.6 min.

2.2.2 Data analysis

Swimming trajectories and patterns

Three-dimensional swimming trajectories of all daphnids within the test aquarium were estimated following the procedure described by Noss et al. (2013). The raw tracks were initially refined to a minimum length to screen out a large number of very short segmented tracks, and furthermore, tracks which did not cross the laser light sheet were discarded. Moreover, near-wall segments of the refined trajectories were also discarded because daphnids tend to veer from the primary swimming trajectory in the neighborhood of the glass walls. Consequently, the lengths of swimming trajectories chosen for further analysis were typically about 60 mm.

   Instantaneous swimming speeds of the organisms were estimated using the distances between subsequent positions along the swimming trajectory. Mean swimming speeds u_D were obtained from averaging of instantaneous speeds over the entire trajectory. Body Reynolds number of daphnids Re_D was calculated using mean swimming speed and body length ($Re_D = u_D \cdot l_D / \nu$, where ν is the kinematic viscosity of water at 20°C).
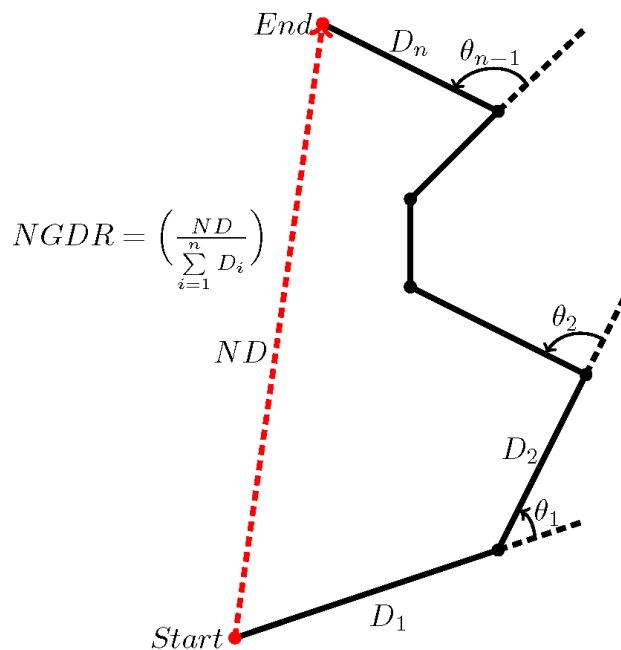
Figure 2.2: *An illustration of different metrics in characterizing swimming trajectories. The mean displacement is the mean of distances D_i traveled between two subsequent observations (black dots). The net displacement ND is the straight-line distance between the initial and final locations, and the gross displacement is the sum of distances D_i. The mean turning angle is the trigonometric mean of angles θ_i formed by changes in direction between observations (Strutton, 2007).*

13

Observed swimming trajectories were further used to categorically characterize the swimming pattern of organisms. A variety of metrics have been proposed for differentiating swimming patterns (Seuront et al., 2004b) (Figure 2.2). All proposed measures (e.g. path length or turning angle) are scale-dependent and no single measure may characterize swimming paths unambiguously (Strutton, 2007). Since both aspects of path length and turning angle are embodied, the Net to Gross Displacement Ratio (NGDR) within a distance of ± 30 mm from the light sheet was adopted in the present study. Three typical swimming patterns were discriminated based on observed NGDR values (Figure 2.3):

- Cruising (NGDR: 1.0-0.9): In this swimming pattern, organisms swim in a near-straight line trajectory (Figure 2.3A).

- Hopping and sinking (NGDR: 0.9-0.6): In this pattern of swimming, organisms tend to discretely ascend and descend from their pathways (Figure 2.3B).

- Looping (NGDR: 0.6-0.25): In this particular swimming pattern, organisms distinctly display a swirling or spiral-like motion (Figure 2.3C).
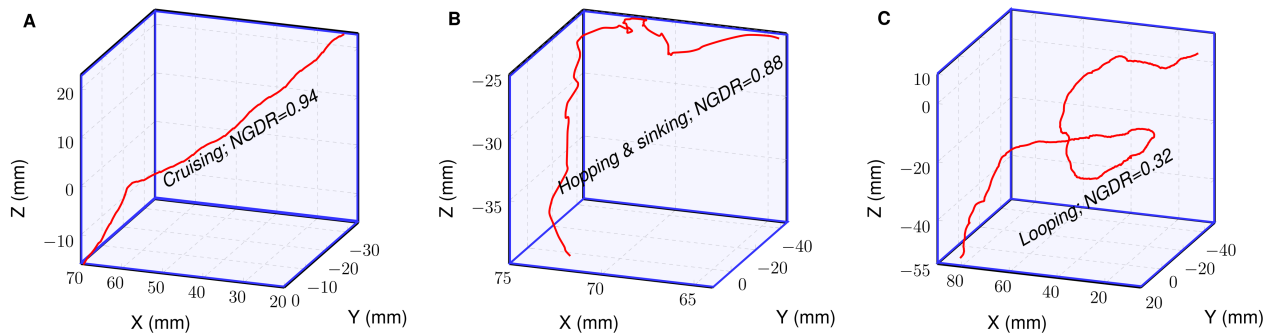
Figure 2.3: *An illustration of swimming patterns of* Daphnia. *The swimming patterns can be distinguished based on NGDR values specified.*

Analysis of trail

Three-dimensional current velocity vectors within the laser light sheet were obtained from stereoscopic PIV analysis (Stamhuis et al., 2002) by using an adaptive correlation method (Dantec Dynamics, 2012) available in DynamicStudio software (version3.20, Dantec Dynamics). The spatial and temporal resolution of the final velocity estimates are 1.8 mm $\times$ 1.5 mm and 0.0676 s respectively.

Dissipation rate of turbulent kinetic energy (Kundu and Cohen, 2008) was estimated from mea-

sured velocity components using;

$$\varepsilon = \nu \left[4\left\langle \left(\frac{\partial u}{\partial x}\right)^2 \right\rangle + 4\left\langle \left(\frac{\partial w}{\partial z}\right)^2 \right\rangle + 4\left\langle \left(\frac{\partial u}{\partial x}\frac{\partial w}{\partial z}\right)^2 \right\rangle + \frac{3}{2}\left\langle \left(\frac{\partial u}{\partial z}\right)^2 \right\rangle + \frac{3}{2}\left\langle \left(\frac{\partial v}{\partial x}\right)^2 \right\rangle \right.$$
$$\left. + \frac{3}{2}\left\langle \left(\frac{\partial v}{\partial z}\right)^2 \right\rangle + \frac{3}{2}\left\langle \left(\frac{\partial w}{\partial x}\right)^2 \right\rangle + 6\left\langle \left(\frac{\partial u}{\partial z}\frac{\partial w}{\partial x}\right)^2 \right\rangle \right] \tag{2.1}$$

Where u, v, and w denote the current velocity components in x, y, and z directions, respectively (Figure 2.1) and velocity gradients were estimated using a central difference scheme (Mathews and Fink, 2004).

The cross-sectional area of fluid disturbances induced by swimming daphnids crossing the laser light sheet were identified using a threshold of 5×10^{-8} W/kg in energy dissipation rates (Noss and Lorke, 2012). It should be noted that the threshold was somewhat arbitrarily chosen depending on the resolution and noise in our measurements. Trail cross-sectional area was estimated as the total area featuring dissipation rates above this threshold for individual PIV images. The three-dimensional distribution of energy dissipation rates in the trails was reconstructed by estimating the unresolved z-coordinate as the product of *Daphnia* swimming velocity obtained from tracking and the time elapsed after it has passed through the PIV field of view (Figure 2.4). The trail volume was estimated by integrating the measured planar dissipation distributions along over all three spatial dimensions. Figure A.1 (provided in the supporting information) shows an example of a trail produced by a cruising *Daphnia*. Assuming a cylindrical trail shape, equivalent trail diameters (d_{trail}) were estimated using the observed trail lengths (l_{trail}) and trail volumes (V_{trail}). Mean dissipation rates of kinetic energy ε_{trail} and total dissipated power P_{trail} were obtained from the log-average of observed dissipation rates within each trail (Baker and Gibson, 1987) and from the multiplication of the log-averaged dissipation rates with trail volume times water density ρ, respectively. For reference, we calculated the wake length of a sphere (l_{Sphere}) sinking in a still surrounding based on velocity scaling in a laminar wake region (Tennekes and Lumley, 1973; Schlichting, 1977). Using the velocity distribution provided in Wu and Faeth (1993) (their Equation 5), l_{Sphere} was estimated (Equation 2.2) as the distance from a sphere having the diameter $d = l_D$ and moving at speed u_D at which the centerline velocity ($\overline{u}$ in Equation 2.2) has decreased to 10% of its maximum value. Thus, the wake length can be formulated as;

$$l_{Sphere} = \frac{\theta^2 U_s}{4\nu(\frac{\overline{u}}{U_s})} = \frac{\theta^2 u_D}{4\nu * (10\%)} = \frac{\theta^2 u_D}{4\nu * 0.1} \tag{2.2}$$

Where θ initial momentum thickness of a wake (Equation 1 of Wu and Faeth (1993)), U_s is the sphere velocity (*Daphnia*) and $\overline{u}$ the mean streamline velocity at distance l_{Sphere}.

Total dissipated power of the swimming daphnids was further estimated using an approach of Huntley and Zhou (2004) for a global assessment of kinetic energy dissipation by swimming organisms. By applying their approach to our observations, the rate of energy utilization $P_{H\&Z}$ (in W) to overcome drag acting on a daphnid can be calculated as:

$$P_{H\&Z} = 1.4 \cdot 10^{-14} \cdot \rho \cdot Re_D^{1.8} \cdot u_D \tag{2.3}$$
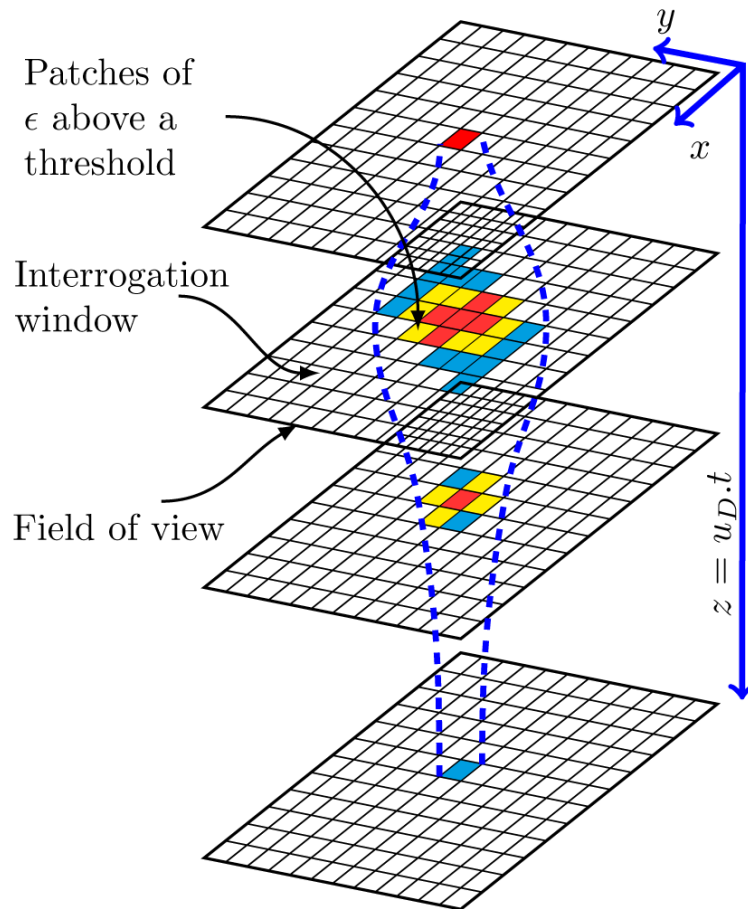
Figure 2.4: *A 3D schematic diagram that illustrates the method of estimating the volume of dissipation rates. The gridded windows indicate the field of view at different time stamps across the laser light sheet while smaller grids represents spatial window of the interrogation area (1.5 mm × 1.8 mm). A* Daphnia *swims in the z-direction, and three different grid colors indicate different levels of dissipation rates induced by the swimming* Daphnia. *The z-coordinate was determined as the product of* Daphnia *swimming velocity (u_D) and time taken to passed through field of view (t) while the trail cross-sectional area was computed by the total area of patches of ϵ above our threshold for each PIV image. The three-dimensional distribution of energy dissipation rates in the trails was reconstructed by the product of z-coordinate and the trail cross-sectional areas. Blue dashed lines represent the boundary of the trail.*

Equation 2.3 was originally derived by considering high-Reynolds number drag acting on a flat plate. As a more appropriate model for daphnids, we modified the derivation of Huntley and Zhou by considering the drag coefficient of a spherical particle, which yields an expression for total dissipated power P_{sphere} of:

$$P_{sphere} = \frac{1}{2}C_d \cdot \rho \cdot \frac{\pi d^2}{4} \cdot u_D^3 \tag{2.4}$$

The drag coefficient C_d of a sphere for the range of $0 < Re < 2 \times 10^5$ is given by:

$$C_d = \frac{24}{Re_D} + \frac{6}{1 + \sqrt{Re_D}} + 0.4 \tag{2.5}$$

The above expression is equivalent to Stokes law if $Re << 1$ (Kundu and Cohen, 2008).

2.3 Results

2.3.1 Swimming kinematics and trail structure

The measured average size of the organisms were $l_D = 2.0$ mm, 3.2 mm, and 3.5 mm in the ascending order of age groups. For each age group, four measurements of each swimming pattern were analyzed, hence, 36 trajectories were analyzed in detail (Table 2.1). The mean swimming velocity of the daphnids increased with increasing organism size from $u_D = 15$ to $u_D = 24$ mm/s, resulting in $Re_D = 32 \dots 84$.

The observed flow fields in the hydrodynamic trails had two possible configurations differing in the directions of current velocity in the trail relative to swimming velocity of the daphnids. An actively swimming daphnid generates a propulsive jet, which is directed opposite to its swimming direction. Fluid drag acting on passively drifting *Daphnia*, on the other hand, generates a fluid wake, with flow velocities in the direction of daphnid motion. Both flow fields are exemplified in Video A.1 of the supplementary information. In both configurations, the trail can be described as a unidirectional and axisymmetric flow structure of cylindrical shape (see animated velocity distribution in the jet behind an upward swimming *Daphnia* in Video A.2 of the supplementary information). 50% of analyzed flow structures were wakes, and 50% jets (Table 2.1), irrespective of the pattern of swimming.

The mean trail diameter in our observations was $d_{trail} = 1.1 \pm 0.5$ cm and did not vary with Re_D (Table 2.1, Figure 2.5A). The observed trail lengths varied over more than one order of magnitude also within the three size groups. For the largest animals considered in the study (i.e., $Re_D > 60$), trail length exceeds the trail diameter approximately by a factor of ten. As shown in Figure 2.5, in particular the long trails of the largest organisms reach the lengths predicted by similarity scaling of laminar trails behind a translating sphere (Equation 2.6, Figure 2.5A). Increasing trail lengths lead to strongly increasing trail volume with increasing Reynolds number (Figure 2.5B). Observed trail volumes (V_{trail}) vary over two orders of magnitude and reaches up to 10^{-5} m^3, corresponding to about 500 times the body volume of the largest daphnids. While trail volume increases with the

Table 2.1: *Summary of analyzed data and results. Note that for the limited number of our observations, the chosen swimming patterns exhibited no systematic dependence with hydrodynamic quantities analyzed. Therefore, only the mean values of all quantified parameters irrespective of swimming pattern are presented with standard deviations within parentheses).*

Age (days)	5	20	35
Size (10^{-3}m)	2.0 ($\pm$0.056)	3.2 ($\pm$0.11)	3.5 ($\pm$0.18)
Speed (10^{-3}ms^{-1})	15.4 ($\pm$3.5)	18.2 ($\pm$4.8)	23.6 ($\pm$4.4)
Reynolds number	32 ($\pm$7.1)	58 ($\pm$15.2)	84 ($\pm$15.8)
No. of observations (wakes, jets)	12 (4, 8)	12 (7, 5)	12 (7, 5)
Cruising (wakes, jets)	(0, 4)	(3, 1)	(2, 2)
Hopping and sinking (wakes, jets)	(1, 3)	(1, 3)	(1, 3)
Looping (wakes, jets)	(3, 1)	(3, 1)	(4, 0)
Mean trail volume (10^{-7}m^3)	5.3 ($\pm$4.4)	10 ($\pm$16.6)	60 ($\pm$31)
Mean trail length (10^{-3}m)	8.6 ($\pm$6.7)	14.1 ($\pm$16.2)	56.3 ($\pm$25.6)
Mean trail diameter (10^{-3}m)	10.0 ($\pm$4.4)	9.5 ($\pm$1.3)	12.9 ($\pm$7.6)
Mean dissipation rate (10^{-6}Wkg^{-1})	3.4 ($\pm$3.5)	2.4 ($\pm$1.9)	1.8 ($\pm$1.2)
Mean total dissipated power (10^{-9}W)	1.3 ($\pm$1.0)	1.3 ($\pm$0.9)	10 ($\pm$6.5)

third power of Reynolds number (Figure 2.5B), no systematic dependence of trail dimension on flow configuration in the trail (wake or jet) or swimming pattern could be observed (Figure 2.5A).

2.3.2 Trail energetics

Trail-averaged viscous dissipation rates varied between 1.8×10^{-6} W/kg and 3.4×10^{-6} W/kg (Table 2.1). Similar to trail diameter, dissipation rates show no systematic dependence on Reynolds number, flow configuration, or swimming pattern (Figure 2.6A). As a result of increasing trail volume, total dissipated power within the trail, however, is increasing with Reynolds number (Figure 2.6B). Observed magnitudes of total dissipated power within the trail of the swimming daphnids varied between 1.3×10^{-9} W and 1×10^{-8} W. For our observations, the total dissipated power estimated according to Huntley and Zhou (Equation 2.3) provides a lower bound while the same approach applied to spherical organisms moving at intermediate Reynolds numbers (P_{sphere}, Equation 2.4) provides an upper bound (Figure 2.6B).

To assess the consistency of observed trail dimension and dissipated power, we estimated the length of an axis-symmetric trail of d_{trail} and of mean longitudinal velocity u_D, which is subject to viscous friction. Under these conditions, the power dissipated in the trail P_{trail} is equal to the product of viscous force acting on the cylindrical surface area of the trail and mean current velocity within the trail ($P_{trail} = F \cdot u_D = (\pi d_{trail}^2/2) \cdot \eta \cdot (u_D^2/d_{trail})$). P_{trail} can further be expressed as the mean dissipation rate in the trail ε_{trail} times trail volume ($\varepsilon = P_{trail} \cdot V^{-1} = P_{trail} \cdot (\rho \cdot (\pi d_{trail}^2/4) \cdot l)^{-1}$), resulting in a relationship between trail length l_{diss} and mean kinetic energy dissipation within
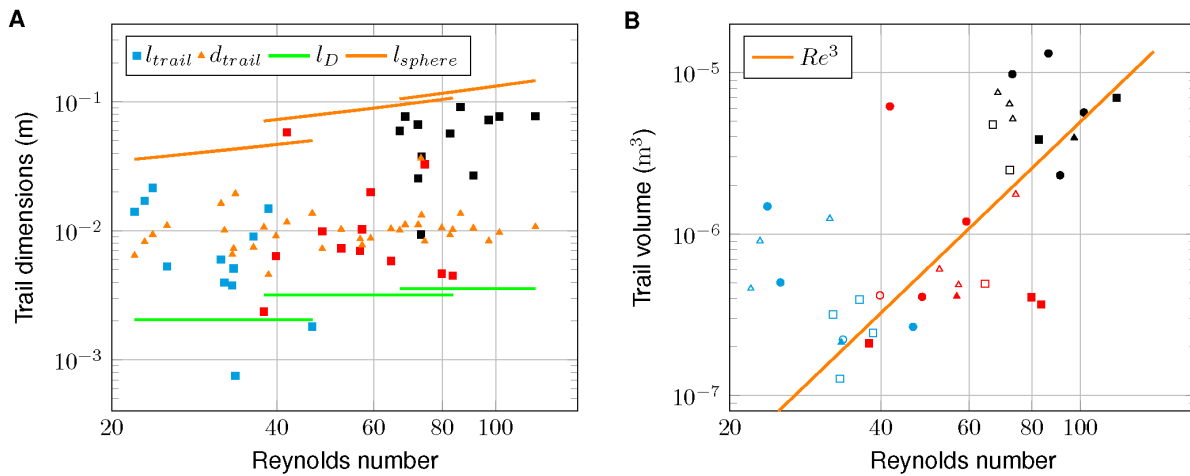
Figure 2.5: *Observed trail dimensions vs. Reynolds number. (A) Observed trail length (squares) and trail diameter (triangles) vs. Reynolds number. Distinct colors of square markers indicate different age groups (cyan-5 days, red-20 days, and black-35 days).* Daphnia *length (green lines) and the length of corresponding sphere wakes (Equation 2.4) are shown for mean Reynolds number of the three age groups. (B) Observed trail volume vs. Reynolds number. Symbol color indicates age group, filled markers represent wakes and open markers jets. Distinct swimming patterns are indicated by square (cruising), triangle (hopping and sinking), and circle (looping). The line represents a proportionality to the Re^3.*
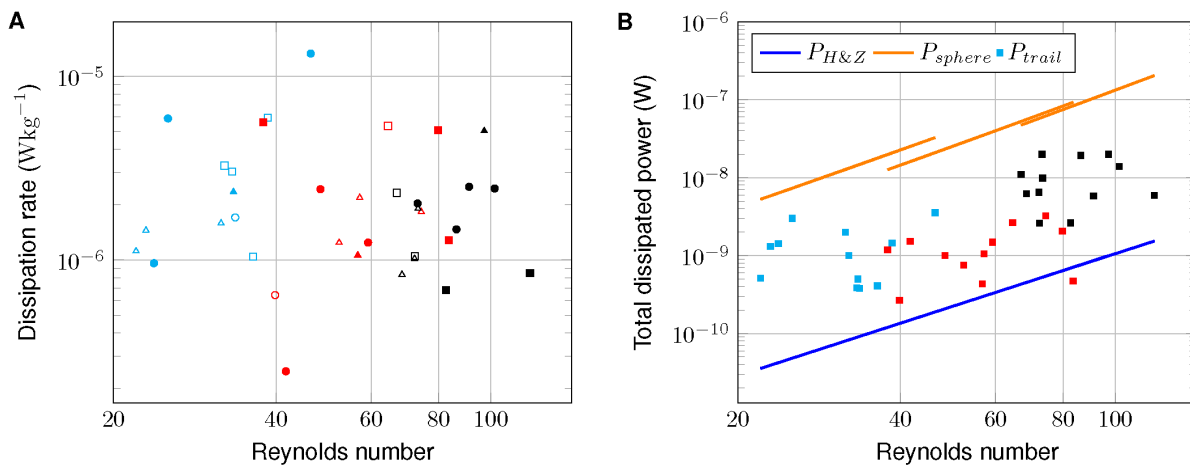
Figure 2.6: *Trail-averaged viscous dissipation rates and total dissipated power within the trail vs. Reynolds number. (A) Trail-averaged viscous dissipation rates (total dissipated power / trail volume) vs. Reynolds number. Distinct colors indicate age groups (cyan-5 days, red-20 days, and black-35 days), filled markers represent wakes and open markers jets. Different swimming patterns are indicated by square (cruising), triangle (hopping and sinking), and circle (looping). (B) Total dissipated power within the trail vs. Reynolds number. Colors indicate age groups. The blue line shows dissipated power estimated according to Huntley and Zhou (2004) (Equation 2.3), and the orange line the modified approach for a sphere (Equation 2.4).*
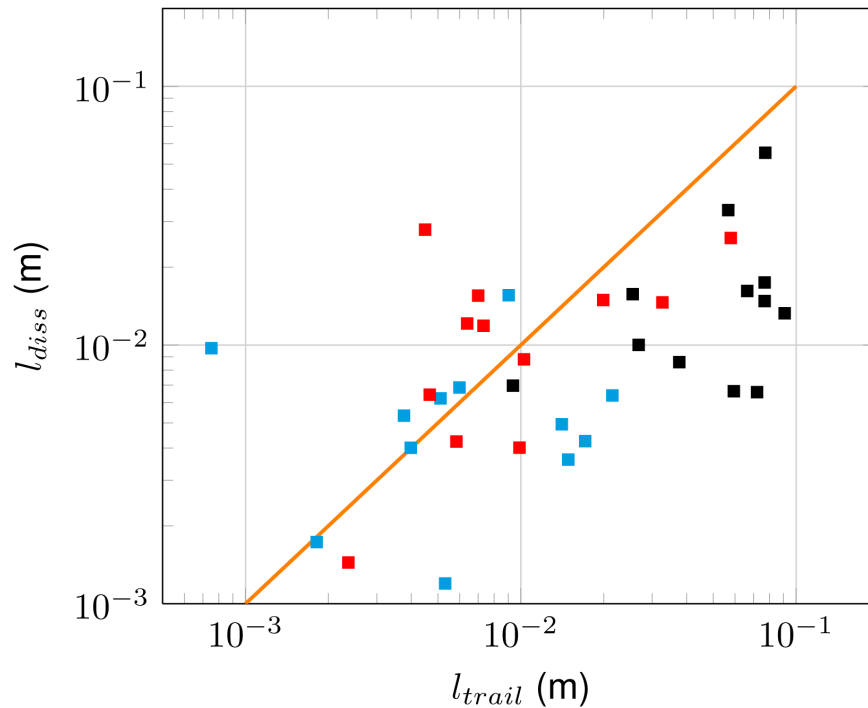
Figure 2.7: *Trail length l_{diss} estimated from observed dissipation rates (equation 2.6) vs. observed wake length l_{trail}. Distinct colors of square markers stand for age groups (cyan-5 days, red-20 days, and black-35 days) and the line represents a 1:1 relationship.*

the trail:

$$l_{diss} = \frac{2\eta \cdot u_D^2}{\varepsilon \cdot \rho \cdot \pi \cdot d_{trail}} \qquad (2.6)$$

Trail lengths estimated from Equation 2.6 using measured dissipation rates and trail diameter d_{trail} indicate a similar order of magnitude with observed trail lengths and also reproduce its dependence on *Daphnia* Reynolds number (Figure 2.7).

2.4 Discussion

2.4.1 Swimming speed, jets and wakes

Huntley and Zhou (2004) have analyzed the hydrodynamics of swimming by 100 marine species ranging in size from bacteria to whales and found close empirical relationships between organism Reynolds number and cruising (u_c), and escape (u_e) swimming speeds, respectively. These relationships have been converted to functions of body size by Kunze (2011), resulting in $u_c = 3.23 \cdot l^{0.83}$ and $u_e = 7.76 \cdot l^{0.53}$. While having body length in between those of copepods and krill, the observed swimming velocities of *Daphnia* closely follow the relationship for cruising speed, (Figure 2.8A). The close correspondence to u_c is expected, because escape behavior was not observed in
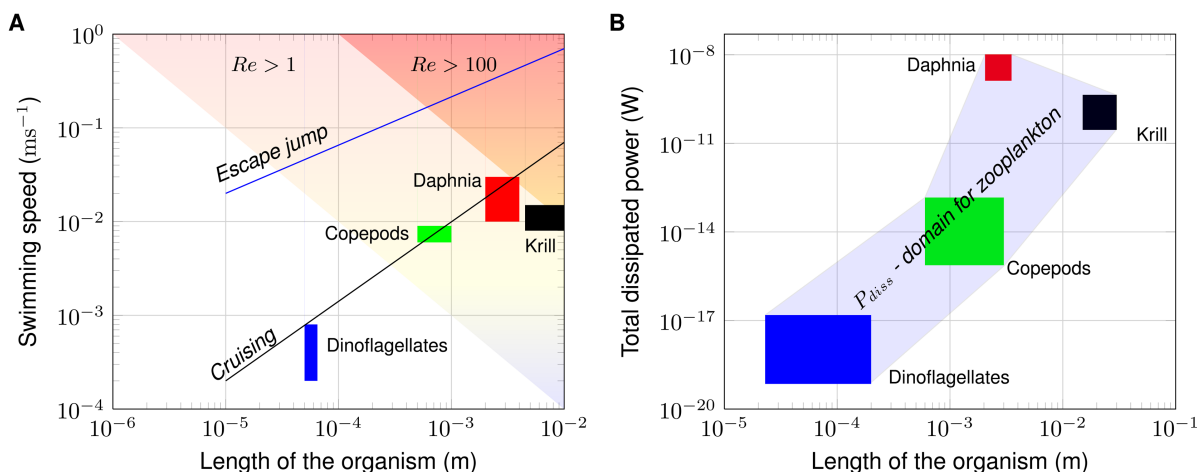
Figure 2.8: *Comparison of* Daphnia *with other zooplankton. (A) Comparison of swimming speed. Regions for* $Re > 1$ *and* $Re > 100$ *are denoted by light and dark pink colors. Lines show the empirical relationships for cruising and escape speeds for aquatic organisms as a function of organism size obtained by Huntley and Zhou (2004). Labeled boxes in color indicate the range of organism size and swimming speed for three zooplankton species considered in the analysis of Huntley and Zhou, as well as the present results for* Daphnia *(figure adopted from Kunze (2011) with modifications). (B) Comparison of total dissipated power of* Daphnia *with empirical estimates for other zooplankton (Huntley and Zhou, 2004). Labeled colored boxes indicate the range of organism size and dissipated power. Shaded area indicates a potential domain for dissipated power (* P_{diss} *) of kinetic energy produced by swimming zooplankton of different size.*

our measurements. Nevertheless, daphnids are capable of performing escape reactions by increasing antenna beat frequencies up to five-fold (up to 23 Hz (Kirk, 1985)).

The hydrodynamic footprint of *Daphnia* can either be a propulsive jet, which is generated by antenna motion and entrainment of ambient fluid (Gries et al., 1999; Kirk, 1985), or it can be a wake of fluid dragged behind the translating body (Leal, 1980). Although the direction of the current velocity relative to the direction of body translation (swimming direction) is reverse, we use the term trail for both flow configurations. Irrespective of the pattern of swimming, each age group exhibited an almost equal distribution of wakes and jets in our observations.

The direction of the trail does not yield a distinct pattern in the distributions of trail volume, dissipation rate, or total dissipated power. These findings indicate similar duration of time periods of active propulsion and of inertial or gravitational movement, as well as a comparable momentum balance between the traversing organism and their trail under both conditions. The direction of flow in the hydrodynamic footprints of *Daphnia* therefore does not provide directional information for locating the organism and potentially reduces the risk of predation. However, the exact information about the nature of a predator's perception of hydrodynamic cues is not known, therefore, the intensity of the signal may still provide guidance to the source.

Our Video A.2 shows that a body vortex is formed around the body of the swimming *Daphnia*. Though the analyses of these vortices are beyond the scope of our work as we focused on the far-field, formation of similar vortex rings have been observed for other organisms and spheres (Jiang and Kiørboe, 2010; Yen and Strickler, 1996; Fields and Yen, 1997). In the case of repositioning jump made by copepods, two counter-rotating viscious vortex rings are formed in the wake and around the body of the copepod (Jiang and Kiørboe, 2010). Shedding of conspicuous vortices during escape jumps of copepods have also been reported elsewhere, copepod mechanoreceptors can detect jet-like wakes produced by their preys during escape hops in the vortex flow field initially created by copepods (Yen and Strickler, 1996). In a separate study, the flow vorticity produced in a feeding current by copepods increases along the antennae (Fields and Yen, 1997).

2.4.2   Trail size and energy dissipation

Our results for the trail dimensions are in good agreement with the empirical estimations suggested by Gries et al. (1999). Using their empirical formulae provided for the trail volume at the lowest density gradient ($3 \ \mathrm{kgm}^{-4}$) that they have used and considering a fully developed trail (i.e. after 6 s of the trail evolution) of *Daphnia* having a length of 2.12 mm, the trail volume is approximately $4 \times 10^{-7} \ \mathrm{m}^3$. This is closely comparable to the mean trail volume estimated in our study ($5.3 \times 10^{-7} \ \mathrm{m}^3$) for *Daphnia* with 2 mm length (Table 2.1). Similarly, the trail length estimated using the empirical formulae by Gries et al. (1999) for the same density gradient is about 8.3 mm whereas our estimations yielded a mean trail length of 8.6 mm (Table 2.1) for similar *Daphnia* size. However, the estimations using the approach by Gries et al. (1999) should still be corrected to avoid underestimating the trail dimensions, because their lowest density gradient is still large. Assuming that the maximum length of the trail remains constant at gradients less than $1 \ \mathrm{kgm}^{-4}$ (Gries et al., 1999), trail length is about 10.6 mm at smaller gradients which overestimates our estimations of the mean trail length by a factor of 1.2. The discrepancy can be attributed to the different species ((Gries et al., 1999) used *Daphnia pulicaria*), larger fluctuations of trail length at gradients less than $1 \ \mathrm{kgm}^{-4}$, and other unknowns.

With increasing Reynolds number, an increasing fraction of power is dissipated at scales significantly exceeding the size of the organism. For the observed range of Reynolds number, our results indicate that the length of the trail increases whereas the width of the trail remains approximately constant. This is in accordance with velocity scaling in a laminar sphere wake (Wu and Faeth, 1993), which predicts that velocity perturbations decrease exponentially in the radial direction and reciprocally along the centerline of a wake. Increasing trail length, due to increasing inertia of the displaced fluid at higher Reynolds number, results in an increase of the fraction of power dissipated in the trail. The category of swimming pattern or the trajectory of swimming neither affects the size nor the energetics of the trails.

Our measurements did show similar dissipation rates of kinetic energy for the different patterns of swimming. While trail sizes and energetics being independent of swimming patterns may be ascribed to the unique propulsion mechanism of *Daphnia* (beating their antennas), it still poses the question why organisms choose different swimming patterns. In addition to dissipate energy, the

organisms need to perform other functions that may demand to differ their trajectories. In order to seize a patch at a faraway distance, organisms may need to cruise to travel a greater distance within a short time (Kiørboe, 2007). Moreover, cruising may also help to evade slower moving predators. Looping may be required to search for a good food patch in the neighborhood of the organism and remain in the patch during its area-restricted food search (Price, 1989; Tiselius, 1992; Woodson and Mcmanus, 2007). Looping can be additionally useful to escape from predators that largely rely on linear perception. Hop and silent sinking may need to perform evasive actions to evade mechanoreceptive predators.

Total dissipated power measured in the trail of swimming daphnids exceeds the estimates of Huntley and Zhou (2004) by one to two orders of magnitude (Figure 2.8B). Also, the total dissipated power estimated by Huntley and Zhou (2004) for different zooplankton species along with the total dissipated power measured in the trail of swimming daphnids provide a potential likelihood region of dissipated power for zooplankton (P_{diss} in Figure 2.8B), and the total dissipated power measured in the trail of swimming daphnids exceeds the smallest zooplankton species considered by about 10 orders of magnitude. Applying the theoretical approach of Huntley and Zhou to a moving sphere, instead of a flat plate, and using a drag coefficient which takes low-Reynolds number effects into account (P_{sphere}, Equation 2.4), results in much higher estimates of power (Figure 2.6B). It should be noted, that our measurements, which result in power estimates in between those of Huntley and Zhou (2004) and P_{sphere}, did not resolve the entire power dissipated in the flow field due to limitations in resolving velocity gradients in close proximity of the organism. Particularly at low Reynolds numbers, most of the energy is dissipated in close proximity of the organism. Hence, our measurements potentially underestimate total dissipated power and energy expenditure of swimming daphnids. However, they provide estimates of power, which is dissipated at larger spatial scales, exceeding the size of the animal by more than a factor of ten.

Mean volume, dissipation rate and total dissipated power of the 5 and 20 days old daphnids in the current study correspond to the values Noss and Lorke (2012) observed in the trail of an approximately 4 mm large *Daphnia magna* swimming in a weak density stratification of $d\rho/dz = -0.7$ kgm^{-4}. Although Gries et al. (1999) observed that a weak stratification ($d\rho/dz \leq 1$ kgm^{-4}) has negligible effects on the trail length of swimming *Daphnia*, the density stratification in Noss and Lorke (2012) might be the main reason for the difference in comparison to our values obtained for the 35 days old daphnids. Numerical simulations of Ardekani and Stocker (2010) revealed that the flow field and fluid transport generated by similar sized organisms is affected also by weak density stratification.

2.4.3 Implications for biomixing

The significance of zooplankton-induced fluid motion for vertical mixing of density-stratified waters at larger scale has been the subject of a recent scientific debate. While different modeling approaches suggest significant contributions to energy production (Dewar et al., 2006; Huntley and Zhou, 2004) and also fluid mixing (Katija and Dabiri, 2009; Leshansky and Pismen, 2010), particularly the latter has been questioned based on scaling arguments (Kunze, 2011; Visser, 2007).

These arguments were based on the assumption that the spatial extent of the hydrodynamic disturbances produced by zooplankton is comparable to organism size. This assumption is only valid for low Reynolds number flow (i.e. $Re << 1$). The turbulent drag law applied by Huntley and Zhou (2004), in contrary, is only valid for high Reynolds number flow ($Re >> 1$). Swimming of most zooplankton organisms, however, is associated with Reynolds numbers in the transitional range (Yen, 2000; Duren et al., 2003; Borazjani et al., 2010), where both approaches are not valid. Our measurements show that in the hydrodynamic trails of *Daphnia*, kinetic energy is dissipated at rates even exceeding current estimates. This finding indicates that more detailed numerical simulations of fluid transport by swimming organisms obtained for Stokes flow (Dabiri, 2010; Doostmohammadi et al., 2012; Eames et al., 1994) (neglecting fluid inertia and trails) cannot unrestrictedly be applied to *Daphnia* and potentially other zooplankton species swimming at intermediate Reynolds number.

Enhanced dissipation rates were observed at spatial scales about 10-fold larger than the size of the organisms. Kinetic energy dissipation is associated with current shear, which also enhances small-scale gradients of dissolved substances. The corresponding mixing, i.e. the dissipation rate of concentration variance by molecular diffusion, can be described by an apparent (eddy) diffusivity. The quadratic dependence of eddy diffusivity on the size of fluid disturbances (Kunze, 2011) results in a 100-fold increase of diffusivity and scalar mixing rates if the size of the hydrodynamic trail instead of the commonly (Kunze, 2011; Visser, 2007) applied organism size is considered. Because molecular diffusivities of dissolved substances are about three orders of magnitude smaller than the diffusivity of momentum, concentration variance is dissipated more slowly than velocity variance. This results in larger dimensions of the trail behind the swimming organisms if it is defined based on concentration measurements. Using a fluorescent tracer, Noss and Lorke (2014) have estimated the size of the trail behind swimming daphnids in terms of dissipation rates of concentration variance to be between 1 and 13×10^{-5} m^{-3}, about one hundred times larger than the hydrodynamic trails observed in the present study. The relevant size of the hydrodynamic trail is defined by the particular context and can be expected to differ strongly, e.g., for hydromechanical and chemical signaling.

Acknowledgments

Daphnia pushed to the limits: kinematics and energetics of swimming in turbulence

Lalith N. Wickramarathna, Christian Noss, and Andreas Lorke

Institute for Environmental Sciences, University of Koblenz-Landau, Landau, Germany.

Abstract

Motile zooplankton generally needs to make a trade-off between efficient swimming, feeding, and leaving hydrodynamic traces that may be detected by predators. Achieving this balance can be challenging in the presence of turbulence. Therefore, an important question is to what extent zooplankton can respond to increasing turbulence by adapting their swimming behaviour and kinematics? We quantify the influence of turbulence on swimming kinematics and the energetics of the resulting flow field using *Daphnia* swimming in a range of turbulent environments with energy dissipation rates ranging between 10^{-8} m^2s^{-3} and 10^{-4} m^2s^{-3}. We show that at the turbulent intensities *Daphnia* are likely to encounter in their natural habitats (10^{-8} m^2s^{-3} -10^{-6} m^2s^{-3}), they increase their swimming activity and speed in response to increasing turbulence. Increasing turbulence intensity to unrealistically high values (10^{-4} m^2s^{-3}), they begin to withdraw from active propulsion at a threshold level of about 10^{-6} m^2s^{-3}. In the intermediate range of turbulence (10^{-7} m^2s^{-3}-10^{-6} m^2s^{-3}), kinetic energy dissipation rates in the vicinity of the organisms are consistently one order of magnitude higher than in the background turbulent flow.

3.1 Introduction

Zooplankton plays a vital role in the food webs of both freshwater and marine ecosystems. They are exposed to fluctuations of their physical environment at a broad range of spatial and temporal scales (Crossland et al., 2005; Kiørboe, 2011) that often test the tolerance of these organisms to the limit (Carrasco et al., 2013). Among the environmental conditions, turbulence is a consistent hydrodynamic feature of all aquatic ecosystems (Thorpe, 1985; Wüest and Lorke, 2003).

To understand the interaction between zooplankton and physical processes in aquatic ecosystems the effects of turbulence on zooplankton swimming have been studied by means of laboratory experiments (Alcaraz et al., 1994; Saiz et al., 2003; Fuchs et al., 2013), field measurements (Visser and Stips, 2002; Maar et al., 2003), and numerical simulations (Mackenzie et al., 1994; Zhan et al., 2014). A substantial amount of effort has so far been made to understand how turbulence in aquatic ecosystems affects swimming behaviour (Haury et al., 1992; Prairie et al., 2012), predator-prey encounter rates (Rothschild and Osborn, 1988; Mackenzie et al., 1994), feeding patterns (Saiz and Kiørboe, 1998), metabolism (Saiz and Alcaraz, 1992; Alcaraz et al., 1994), and growth rates (Alcaraz et al., 1988; Saiz et al., 1992), although these studies have not essentially yielded consistent results as discussed below.

The majority of existing studies were focused on behavioural responses of marine copepods to varying turbulence intensities (Granata and Dickey, 1991; Saiz and Kiørboe, 1998; Saiz et al., 2003). While some previous studies have used undefined turbulence intensities (Oviatt, 1981; Alcaraz et al., 1988), copepods exposed to a range of turbulent energy dissipation rates (5×10^{-6}-1.5×10^{-5} m^{2}s^{-3}) indicated a potential three-fold energetic gain in turbulence in comparison to non-turbulent conditions at low food concentrations (Marrasé et al., 1990). Several other studies have suggested threshold levels for the dissipation rate of turbulent kinetic energy at which copepods begin to avoid turbulence ($10^{-6.5}$ m^{2}s^{-3} (Incze et al., 2001), 10^{-7} m^{2}s^{-3} (Pringle, 2007)). For a range of turbulence (3.8×10^{-8} - 1.1×10^{-4} m^{2}s^{-3}) copepod Temora longicornis showed an increase in escape response with increasing turbulence, and their swimming patterns exhibited a strong adaptation to highly turbulent environments (Seuront et al., 2004). Yen et al. (2008) showed that copepods could control their position and movements at low turbulence intensity and their movement was dominated by passive displacement at higher turbulence intensity while the transition occurred at a dissipation rate of 9×10^{-7} m^{2}s^{-3}. Further strengthening the argumentation that zooplankton have an optimum fitness level under turbulent conditions, Visser et al. (2009) found a dome-shaped relationship between copepod swimming activity and ambient turbulence intensities. According to their findings, the zooplankton fitness starts to reduce swimming activity at a turbulence level about 10^{-4} m^{2}s^{-3} which they attribute to a behavioural change from cruise to ambush feeding. This dome-shaped relationship may affect the vertical distribution of organisms. Because, as turbulence increases, predation risk increases more than foraging benefit (Visser et al., 2009), downward migration to lower turbulence intensities can reduce the predation risk at a marginal decrease in ingestion rates due to decreasing prey concentration.

A recent study demonstrated that active swimming contributed substantially to the swimming

velocity of copepods even when turbulence is significant (Michalec et al., 2015). Webster et al. (2015) investigated the response of two copepod species in two turbulence levels with mean dissipation rates of turbulence (9×10^{-7} m^{2}s^{-3} and 9.6×10^{-6} m^{2}s^{-3}) and found that Acartia tonsa did not significantly responded to the lower turbulence level but significantly altered their swimming behaviour in the higher turbulence level by increasing the relative speed of swimming. In contrast, T. longicornis did not indicate a behavioural response to both levels.

In addition to zooplankton, meroplankton (mainly marine vertebrate larvae) have been reported to trigger changes in larval swimming behaviour actively or passively in response to turbulence (Roy et al., 2012). Fast swimming larvae crab zoea observed to actively change their swimming speeds (Welch and Forward, 2001) while barnacle cyprids opposed downwelling currents by swimming upwards (DiBacco et al., 2011). Moderately fast swimming oyster larvae has shown to sink (Fuchs et al., 2013) or swim upward (Wheeler et al., 2013; Fuchs et al., 2015; Wheeler et al., 2015) in high turbulence. At turbulence intensity equivalent to the kinetic energy dissipation rate of 10^{-6} m^{2}s^{-3}, an active upward swimming of sand dollar and a passively stable swimming of purple sea urchin have been observed (McDonald, 2012). Sea urchin exposed to two levels of turbulent dissipation rates (9×10^{-9} m^{2}s^{-3} or 4×10^{-7} m^{2}s^{-3}) showed that under no flow and low turbulence conditions, animals moved towards the water surface whereas in high turbulence, larvae were passively transported with the flow (Roy et al., 2012). Some studies suggested that increasing turbulence enhances larval settlement (Fuchs et al., 2015), whereas others observed a reduced settlement in scallop larvae (Pearce et al., 1998). Among various other studies that have reported an active response of larvae to turbulence; larval boat snails Crepidula fornicata increased upward swimming with increasing turbulence level (Fuchs et al., 2010), and larval eastern oysters Crassostrea virginica dived in the presence of high fluid acceleration over short time spans (Wheeler et al., 2015). Turbulent shear has been suggested to provide habitat-scale cues for larval settlement of sea urchin (Gaylord et al., 2013), and can induce cloning by fragmenting individuals in coral larvae (Heyward and Negri, 2012).

Less is known about how turbulent flows affect the swimming and energetics of freshwater zooplankton. *Daphnia*, commonly known as water fleas, adults range in size from 0.2 mm to 1 cm, are a freshwater zooplankton found in ponds and lakes (Ebert, 2005). They use a pair of stretched appendages and erected swimming hairs during its power stroke while appendages and hairs are concurrently folded and collapsed during its recovery stroke. The forward propulsive force is achieved by beating the appendages at frequencies of 3-5 Hz (Gries et al., 1999), but the rate can increase up to 23 Hz during escape reactions (Kirk, 1985). During each stroke, *Daphnia* produce a peak displacement in the order of the *Daphnia* radius. *Daphnia* exhibit distinctive swimming patterns in calm water, namely; cruising, hop and sink, and looping (Wickramarathna et al., 2014).

A few studies have focused on understanding behavioural changes of *Daphnia* in the presence of turbulence (Brooks, 1947; Alcaraz et al., 1994; Laforsch and Tollrian, 2004). Spitael (2007) observed that *Daphnia magna* tolerated higher levels of turbulence to remain in the oxygen-rich surface zone. Seuront et al. (2004) investigated swimming speed and behaviour of *Daphnia* pulicaria for a range of turbulent dissipation rates (3.8×10^{-8} m^{2}s^{-3} - 1.1×10^{-4} m^{2}s^{-3}) and found

increased escape responses with increasing turbulence.

Thus, despite a number of investigations on zooplankton and meroplankton swimming in turbulence, the extent to which they adapt their swimming behaviour or avoid turbulence often remains ambiguous. This ambiguity can mainly be attributed to experimental methods which have largely focussed on the analysis of organism behavioural change, while observations of actual flow fields were neglected. Only a few studies have deployed simultaneous measurements of organism swimming and the flow field around the organisms (Yen et al., 2008; Adhikari et al., 2015; Michalec et al., 2015).

A previous study showed that among zooplankton species, *Daphnia* exhibited swimming speeds exceeding those of copepods and krill (Wickramarathna et al., 2014) in still-water. Turbulence enhances *Daphnia* metabolism, as indicated by 14.3% increase in heart rate compared to calm water conditions (Alcaraz et al., 1994). This suggests that *Daphnia* may be more resilient and can potentially enhance their swimming activity in response to turbulence. Therefore, we hypothesize that *Daphnia* intensify their swimming activity in response to increasing turbulence up to a threshold, beyond which, the animals gradually withdraw from active swimming.

Here we analyse laboratory observations of *Daphnia* swimming in turbulent flows of different intensity. We follow a novel approach of simultaneously obtaining time-resolved trajectories and the flow field around planktonic organisms (Adhikari et al., 2015). The measurements resolve both behavioural changes in animals' motility and the corresponding characteristics of the turbulent and animal-induced flow fields, which allow for direct estimates of dissipation rates of turbulent kinetic energy.

3.2 Materials and Methods

3.2.1 Experimental set-up

Experiments were conducted in a laboratory tank with a length, width, and water depth of 3 m, 0.36 m and 0.4 m respectively (Table 3.1). Turbulence was generated by horizontal oscillations of a rigid grid (35 cm × 35 cm) with a stroke amplitude of 10 cm. The grid had vertical and horizontal bars of 1 cm thickness with a mesh size of 4.5 cm × 4.5 cm, resulting in a solidity of 40%. The distance between the tank's bottom and the bottom most edge of the grid was 2 cm. Grid oscillation was driven by an electric motor and experiments were conducted without turbulence and at four different turbulence levels, referred to hereafter as TL0 (grid-turbulence generator switched off), TL1, TL2, TL3, TL4.

For organism tracking, the tank was illuminated from below using a dimmable natural white Light-Emitting Diode (LED)-panel. Light intensity was adjusted (454 lm) to provide sufficient illumination for organism tracking. Swimming trajectories of daphnids were observed using two orthogonally mounted Charge Coupled Device (CCD)-cameras (FlowSense4M, Dantec Dynamics, 2048 × 2048 pixels, 8 bit grey-scale resolution) (Fig. 3.1). Tracking cameras captured images

Table 3.1: *Summary of experimental data.*

Tank	Length × Width × Water depth	3 m × 0.36 m × 0.4 m
Grid	Width × Height	35 cm × 35 cm
	Mesh size	4.5 cm × 4.5 cm
	Bar size (vertical and horizontal)	1 cm
	Stroke amplitude	10 cm
Tracking	Volume	14 cm × 14 cm × 16 cm
	Luminous flux	454 lm
PIV data	Field of view	14 cm × 14 cm
	Spatial resolution	1.12 mm × 1.13 mm
	Temporal resolution	0.135 s
	Interrogation window	32 × 32 pixels
	Light sheet thickness	5 mm
	Tracer particle size (diameter)	20 μm
Daphnia	size	2.9±1.0 mm
	Number of organisms	75-100
	Initial acclimatization time (light)	20 min
	Acclimatization time (at each turbulence)	20 min

within a volume 14 cm × 14 cm × 16 cm. In combination with the tracking cameras, we used two additional CCD cameras for simultaneous measurements of the three-dimensional flow velocities using stereoscopic Particle Image Velocimetry (PIV). The velocities were measured within a vertical plane located in the centre of the tank. The plane was illuminated by short laser pulses (model: Litron Nano L 200-15 PIV double pulse laser, wavelength: 532 nm, pulse duration: 4×10^{-9} s, light sheet thickness: 5 mm with Gaussian intensity distribution), and the displacement of neutrally buoyant seeding particles (20 μm diameter polyamide particles, Dantec Dynamics) was observed from two different perspectives (Fig. 3.1). Based on our former investigation (Table S1 in Wickramarathna et al. (2014)), we do not expect the swimming behaviour of daphnids to be affected by the green laser light. The PIV field of view covered 14 cm × 14 cm , and the spatial and temporal resolution of the final velocity estimates were 1.12 mm × 1.13 mm and 0.135 s respectively. The two PIV cameras captured image pairs during the exposure of the double-pulse laser, while the two tracking cameras captured images during the time window in which the laser light was off. Video B.1 (provided in the supplementary information) exemplifies a sequence of raw images illustrating passive tracer particles and a *Daphnia* swimming in turbulence. The timing of laser pulses and image acquisition of all four cameras were controlled using Dantec Dynamicstudio software (version 4.00).

3.2.2   Organisms and measurements

Test organisms, *Daphnia magna*, were cultured following standard regulatory requirements (OECD, 2004), and transferred to a separate vessel with an adequate supply of algae and a similar medium
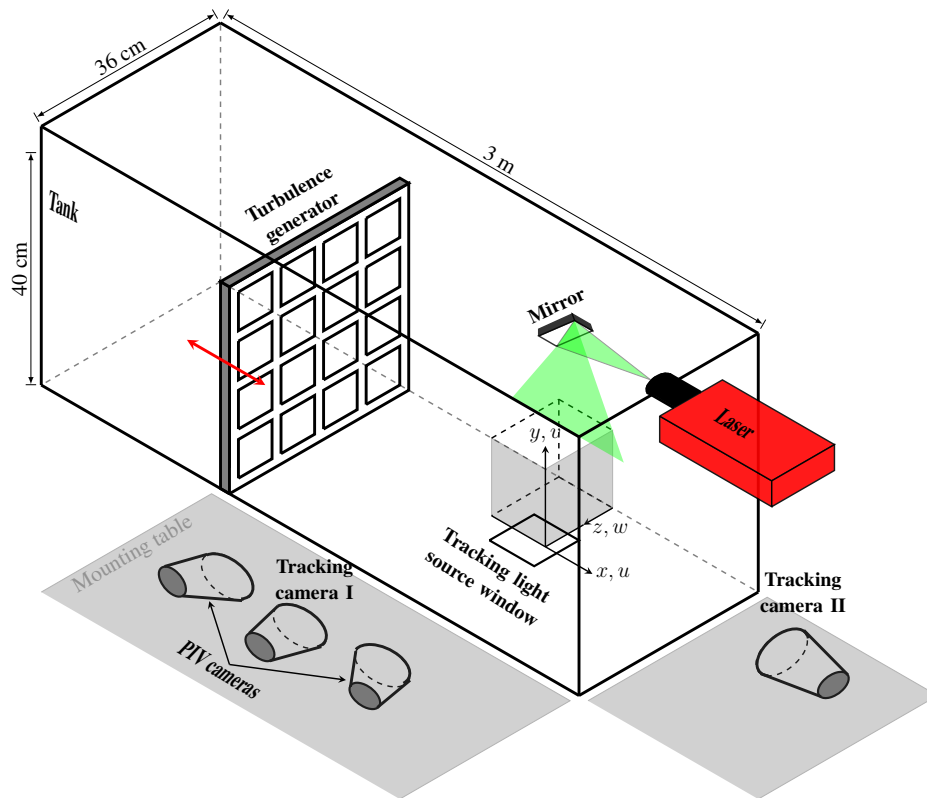
Figure 3.1: *A three-dimensional depiction of the experimental set-up (not to scale). Turbulence is generated in a tank by a longitudinally oscillating grid, and the interrogation volume is shown by the shaded volume in the middle of the tank. The grid translation is indicated by the double-sided arrow at the grid, the grid-translation mechanism is not shown.*

as in the test tank prior to measurements. For the measurements, groups of 75-100 individuals of mixed sizes (2.9±1.0 mm in length) were put into the tank and allowed to acclimatise to the light. Estimates of core body length (head to the proximal end of the caudal spine (Ranta et al., 1993)) were based-on recorded images from the tracking cameras. The relatively low organism densities were chosen for two reasons: (1) the applied tracking algorithm fails to identify organisms which overlap in any camera perspective and if individuals disappear for longer time periods (Noss et al., 2013b), and (2) we strictly intended to observe individual swimming of animals, which are not affected by neighbours in dense animal groups or swarms.

At a distance of 60 cm from the oscillating grid (measured between the centre of the grid's stroke length and the centre of camera field of view) *Daphnia* tracks and flow velocities were recorded at 7.4 Hz for at least 1.5 min at selected turbulence intensities. Turbulence was increased from TL0, in four increments, with a 20 min pause in measurements to allow for flow stabilisation and acclimation of the animals, after each increment.

3.2.3 Data analysis

Swimming trajectory and speed

Three-dimensional swimming trajectories of daphnids within the field of view of the tracking cameras were reconstructed using the algorithm described by Noss et al. (2013b), which identifies the centroids of daphnias in each image and camera perspective and determines the 3D coordinates of the organisms. Only continuous trajectory fragments of individual organisms that were observed for more than 1.3 s were considered. The detection and tracking of the organisms was not affected by the presence of the PIV tracer particles, which were only observable during laser illumination, when no tracking images were recorded. Instantaneous swimming speeds were estimated from the distance travelled within each 0.135 s along the observed trajectories. Mean swimming speeds were estimated by averaging instantaneous speeds over the entire trajectory of about 20 subsequent positions. The estimated swimming speeds represent the sum of both organism swimming velocity and advection of the organism by fluid motion. Swimming trajectory convolution was characterized from the Net to Gross Displacement Ratio (*NGDR*) (Seuront et al., 2004b), and about 5-15 trajectories for each turbulence level were analysed.

To verify that the observed *NGDR* were the result of organism swimming and not passive advection with the turbulent flow, we additionally estimated the *NGDR* of PIV seeding particles using the 2D particle tracking tool (Chenouard et al., 2014) in ImageJ. Twenty trajectories of seeding particles having a time span of 5.4 s were considered for each turbulence level. To compare the relative importance of organism swimming behaviour over background flow, the motility number was estimated for all turbulence levels. The motility number is defined as the ratio of observed swimming speed to the root mean square of the turbulent velocities, and a motility value of greater than unity suggests that behaviour dominates over turbulence (Gallager et al., 2004).

We performed a one-way analysis of variance (ANOVA) and a multiple comparison test to see if the *NGDR* is significantly different among different turbulence levels and if they differ between pairs of turbulence levels.

Vorticity and energy dissipation rate

Instantaneous current velocities (u, v, w) within the laser light sheet in x, y, and z directions (i.e. horizontal, vertical, and transversal directions respectively) were obtained from stereoscopic PIV analysis (Fig. 3.1). PIV images were processed using an adaptive correlation algorithm (Theunissen et al., 2006) available in the DynamicStudio software using 32×32 pixels interrogation windows with a 50% overlap. Outliers, which were mainly caused by the moving animals, were detected using a universal outlier detection algorithm (Westerweel and Scarano, 2005) and removed.

Velocity gradients, estimated using a two-point central difference scheme, were used to calculate the z component of vorticity (ω) (Fig. 3.1):

$$\omega = \frac{\partial v}{\partial x} - \frac{\partial u}{\partial y} \tag{3.1}$$

The turbulent fluctuations of the current velocity were obtained by subtracting the mean velocity from the measured instantaneous velocities. Dissipation rates of turbulent kinetic energy (ε) were estimated from the fluctuating components (u', v', w') in two different ways. In the first approach, the dissipation rates were calculated from the of root-mean-square (r.m.s.) velocity fluctuations ($u_{rms} = \sqrt{u'^2 + v'^2 + w'^2}$)) following Taylor (Taylor, 1935),

$$\varepsilon = D\frac{u_{rms}^3}{l} \tag{3.2}$$

Where D is a constant ($D = 1$, according to Stiansen and Sundby (2001)), and l is the integral length scale of turbulence (characteristic length scale representing the energy-containing turbulent eddies). l increases with the distance from the grid (i.e. direction x in Fig. 3.1) (Thompson and Turner, 1975):

$$l = kx \tag{3.3}$$

Where k is a constant ($k = 0.1$).

In the second approach, turbulent kinetic energy dissipation rates were directly calculated from the gradients of fluctuating velocities (Steinbuck et al., 2010):

$$\varepsilon = \nu\left[4\left\langle\left(\frac{\partial u'}{\partial x}\right)^2\right\rangle + 4\left\langle\left(\frac{\partial w'}{\partial z}\right)^2\right\rangle + 4\left\langle\left(\frac{\partial u'}{\partial x}\frac{\partial w'}{\partial z}\right)^2\right\rangle + \frac{3}{2}\left\langle\left(\frac{\partial u'}{\partial z}\right)^2\right\rangle + \frac{3}{2}\left\langle\left(\frac{\partial v'}{\partial x}\right)^2\right\rangle \right.$$
$$\left. + \frac{3}{2}\left\langle\left(\frac{\partial v'}{\partial z}\right)^2\right\rangle + \frac{3}{2}\left\langle\left(\frac{\partial w'}{\partial x}\right)^2\right\rangle + 6\left\langle\left(\frac{\partial u'}{\partial z}\frac{\partial w'}{\partial x}\right)^2\right\rangle\right] \tag{3.4}$$

With ν denotes the kinematic viscosity of water.

The Kolmogorov length scale (η_k) that represent the smallest eddies with which *Daphnia* may interact was calculated as, $\eta_k = (\nu^3/\varepsilon)^{0.25}$.

Log-averaged background energy dissipation rates (i.e. turbulence dissipation in the absence of daphnids) were estimated for each turbulence level for the entire view field of the PIV cameras and time periods of about 40 s. Maximum vorticity and log-averaged energy dissipation rates in the vicinity of the swimming *Daphnia* were estimated for areas of 5 mm × 5 mm along selected trajectories which remained within the laser light sheet. Due to high temporal fluctuations of flow signatures in turbulence flows, we only used a few number of frames for estimating dissipation rates induced by *Daphnia* (Table 3.2).

The fluid volume which contained velocity fluctuations caused by swimming *Daphnia* (i.e. trail volume) was estimated using a threshold of energy dissipation rate of 5×10^{-8} m^{2}s^{-3}. The threshold was chosen by considering the resolution and noise in our measurements at TL0. To compare trail volumes between flow conditions, the same threshold was used. It should, however, be noted that estimation of trail volume was only possible when background dissipation rate did not exceed the

selected threshold. In each PIV image with a *Daphnia* crossing the light sheet, the trail cross-sectional area was determined as the total area of dissipation rates exceeding this threshold. The trail length was estimated as the product of the *Daphnia* swimming velocity and the time period during which the dissipation rate of fluid disturbances was above the threshold. The trail volume was estimated by integrating the measured (two-dimensional) dissipation rate distributions over all three spatial dimensions (Wickramarathna et al., 2014).

3.3 Results

3.3.1 Turbulence intensities

The mean dissipation rates of turbulent kinetic energy increased with grid translation frequencies (Fig. 3.2). Instantaneous (spatially-averaged) dissipation rates varied by more than one order of magnitude at a given grid frequency. For all turbulence intensities, the gradient [equation (4)] and Taylor [equation (2)] methods for estimating dissipation rates of turbulent kinetic energy yielded mean dissipation rates which differed by up to a factor of 3.9 (Fig. 3.2). Because the Taylor method was not applicable at TL0, the dissipation results based on the gradient method are considered in the following sections unless specified. The mean values of the log-averaged dissipation rates at each turbulence level were 6.4×10^{-8} m^2s^{-3} (TL1), 2.8×10^{-7} m^2s^{-3} (TL2), 1.8×10^{-6} m^2s^{-3} (TL3), and 5.8×10^{-4} m^2s^{-3} (TL4) respectively. The mean values of log-averaged dissipation rates were significantly different among all turbulence levels ($p < 0.05$).

3.3.2 Characteristics of swimming motility

Swimming behaviour

NGDR values of the analysed trajectories varied strongly, but had comparable mean values between 0.5 and 0.6 at the different turbulence levels (Fig. 3.3). This indicates that changing flow conditions from no turbulence to high turbulence did not result in significant differences in the swimming trajectories. Estimates of two-tailed p-values among turbulence levels varied between 0.4 and 0.9 at 95% confidence intervals. There were no statistically significant differences between group means as determined by one-way ANOVA ($F_{4,36} = 0.3$, $p = 0.87$), indicating that *NGDR* did not significantly differ between turbulence levels.

The *NGDR* of the trajectories of neutrally buoyant passive tracer particles varied from 0.5 at TL0 to 0.8 at TL4 (Table 3.2). One-way ANOVA ($F_{4,100} = 29.3$, $p < 0.00001$) indicated that the *NGDR* of tracer particles did differ significantly among turbulence levels.

The mean daphnid swimming speed increased with increasing turbulence intensity and exceeded speeds observed in the absence of turbulence by 20 40% (Fig. 3.4A). The mean of the swimming velocity component in the direction of grid oscillation (i.e. longitudinal) was close to zero ($<$ 1.4 mm s^{-1}) at low and medium turbulent levels (Fig. 3.4B), indicating that the grid-generated turbulence did not create artificial bias in the swimming direction of the organisms.
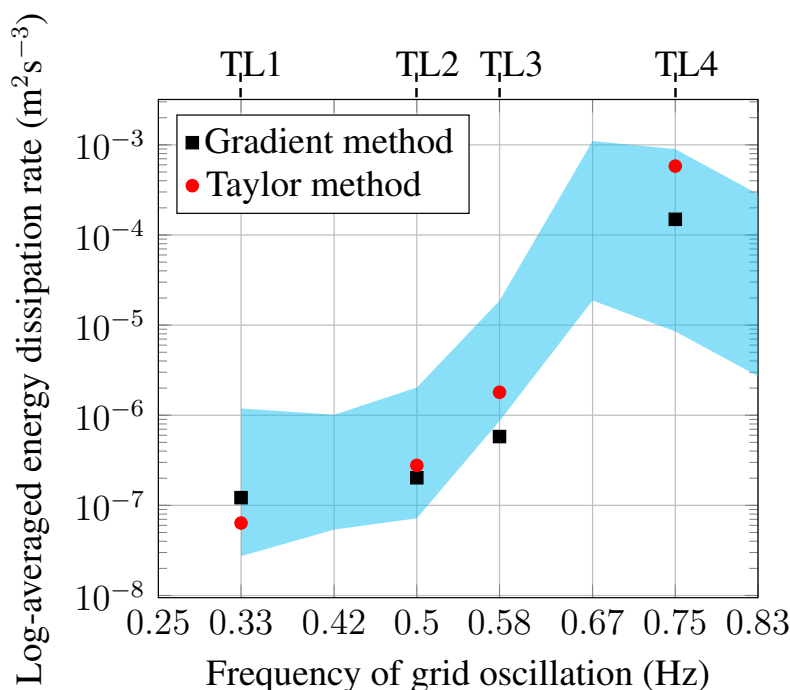
Figure 3.2: *Energy dissipation rates induced by the oscillating grid at various oscillation frequencies. Square symbols represent the mean log-averaged dissipation rates estimated using the gradient method [equation 3.4] whereas those estimates using Taylor method [equation 3.2] are indicated in filled circles. The blue shaded area shows the range of dissipation rate estimates (using the Taylor method).*

The motility number estimated for TL0, TL1, TL2, TL3, and TL4 were 36.8, 10.6, 7.2, 3.6, and 1.1 respectively suggesting a dominance of behaviour over flow.

3.3.3   Characteristics of induced flow field

Vorticity

Except at the highest level of turbulence, the magnitude of vorticity of the flow field in the vicinity of the swimming daphnids increased with increasing turbulence (Fig. 3.5). The mean values of the vorticity magnitude at TL0, TL1, TL2, TL3, and TL4 were 0.02 s^{-1}, 0.08 s^{-1}, 0.1 s^{-1}, 0.2 s^{-1}, and 3.7 s^{-1} respectively (Table 3.2). Temporally and spatially averaged vorticity estimated away from the organism within a smaller region (5cm x 5 cm) at TL0, TL1, TL2, TL3, and TL4 were 0.02 s^{-1}, 0.08 s^{-1}, 0.11 s^{-1}, 0.2 s^{-1} and 3.6 s^{-1} respectively, indicating that vorticity estimated considering the PIV field view and within a smaller region are comparable. We considered vorticity as an indicator for swimming activity because *Daphnia* typically produce a mushroom-shaped pair of vortices behind their body during active propulsion (Gries et al., 1999; Murphy, 2012). These
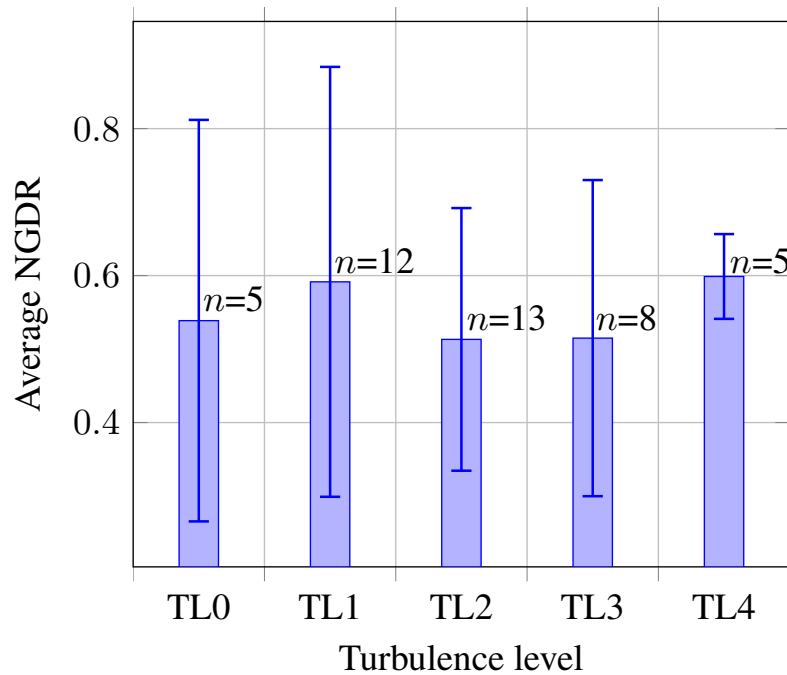
Figure 3.3: *Variation of average NGDR with turbulence level. The mean NGDR values at turbulence levels are shown by the bars, and standard deviations are depicted by the error bars. The number of observations associated with each turbulence level (n) are shown adjacent to the bars.*

counter-rotating vortices were resolved in our measurements (Fig. 3.6). Besides magnitude, also vortex size increased with turbulence (up to TL3), indicating that daphnids endeavour to respond to increasing turbulence by active propulsion, as reported by Alcaraz et al. (1994). Reduced vortex magnitude and spatial extent at TL4 (the highest turbulence level) indicates reduced swimming activity of the organisms.

The maximum vorticity found to be significantly different among turbulence levels up to TL2 ($p < 0.05$) whereas the differences of maximum vorticity beyond TL2 were not statistically significant ($p > 0.05$).

Energy dissipation rate

At all turbulence levels (TL0-TL4), dissipation rates of kinetic energy in the vicinity of *Daphnia* were consistently higher than the background turbulent flow dissipation rates (Fig. 3.7A). Video B.2 (provided in supplementary materials) shows colour maps of the background and *Daphnia* induced dissipation rates as the organism passed through the laser light sheet. The relationship between the background and *Daphnia* proximity dissipation rates, although close to linear, could be described by a power law ($\epsilon_d = 10.5\epsilon_b^{0.9}$) with a coefficient of determination of 0.94, Fig. 3.7B). To test if the difference between the dissipation rates were caused by the different scales of spatial averaging, we
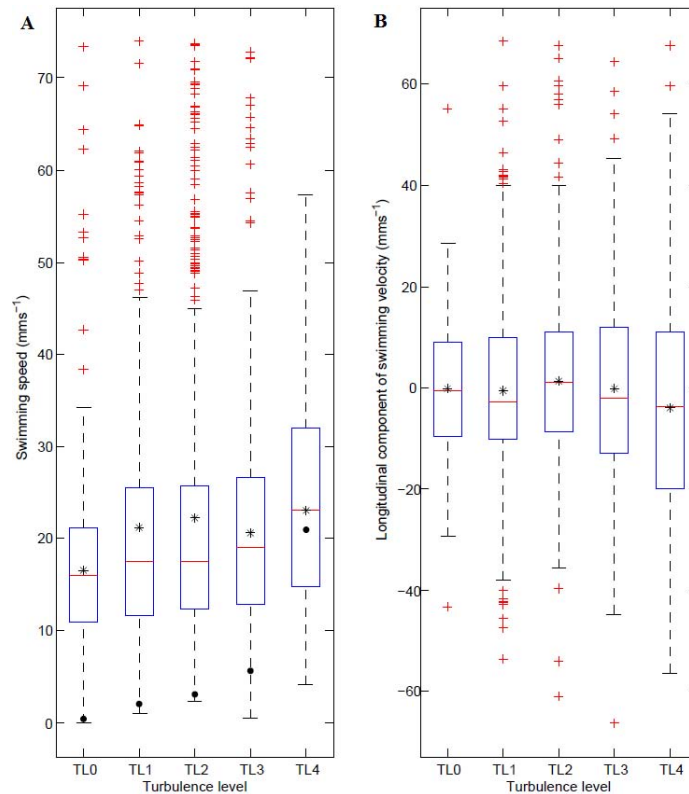
Figure 3.4: *Instantaneous swimming speed and longitudinal component of the swimming velocity. (A) boxplot of the magnitude of the swimming velocity at different turbulence levels. Black asterisks and circles represent the mean swimming speeds and turbulent velocities (u_{rms}), respectively. (B) boxplot of the longitudinal component of the swimming velocity (u in Fig. 3.1). Median values are marked by the red horizontal lines within boxes, and the boxes encompass the 25th (first quartile) & 75th (third quartile) percentiles. Black whiskers mark the highest and lowest values of the data that are within 1.5 times the inter-quartile range. Outliers (i.e. outside 1.5 times the inter-quartile range) are indicated by crosses.*

additionally estimated the dissipation rates of the background flow over a smaller volume (5 cm × 5 cm). The resulting dissipation rates were 1.1×10^{-8} m^{2}s^{-3}, 5.6×10^{-8} m^{2}s^{-3}, 2.7×10^{-7} m^{2}s^{-3}, 1.7×10^{-6} m^{2}s^{-3}, and 4.4×10^{-4} m^{2}s^{-3} for TL0, TL1, TL2, TL3, and TL4 respectively, which are closely comparable to values obtained by averaging over the entire PIV field of view (Table 3.2).

The trail volumes, in which the dissipation rates were enhanced by swimming organisms, were $3.45\ (\pm2.76)\times10^{-7}$ m^3 (for a *Daphnia* of size 3.5 mm) and $1.15\ (\pm0.48)\times10^{-7}$ m^3 (for a *Daphnia* of size 3.2 mm) at the turbulence levels of TL0 and TL1, respectively. At higher turbulence levels, the trail volumes could not be estimated because the mean background dissipation rates exceeded the threshold value (5×10^{-8} m^{2}s^{-3}) used for the trail identification.

Because the dissipation rate estimates are based on instantaneous observations of velocity gradi-
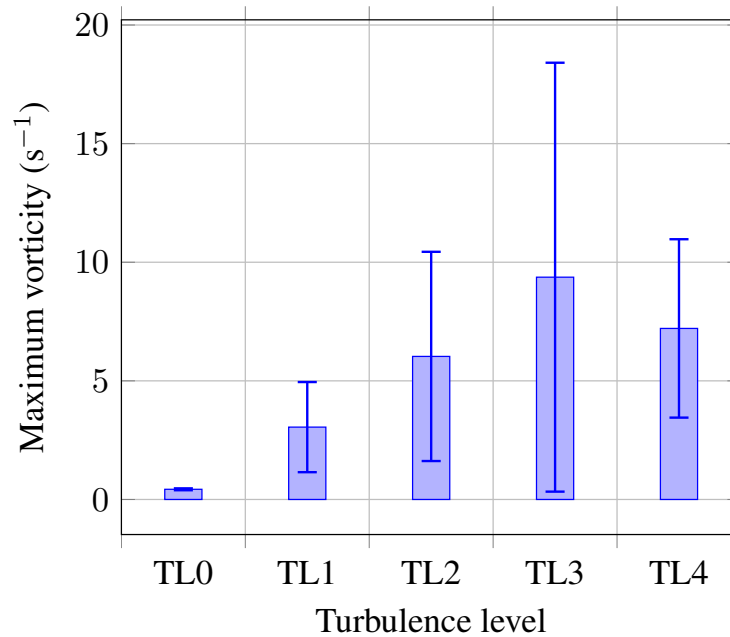
Figure 3.5: *Maximum vorticity induced by swimming animals at different turbulence levels. Standard deviations are depicted by the error bars.*

ents, they were not affected by the PIV measurement frequency. To test if the spatial resolution was sufficient to resolve energy dissipation rates at all turbulence levels, we estimated the Kolmogorov microscales. The Kolmogorov micro scale for TL1, TL2, TL3, and TL4 were 1.9 mm, 1.3 mm, 0.9 mm, and 0.2 mm respectively. The spatial resolution of our measurements is nearly an order of magnitude larger than the smallest microscale. Hence, the dissipation rate estimated for TL4 may have potentially underestimated.

3.4 Discussion

3.4.1 Turbulence and zooplankton motility

Turbulence intensities used in early laboratory experiments with plankton were typically several orders of magnitude greater than those encountered in natural habitats (Peters and Redondo, 1997; Mann and Lazier, 2006), which hindered the extrapolation of observations to natural systems (Seuront et al., 2004). However, more recent measurements particularly in coastal waters have suggested that turbulence intensities were 1-2 orders of magnitude greater than highest values previously reported (Mann and Lazier, 2006), which makes the turbulence levels used in laboratory measurements comparable to the levels found in plankton habitats. In the natural habitats of *Daphnia* (lakes or ponds (Ebert, 2005)), the major source of turbulence is wind (Wüest and Lorke, 2003), and the depth-dependent turbulence dissipation rate can be estimated from wind speed using boundary-layer
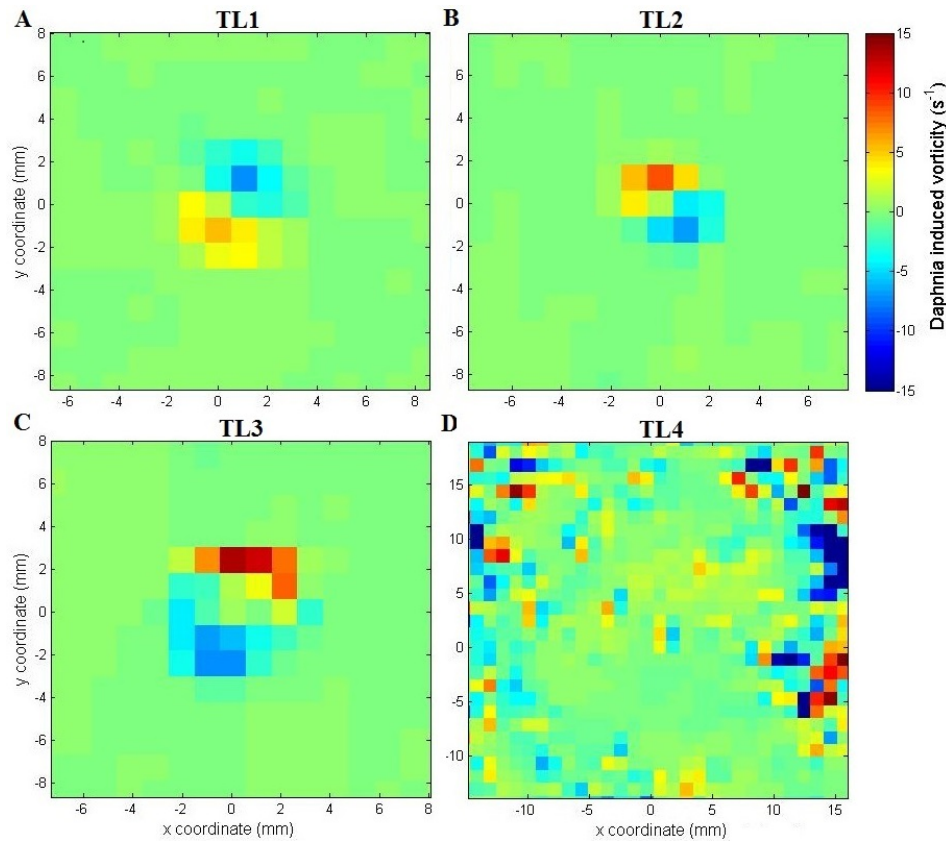
Figure 3.6: *Vorticity generated by swimming* Daphnia *at different turbulence levels. Panels A-D depict colour maps of* Daphnia *induced vorticity estimated at turbulence levels TL1-TL4, respectively. The origin of the coordinate system was located at the approximate location of* Daphnia. *It should be noted that the magnitude of the vorticity increased with increasing turbulence level (A-C) until it faded away with very high perturbations in the flow at the highest turbulence level (D). The regions of high vorticity in panels A, B, and C show pairs of counter-rotating vortices behind a* Daphnia *which passed the light sheet.*

scaling (Mackenzie et al., 1994) such that,

$$\varepsilon = \left(\frac{5.82 \times 10^{-9} u_w^3}{z}\right) \tag{3.5}$$

where u_w and z are wind speed and depth.

Assuming a mean residence depth of 2.5 m (Brosseau et al., 2012), *Daphnia* are likely to encounter dissipation rates corresponding to intermediate turbulence levels (TL1-TL3) in our experiments (Fig. 3.8). TL3 corresponds to a wind speed of up to 10 m s^{-1}, which already amounts to a storm. Other than under breaking surface waves, it is very unlikely that daphnids would encounter the high turbulence regime (TL4), which corresponds to wind speeds >40 ms^{-1}.

In contrast to the distinct swimming patterns of *Daphnia* observed in still-water experiments (Wickramarathna et al., 2014), the mean values of *NGDR* did not significantly differ between the

38
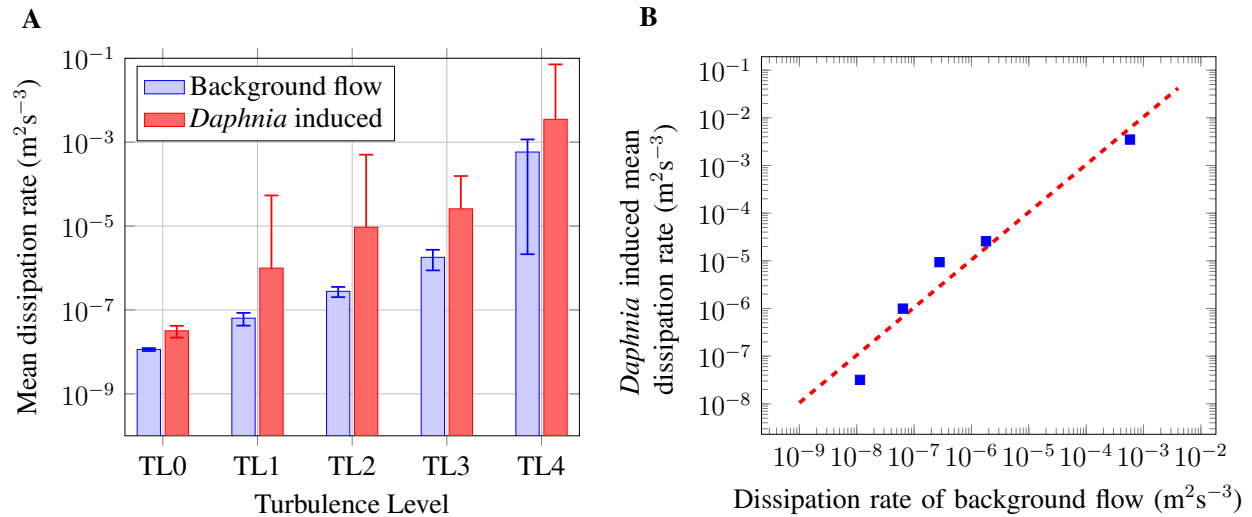
Figure 3.7: *(A) Mean dissipation rates and standard-deviations in the background turbulent flow and in the vicinity of the swimming animals at different levels of turbulence. (B) Relationship between mean turbulence dissipation rates and dissipation rate in the vicinity of the swimming organism. The dashed line shows a power-law fit ($\epsilon_d = 10.5\epsilon_b^{0.9}$).*

different turbulence treatments in the present experiments. This observation is in accordance with previous studies. Responses of three copepod species to a range of turbulence intensities (i.e. $(0.2\text{-}25)\times10^{-6}$ m^{2}s^{-3}) showed that the *NGDR* of the swimming trajectories of the copepod T. longicornis was not significantly affected by turbulence (Yen et al., 2008). In the range of turbulence produced in laboratory ($\epsilon = 0.51.4\times10^{-6}$ m^{2}s^{-3}), planktonic predators, ctenophore Mnemiopsis leidyi indicated no significantly different *NGDR* between calm water and turbulence (Sutherland et al., 2014). Also the *NGDR* of swimming trajectories of blue crabs (Callinectes sapidus) was observed to be almost unaffected by bottom roughness (Jackson et al., 2007).

The mean *NGDR* of the tracer particles were comparable to those of *Daphnia* (Table 3.2). This indicates that *NGDR* was not affected by active swimming or relatively high *NGDR* of the background flow did not permit to resolve *NGDR* of active swimming. It can also be argued that *NGDR* of *Daphnia* being significantly unaffected in significantly different flows shows a persistence swimming behaviour of *Daphnia* across turbulence levels. However, it is not appropriate to compare *NGDR* of *Daphnia* and tracer particles, which are different in size, shape, density, and inertia effects because these differences affect how they behave in turbulent flows. It should be noted that *NGDR* is scale-dependent, i.e., it differs depending on the physical or temporal scales at which it is measured (Seuront et al., 2004b). Therefore, organisms behaviour at different turbulent levels could not be unambiguously compared based on differences in *NGDR*.

The swimming speeds of *Daphnia* under turbulence were comparable to the swimming speeds observed in still water (Wickramarathna et al., 2014) and generally agree with typical zooplankton swimming speeds estimated using an empirical relationship with animal size obtained by Yamazaki

Table 3.2: *Kinematics of swimming* Daphnia, *tracer particles and energetics of flow perturbation.* u_d*: Observed swimming speed of* Daphnia*;* $NGDR_d$*: Observed NGDR of* Daphnia*;* $NGDR_{tr}$*: Observed NGDR of tracer particles;* u_{rms}*: R.M.S velocity of the flow;* ε_d*:* Daphnia *induced dissipation rate;* ε_b*: Background dissipation rate;* ω_d*:* Daphnia *induced vorticity;* ω_b*: Background vorticity. Standard deviations are shown in parenthesis. *Number of frames used in the analysis are shown in square brackets.*

Flow	Kinematics of *Daphnia* and tracer particles			Energetics of flow perturbation				
	u_d (mms^{-1})	$NGDR_d$	$NGDR_{tr}$	U$_{rms}$ (mms^{-1})	*ε_d (m^{2}s^{-3})	ε_b (m^{2}s^{-3})	ω_d (s^{-1})	ω_b (s^{-1})
TL0	16.6 ($\pm$12.2)	0.53 ($\pm$0.27)	0.51 ($\pm$0.10)	0.45 ($\pm$0.01)	3.18×10^{-8} [5] ($\pm1.0\times10^{-8}$)	1.14×108 ($\pm0.0910^{-8}$)	0.43 ($\pm$0.04)	0.02 ($\pm7.4\times10^{-4}$)
TL1	21.1 ($\pm$10.8)	0.59 ($\pm$0.29)	0.54 ($\pm$0.08)	2.0 ($\pm$0.24)	9.93×10^{-7} [5] ($\pm5.26\times10^{-5}$)	6.37×10^{-8} ($\pm2.14\times108$)	3.05 ($\pm$1.9)	0.08 ($\pm$0.02)
TL2	22.2 ($\pm$9.8)	0.51 ($\pm$0.18)	0.61 ($\pm$0.05)	3.1 ($\pm$0.28)	9.37×10^{-6} [5] ($\pm4.93\times10^{-4}$)	2.78×10^{-7} ($\pm0.76\times10^{-7}$)	6.03 ($\pm$4.4)	0.1 ($\pm$0.01)
TL3	20.6 ($\pm$12.8)	0.51 ($\pm$0.22)	0.65 ($\pm$0.07)	5.7 ($\pm$1.5)	2.57×10^{-5} [5] ($\pm1.3\times10^{-4}$)	1.80×10^{-6} ($\pm0.92\times10^{-6}$)	9.37 ($\pm$9.0)	0.2 ($\pm$0.14)
TL4	23.0 ($\pm$9.8)	0.6 ($\pm$0.06)	0.8 ($\pm$0.14)	21 ($\pm$10.7)	3.50×10^{-3} [3] ($\pm6.79\times10^{-2}$)	5.81×10^{-4} ($\pm5.79\times10^{-4}$)	7.21 ($\pm$3.8)	3.7 ($\pm$0.9)

and Squires (1996) for various organisms ranging from phytoplankton to fish.

Swimming zooplankton have been reported to be capable of overcoming water currents which are exceeding their swimming speed under certain environmental conditions. For instance, in stratified waters, estimates of swimming speeds of zooplankton showed that they can overcome small scale turbulent velocity fluctuations encountered in their natural environments by swimming at higher speed (Yamazaki and Squires, 1996) although experimental validation of this notion for freshwater zooplankton such as *Daphnia* was lacking. Seuront et al. (2004) observed that daphnia pulicaria can overcome flow velocities up to 2 orders of magnitude greater than their nominal swimming velocity while this capability of copepod T. longicornis was up to 3 orders of magnitude, and concluded that the motion of both organisms was independent of local turbulent conditions. However, their findings were not supported by simultaneous observations of organisms and flow. Genin et al. (2005) also suggested that copepods are capable of overcoming flow velocities much greater than their typical swimming speed. They tracked zooplankton at two coastal sites in the Red Sea using a three-dimensional acoustic imaging system, which showed that the animals swam against upwelling and downwelling currents moving at rates of more than ten body lengths per second to maintain their depth. These former suggestions have been recently confirmed by Michalec et al. (2015), who demonstrated that swimming contributes substantially to the dynamics of copepods even when turbulence is significant, i.e. self-induced motion of the organisms is comparable to or stronger than their typical swimming velocity.

In our experiments, the swimming speeds of *Daphnia* were much higher than r.m.s turbulent velocities typical of natural habitats (i.e. TL1-TL3), but at higher turbulence levels (TL4), the r.m.s turbulent flow velocity became comparable to mean swimming speed. The motility number
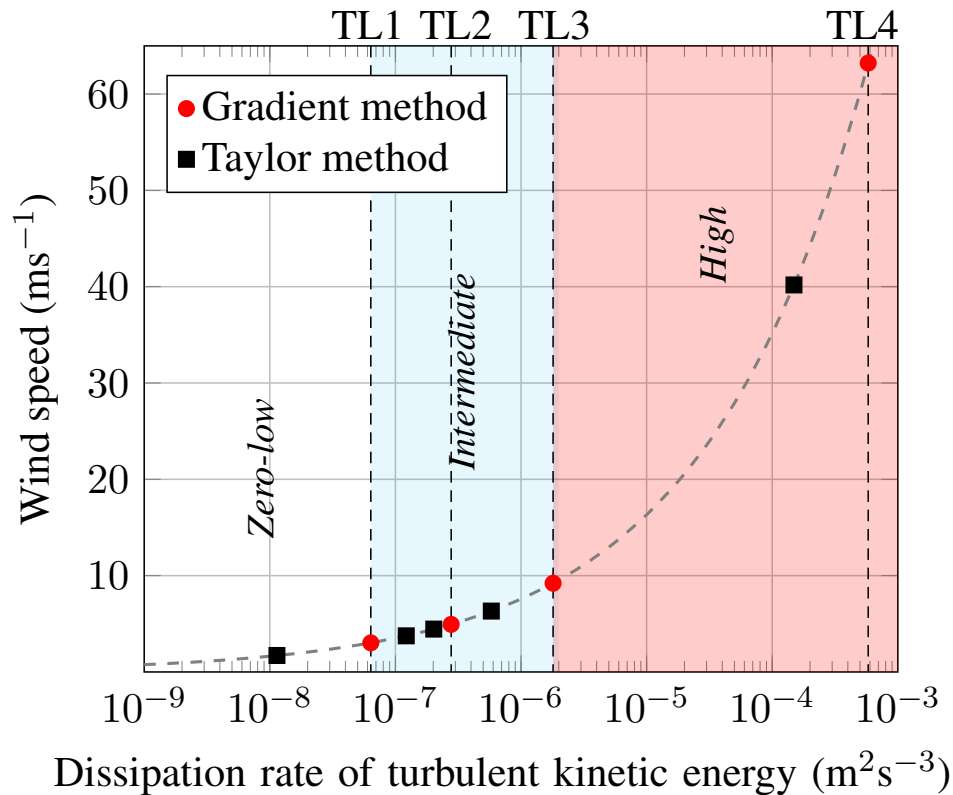
Figure 3.8: *Wind speed vs. dissipation rates of turbulent kinetic energy at 2.5 m depth. The dissipation rate estimates in our experiments based on the Taylor method and on the gradient method are shown by filled circles and square markers, respectively. The grey dashed line indicates the functional relationship [equation 3.5]. The shaded regions show intermediate turbulence levels (TL1–TL3) and high turbulence levels (TL3–TL4). It should be noted that Taylor method is not applicable at TL0.*

estimated suggests that the dominance of behaviour over flow reduces with increasing turbulence. Therefore, unlike Copepods, *Daphnia* responded to strong turbulence by reducing their swimming activity and therefore withdrew from active propulsion. The rate of energy dissipation at which this transition in behaviour occurred (about $\times 10^{-6}$ $m^2 s^{-3}$) was at least two orders of magnitude smaller than the turbulent energy dissipation rate which was required to trigger escape reactions of adult Copepods (Visser et al., 2009). This difference can be attributed to the fact that Copepods commonly live in temperate shelf seas and are, therefore, adapted to stronger turbulence (Fields and Yen, 1997).

Our methodological approach, however, did not consider a potential adaption of *Daphnia* to the successively increasing turbulence intensity in our experiments. Because *Daphnia* showed no significant differences in heartbeat rate when they were exposed to two alternate periods of calm and turbulence flow conditions (Alcaraz et al., 1994), we assume that our findings are not affected by

such short-term adaption. Respiration measurements conducted with *Daphnia* revealed that a decrease in respiration was only observed after 10-15 hours of reduced food concentration (Schmoker and Hernndez-Len, 2003). Even if their measurements were not conducted in turbulence, this implies that we are far below the time limit that *Daphnia* may start to starve, thus fatigue was unlikely a major concern within the period of our experiments.

Moreover, we do not expect that the presence of PIV seeding particles may have affected the swimming behaviour. This can be sufficiently addressed based on long-term tracking of *Daphnia* swimming in calm water without seeding particles and TiO_2 exposure (controlled group) conducted by Noss et al. (2013b). In the controlled measurements, *Daphnia* with a mean body length of 2 mm indicated a mean swimming velocity of 10.3 mm s^{-1}, and a linear relationship between the mean swimming velocity and mean body length was proposed (dv/dL=4.41 s^{-1}). Following this relationship, for a mean body length of 2.9 mm used in the present study, the mean velocity of *Daphnia* swimming in calm water would be 14.2 mm s^{-1}. The mean velocity of *Daphnia* swimming in polyamide particles seeded calm water (TL0) is 16.6 mm s^{-1}.

The overestimation of swimming speed in the presence of seeding particles (TL0) over the case without tracer particles may be attributed to differences in container size and number of individuals. Noss et al. (2013b) used chambers with a side length of 8 cm in comparison to the larger tank in the present work. A smaller container size has shown to underestimate swimming speed of *Daphnia*. *Daphnia magna* in a smaller container showed a mean speed of 6.03 mm s^{-1} in comparison to 17.99 mm s^{-1} in a large tank (Dodson et al., 1997). And, our overestimation in the present study could well be attributed to the number of individuals used (controlled group in Noss et al. (2013b) included only ten individuals).

3.4.2   Hydrodynamic trails and ecological implications

Hydrodynamic trails

The kinetic energy dissipation rates in the vicinity of swimming *Daphnia* were consistently higher than, and almost linearly related to, those of the background turbulent flow. The enhanced energy dissipation rate could be caused by kinetic energy production of the swimming daphnids, i.e. by increasing antenna beating frequencies. Although we did not measure the antenna beating frequency of animals (mainly due to lack of temporal and spatial resolution), it is unlikely that they can increase the rate of energy production by several orders of magnitude. Alternatively, the *Daphnia*-induced flow field could have caused increasing dissipation rates by disturbing the energy cascade transporting kinetic energy from larger to smaller scales. The turbulence in our experiments was mainly produced at the oscillating grid and decayed with increasing distance from it (De Silva et al., 1994). Disturbance of the energy cascade by *Daphnia*-induced small-scale velocity perturbations can be expected to lead to a stronger longitudinal decay of turbulence with increasing distance from the grid. Therefore kinetic energy dissipation rates predicted by the Taylor method [equation 3.2] would have underestimated the actual dissipation rate when *Daphnia* were present compared to the measurements in the absence of *Daphnia* and in comparison to direct dissipation estimates from small-scale current shear [equation 3.4].

A third possible explanation for increasing dissipation rates in *Daphnia* trails with increasing background turbulence is that the trails of the *Daphnia*, where the entire energy that they impart on the surrounding fluid gets dissipated, was confined to smaller volumes with increasing turbulence intensity. As a matter of fact we did not observe large trails, as in a previous still-water study (Wickramarathna et al., 2014), in the presence background turbulence. In still water, the mean trail volume varied between 5.3×10^{-7} m^3 for *Daphnia* having a length of 2 mm, and 60×10^{-7} m^3 for *Daphnia* with a length of 3.5 mm. Although we did not specifically investigate the dependency of animal size on trail volume, estimates of trail volume in calm water (TL0) and TL1 suggest a reduction of trail volume in turbulent environments. At higher turbulence levels (TL2-TL4), the fixed threshold-based approach for the estimation of trail volume could not be applied because of high dissipation rates in the background flow.

Both ambient levels of turbulent kinetic energy and swimming velocity affect how quickly swimming-induced flows dissipate and the volume at which they enhance background turbulence. Velocity perturbations induced by larvae swimming has been reported to attenuate more rapidly with the distance from the organism (r) in turbulence than in still water conditions (Gallager, 1993). Gallager (1993) also claimed that velocity magnitudes of 3 mm s^{-1} and 6 mm s^{-1} of larva swimming in turbulence attenuated from the organism distance as $1/r^{1.9}$ and $1/r^{2.9}$. This indicates that flow signatures produced by faster swimming organisms in turbulence dissipate faster than those produced by slow swimming individuals.

Ecological implications

Simultaneous observations of the local flow and organism behaviour can facilitate to understand how the environmental flow affects ecological interactions of plankton (Sutherland et al., 2011). From an ecological perspective, our findings help to better understand whether the choice of habitat of zooplankton tends to be dependent on turbulence intensity (Pringle, 2007). Under small-scale turbulence marine copepods avoided high turbulence levels by swimming towards calmer waters (Incze et al., 2001; Visser et al., 2001), however, the dispersive effect of turbulence can increase the average depth of organism distribution (Haury et al., 1990) or the vertical distribution remained unaffected irrespective of stratification (Lagadeuc et al., 1997).

It is a well-known notion that turbulence can enhance predator-prey encounter rates leading to increase the predation risk of *Daphnia*. Previous studies investigating hydrodynamic cues generated by swimming *Daphnia* in still-water (Gries et al., 1999; Wickramarathna et al., 2014) yielded estimates of trail volumes up to 500 times the size of the organisms. Because in the absence of turbulence, the diffusivities of solutes are several orders of magnitude smaller than those of fluid momentum, the footprint in terms of concentration or density fluctuations may far exceed even this value (Noss and Lorke, 2014). These large and long-lasting trails provide potential hydrodynamic or chemical cues for predators (Gries et al., 1999) and increase predation risk during active propulsion. Despite this, we demonstrate here that the large hydrodynamic trails produced by swimming *Daphnia* are offset by the ambient turbulence (e.g. TL4 in Fig. 3.6). We expect that this finding also applies to concentration fluctuations, because momentum and solute diffusivities are of equal

magnitude in turbulent flows.

Acknowledgements

The kinematics and energetics of *Daphnia* swarms

Lalith N. Wickramarathna, Christian Noss, and Andreas Lorke

Institute for Environmental Sciences, University of Koblenz-Landau, Landau, Germany.

Abstract

The interaction of physical and biological processes has been observed to trigger dense aggregations of many zooplankton species. This study quantifies the influence of animal abundance and density on the swimming kinematics and energetics of the flow field induced by *Daphnia* swarms. In a series of laboratory experiments, light-induced swarming behaviour was observed using four different animal abundances of mixed sizes. We combined three-dimensional tracking of swimming trajectories with observations of the swarm-induced flow field using particle image velocimetry. Our findings demonstrate that *Daphnia* aggregated in swarm densities of $(1.1\text{-}2.3)\times10^3$ L^{-1}, which exceeded the abundance densities in our experiments (1.7 - 6.7 L^{-1}) by two orders of magnitude. For the same swarm density range, the estimated swarm volume decreased from 52 cm^3 to 6.5 cm^3, and the mean neighbouring distance dropped from 9.9 to 6.4 body lengths. We also illustrate that mean swimming trajectories were primarily horizontal concentric circles around the light source. Mean flow speeds found to be one order of magnitude lower than the corresponding swimming speeds of *Daphnia*. Furthermore, we also show that the flow fields produced by swarming *Daphnia* differed considerably between unidirectional vortex swarming and bidirectional swimming at low and high abundances respectively.

4.1   Introduction

Animal aggregation has been observed among a great variety of mammals, birds, fishes and zoo-plankton as a mechanism to increase food exploitation, mating encounter rates, offspring rearing success, and to avoid predators (Parrish and Edelstein-Keshet, 1999). An animal swarm may be defined as a dense three-dimensional patch in which the moving organisms are not aligned in parallel to each other (Leising and Yen, 1997). Thus, swarming differs from schooling in such a way that it is non-arrayed and largely uncoordinated between individuals, yet it is far from being a set of completely random movements in which animals spread out over time and disperse as drifting particles (Banas et al., 2007).

The aggregation of zooplankton in swarms can be a passive process, which is caused by the physical characteristics of water currents such as eddies, fronts, shear layers (Okubo and Anderson, 1984; Huber et al., 2011). Active swarming behaviour is a type of swimming motion that resists dispersion without orienting or distributing animals in an organized way (Banas et al., 2007). Both passive and active swarming affect predator-prey encounter rates (Pijanowska Kowalczewski, 1997; Lorke et al., 2008), food capturing success (Davis et al., 1991), and encountering mates (Hebert et al., 1980; Gendron, 1992). Formation, maintenance, and decay of plankton swarms are governed by the interaction of physical and biological processes (Folt and Burns, 1999), and the relative significance of both is dependent on the spatial scale (Pinel-alloul, 1995), where the importance of physical processes is most pronounced at large scales.

Swarming that resists diffusion by forming a non-random yet non-uniform aggregation (Bertrand et al., 2014) can be based on either social or non-social interactions (Banas et al., 2007). In socially interactive aggregations, a swarm is formed as a result of density-dependent responses of individual organisms to their neighbours (Flierl et al., 1999; Ritz et al., 2011). For instance, copepod aggregations can be be induced by long-distance interactions along neighbours' scent trails (Weissburg et al., 1998) and along trails in the shear or pressure fields (Fields and Yen, 1997). Social aggregations of zooplankton can also be triggered as a result of attempting to improve probability of encounter (Gerritsen, 1980) so that mating among conspecific adults is enhanced (Ambler et al., 1996). Collective avoidance of their predators (Ambler, 2002), thereby aggregate in relatively safer areas (Yen et al., 1998) are some other examples of social zooplankton swarms.

Unlike the self-organizing nature of social aggregations, in non-social aggregations, zooplankton swarms are formed as a result of external cues such as light, food, or predators (Van Gool and Ringelberg, 1997; Cohen and Forward, 2009). Functional response of zooplankton to the presence of predators as a biological trigger for migration, swarming and patchiness has been extensively studied (Kvam et al., 1995; Buskey et al., 1996; Kleiven et al., 1996; Pijanowska Kowalczewski, 1997).

The phototactic behaviour of the widespread freshwater zooplankton *Daphnia* has been extensively studied and considered as a model organism for mechanistic explanations of diel vertical migration (Ringelberg, 1999). Aligned synchronization of swimming has not been detected among *Daphnia* (Okubo and Levin, 2001) as they are unable to form an image with their eyes (Buchanan

and Goldberg, 1981) and there is no known mechanism of long-range communication between *Daphnia* (Larsson and Dodson, 1993) to trigger social interactions. Numerical simulations, however, suggested that short-ranged hydrodynamic interactions, e.g., collision avoidance can induce aligned swimming directions in high-density *Daphnia* swarms (Ordemann et al., 2003; Mach and Schweitzer, 2007). These numerical studies suggest that unidirectional vortex swarming can be expected if swarm the density exceeds a critical value, which is related to the size of the hydrodynamic disturbances which are produced by the swimming organisms, as well as the perception range.

Among zooplankton species, *Daphnia* exhibit the largest total dissipated power in their trails with swimming speeds exceeding those of copepods and krill. Furthermore, the trails produced by swimming daphnids were found to be several folds bigger than the size of organisms (Wickramarathna et al., 2014). The flow field induced by swarming zooplankton has rarely been observed in existing studies, although it accounts for important physiological and ecological consequences at organism and population scale such as feeding strategies and success (Kiørboe, 2011), reception of chemical (Lombard et al., 2013) and hydro-mechanical cues (Visser, 2001) to detect prey or predators (Kiørboe et al., 2010), and being a potentially significant energy source for vertical mixing in density-stratified waters (Huntley and Zhou, 2004; Dewar et al., 2006).

Here we analyse laboratory observations of the swarming behaviour and kinematics of *Daphnia* in combination with measurements of the swarm-induced flow fields. The swarming was induced by a light beam and by performing experiments with variable organism abundance, we investigated if hydrodynamic interactions can cause an alignment of swimming directions in dense swarms. Further, we characterized the swarm-induced flow fields to detect large scale flow patterns induced by swarming *Daphnia*.

4.2 Materials and Methods

4.2.1 Experimental set-up

The test aquarium with a cross-sectional area of 30 cm×20 cm and a height of 25 cm was illuminated from above using a circular opening (4 cm in diameter) in a dimmable natural white Light Emitting Diode (LED) panel, while light intensity was adjusted (568 lm at the circular opening) so that it provided a light stimulus for organisms to aggregate as well as sufficient illumination for organism tracking (Fig. 4.1). Additionally, tracking in the absence of the light stimulus was aided by providing sufficient background light distributed around the tank. A gap of about 4 cm between the cover of the aquarium and LED-panel was maintained in order to make the light beam more concentric and to minimize convective currents that would have induced by warming up the surface water. We deployed two cameras for tracking in combination with two Particle Image Velocimetry (PIV) cameras for velocity measurements (Fig. 4.1).

Swimming trajectories of all daphnids were tracked using two orthogonally arranged Charge-Coupled Device (CCD) cameras (FlowSense4M, Dantec Dynamics, four-megapixel, 8 bit greyscale resolution) mounted on bi-telecentric lenses (TC 4M, Opto Eng.) having a focal depth of 5.6 cm.
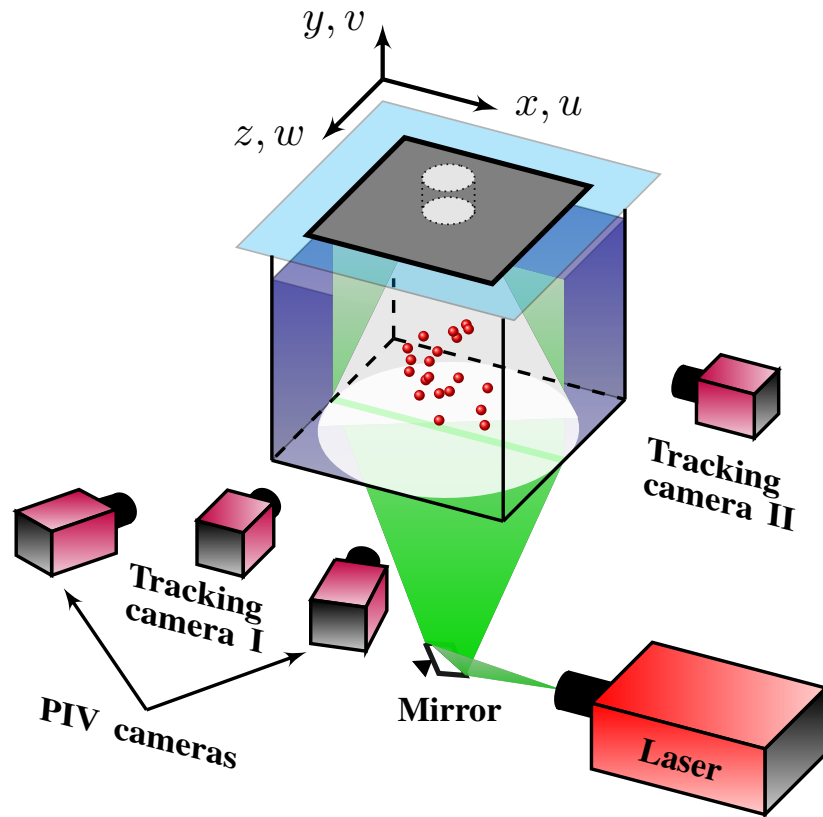
Figure 4.1: *A three-dimensional depiction of the experimental set-up. White light is emitted from a light source placed on the top of the covered aquarium (the lid shown in cyan) and is guided down through a guide (shown in dashed lines). The laser is fired from the bottom of the aquarium (shown in green).* Daphnia *are indicated by red spheres. The origin of the coordinate system lies within the laser light sheet. It should be noted that and mountings for the laser, cameras, and aquarium are not shown.*

The usage of bi-telecentric lenses provided a pixel resolution of 19.5 pixels mm^{-1}, which is independent of location within the sampling volume. The spatial resolution of each camera-lens combination was measured using a custom-made calibration target.

Three-dimensional current velocities were measured within a vertical plane located in the centre of the test aquarium using stereoscopic PIV (Adrian, 1991). The plane was illuminated by short laser pulses (Litron Nano L 200-15 PIV double pulse laser, wavelength: 532 nm, pulse duration: 4×10^{-9} s), and the displacement of seeding particles (50 μm diameter Polyamide particles, Dantec Dynamics) within the 5 mm thick laser light sheet was observed from two different perspectives (Fig. 4.1). A four-megapixel greyscale CCD-camera (FlowSense4M, Dantec Dynamics) and a two-megapixel greyscale PCO camera (HiSense 610, Dantec Dynamics) were used for the PIV measurements. The timing of laser pulses and image acquisition of all four cameras was controlled using Dantec Dynamicstudio software (version 3.20). The two stereoscopic PIV cameras captured

image pairs during the exposure of the double-pulse laser, while two tracking cameras captured images during the time window in which the laser was off.

4.2.2 Organisms and measurements

All test organisms of species *Daphnia magna* were cultured following standard regulatory requirements (OECD, 2004). Experiments were conducted with four different animal abundances of 20, 40, 60 and 80 organisms of mixed sizes (2.42 ± 0.15 mm in length). The core body lengths, i.e., the length from head to the proximal end of the caudal spine (Ranta et al., 1993) were estimated from recorded images of the tracking cameras. In each experiment, the corresponding number of fresh animals was inserted into the test aquarium. After the transfer of the organisms into the test tank, the light shaft was switched on, and tracking and velocity measurements started after providing the organisms an acclimatization time of about 20 minutes (Ekvall et al., 2013). Images from all four cameras were then recorded at 7.4 Hz for about 40 s. The experiments with the different abundance groups of 20, 40, 60, and 80 organisms are hereafter referred to as SW1, SW2, SW3, and SW4, respectively.
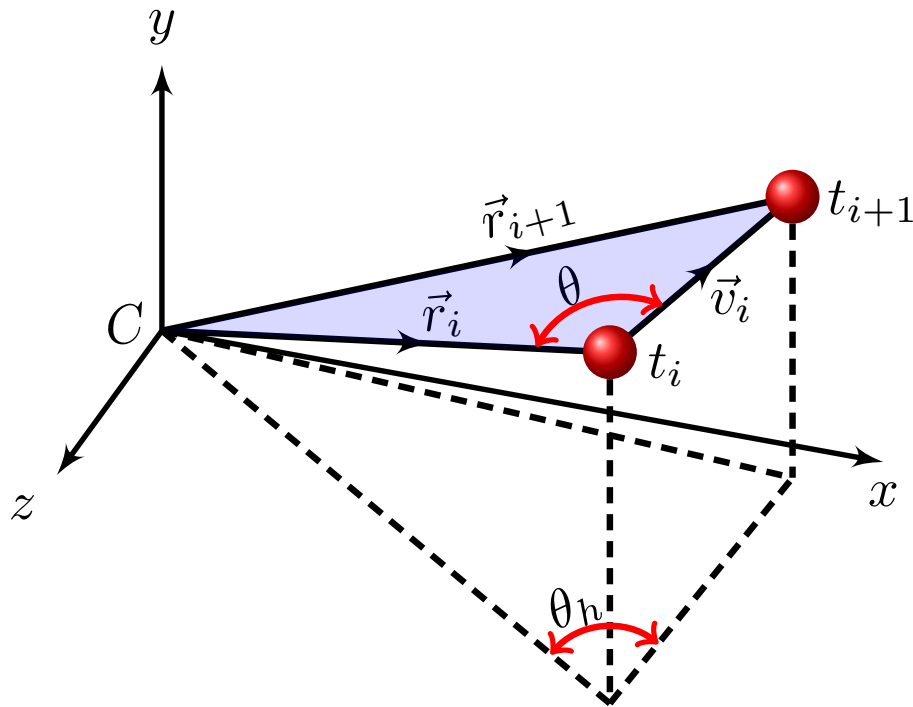
Figure 4.2: *A three-dimensional elaboration of indices used for characterizing the position of a* Daphnia *within the group.* C *is the centroid of the animal group,* $\vec{r}_i$ *and* $\vec{r}_{i+1}$ *are the radial vectors of* Daphnia *positions with respect to the centroid corresponding to subsequent observations at the time* t_i *and* t_{i+1} *respectively. The vector of the swimming velocity of the* Daphnia *and its heading angle estimated on horizontal plane are denoted by* $\vec{v}_i$ *and* θ_h *respectively.*

4.2.3   Characterization of swimming *Daphnia*

An object identification and tracking algorithm (Noss et al., 2013) was used to identify and determine three-dimensional coordinates of swimming *Daphnia* with a temporal resolution of 0.135 s. Because of frequent ambiguity in subsequent position estimates of individual organisms, swimming tracks could not be estimated continuously, but only as fragments greater than 10 times the temporal resolution.

Instantaneous neighbouring distances (*ND*) between the organisms were determined as the mean pairwise Euclidean distances between all possible permutations of identified organisms at a particular time. The mean neighbouring distance (*MND*) was obtained for each experiment by temporal averaging of all *ND*s. We estimated the probability distributions of instantaneous positions along radial and vertical directions. The radial positions were estimated in respect to the horizontal coordinates of the centroid of all organisms at a given time. The mean values of the radial and vertical positions were used as the axes lengths of a prolate spheroid approximately defining the volume occupied by the swarm. Animal density in a swarm was then calculated by dividing the number of *Daphnia* in the swarm by this volume. Swimming velocities of *Daphnia* were estimated using the distances between subsequent positions along the swimming trajectory.

We also estimated heading angle of *Daphnia* as a statistical measure of the animals' motion. The heading angle (θ on the shaded plane in Fig. 4.2), is defined as the angle between the radial vector of a *Daphnia* position at a given time ($\vec{r}_i$) and the swimming velocity vector corresponding to the subsequent positions ($\vec{v}_i$). The probability density distribution of heading angles was calculated using an optimal bin size according to Shimazaki and Shinomoto (2007). To characterize the degree of global ordering of the swarms, we estimated the polarization (Cavagna et al., 2010). For a total number animals within the group N and their instantaneous swimming velocities $\vec{r}_i$, the polarization (ϕ) is given by:

$$\phi = \left\| \frac{1}{N} \sum_{i=1}^{N} \frac{\vec{v}_i}{\|\vec{v}_i\|} \right\| \tag{4.1}$$

Where the vertical double-lines denote the norm of the velocity vector. ϕ can have values between 0 (no alignment on average or completely random swimming directions) and 1 (completely aligned or highly organized) (Tunstrom et al., 2013).

Based on an analysis of the change of swimming directions within a green laser sheet in a similar experimental set-up (Wickramarathna et al., 2014), we assume that the laser light sheet had a negligible effect on the swimming behaviour of *Daphnia*.

4.2.4   Characterization of flow field

Instantaneous current velocities (u, v, w) within the laser light sheet in x, y, and z directions (i.e. horizontal, vertical, and transversal directions respectively) were obtained from stereoscopic PIV analysis (Fig. 4.1). PIV images were processed using the adaptive correlation algorithm (Theunissen et al., 2006) available in the DynamicStudio software, and a universal outlier detection algorithm

(Westerweel and Scarano, 2005) was then applied to detect and remove outliers, which were primarily caused by moving animals. The interrogation area was 32×32 pixels with a 50% overlap, and the spatial and temporal resolution of the final velocity estimates was 3.2 mm $\times$ 3.1 mm and 0.135 s, respectively. Velocity gradients were estimated using a two-point central difference scheme over a distance equivalent to the spatial resolution.

Viscous dissipation rates of kinetic energy (ε) in the laser light sheet were estimated from measured velocity gradients by assuming isotropy in the direction of the unresolved velocity gradient (Steinbuck et al., 2010):

$$\varepsilon = \nu \left[4\left\langle \left(\frac{\partial u}{\partial x}\right)^2 \right\rangle + 4\left\langle \left(\frac{\partial v}{\partial y}\right)^2 \right\rangle + 4\left\langle \left(\frac{\partial u}{\partial x}\frac{\partial v}{\partial y}\right)^2 \right\rangle + \frac{3}{2}\left\langle \left(\frac{\partial u}{\partial y}\right)^2 \right\rangle + \frac{3}{2}\left\langle \left(\frac{\partial w}{\partial x}\right)^2 \right\rangle \right.$$

$$\left. + \frac{3}{2}\left\langle \left(\frac{\partial w}{\partial y}\right)^2 \right\rangle + \frac{3}{2}\left\langle \left(\frac{\partial v}{\partial x}\right)^2 \right\rangle + 6\left\langle \left(\frac{\partial u}{\partial y}\frac{\partial v}{\partial x}\right)^2 \right\rangle \right] \tag{4.2}$$

Where ν is the kinematic viscosity of water and the brackets denote temporal averaging over the entire observation period.
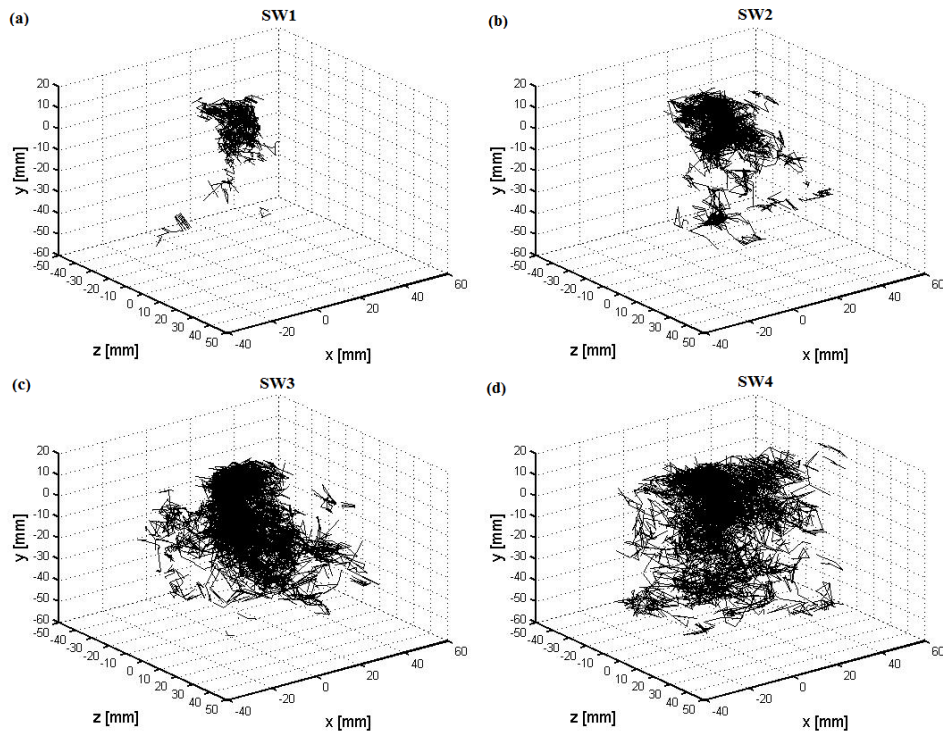
Figure 4.3: *Overview of* Daphnia *tracks (black lines) after formation of swarms. Panels* **(a)**-**(d)** *correspond to SW1-SW4, and the coordinate system in each panel is centred at the centroid coordinate of the corresponding group.*

4.3   Results

4.3.1   Swarming characteristics: position and density

For each abundance group, the trajectories of animals after formation of a swarm showed that animals were aggregated in clusters at the centre of the tank (Fig. 4.3). As the animal abundance increased from SW1 to SW4, the group of aggregated animals was found to elongate in the vertical direction. However, trajectories of animals in the absence of a light stimulus did not show such aggregations at all abundance densities (Fig. C.1).

For each swarming group, the probability density distribution of the radial positions of the daphnids was skewed towards larger radii (Fig. 4.4a). It was observed that for the groups of SW1 and SW2 most animals (75%) swam at a radial distance of 10-20 mm, however, the probability distribution was flattened out at higher abundances (SW3 and SW4) and the animals became more uniformly distributed over a wider radial distance of up to 40 mm. The organisms were distributed over increasing vertical extents as the animal abundance increased (Fig. 4.4b). At SW1, animals were mainly swimming in the upper half of the tank, and the distribution shifted towards the bottom part of the tank for SW2. At SW3, animals became homogeneously distributed in the vertical direction, while they primarily occupied the uppermost and near-bottom regions at the highest abundance (SW4).

(a)   **(b)**
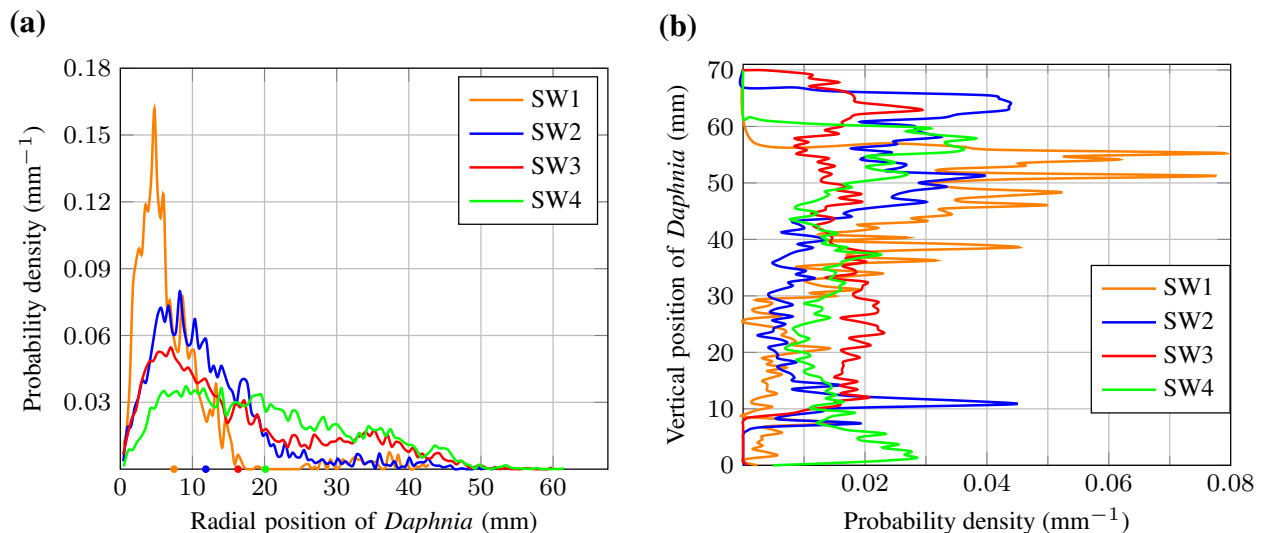
Figure 4.4: *Probability density distributions of occupying positions of swarming groups.* **(a)** *Probability distribution of positions of* Daphnia *in radial direction on the horizontal plane for SW1-SW4. The mean radial distances are indicated by circular symbols with the corresponding color on the x-axis.* **(b)** *Probability distribution of the vertical positions of* Daphnia *for SW1-SW4. The vertical position were measured positively upward from the bottom of the experimental tank.*

In contrast, the probability distribution of radial positions of *Daphnia* without a light stimulus was found to be more variable, indicating that the organisms were swimming in smaller groups. The

Table 4.1: *Statistics of horizontal and vertical swimming speeds of swarming* Daphnia. *Standard deviations are shown in parentheses.*

Group	*Daphnia* abundance density (L^{-1})	Swarm density (10^3 L^{-1})	Horizontal swimming speed (mm s^{-1})		Vertical swimming speed (mm s^{-1})	
			Mean ($\pm$SD)	Median	Mean ($\pm$SD)	Median
SW1	1.7	2.3	21.8 ($\pm$31.2)	4.8	13.9 ($\pm$25.5)	1.8
SW2	3.3	1.54	39.8 ($\pm$41.3)	23.9	21.4 ($\pm$30.0)	5.0
SW3	5.0	1.16	45.7 ($\pm$43.4)	35.4	27.8 ($\pm$34.2)	10.8
SW4	6.7	1.15	53.8 ($\pm$45.4)	47.9	27.4 ($\pm$34.1)	9.4

corresponding radii were much larger (mean radial position: 28 mm) than those of the swarming groups (Fig. C.2a). In the absence of a light stimulus *Daphnia* were mainly swimming close to the bottom of the tank (Fig. C.2a).

The swarm volumes for SW1, SW2, SW3, and SW4 were 6.5 cm^3, 19.4 cm^3, 39 cm^3, and 52 cm^3 respectively, while the organism density in the swarms was decreasing from 2296 L^{-1} to 1152 L^{-1} (Table 4.1). The observed swarm densities were more than two orders of magnitude higher than the organism density in the experimental tank, which varied between 1.7 L^{-1} for SW1 and 6.7 L^{-1} for SW4 (Table 4.1).

4.3.2   Swarming characteristics: kinematics

The probability distributions of *ND*s normalized by body length of *Daphnia* showed sharp probability peaks at SW1-SW2 and more homogeneous distributions at SW2-SW4 (Fig. 4.5a). This indicates that the organisms became more equally distributed over a wider distance. *MND* increased from 6.4 (SW1) and 7.6 (SW2) body lengths to 10.1 (SW3) and 9.9 (SW4) body lengths (Fig. 4.5b). As expected, MND increased for decreasing swarm density.

Without a light stimulus, *ND* was more variable and mainly distributed between 10 and 30 body lengths (Fig. C.2b). The corresponding *MND* of 18.2 body lengths showed that in the absence of the light stimulus the mean nearest neighbor distance was about twice as large as in the swarming experiments (mean of *MND* across all four swarming animal groups was 8.5 body lengths).

The mean horizontal swimming speeds increased with decreasing swarm density from 22 to 54 mm s^{-1} (Table 4.1). For all abundance groups, the mean vertical swimming speed was much lower in comparison to the horizontal speeds.

Under swarming conditions, the estimated heading angles showed a bi-modal distribution with pronounced maxima at $\pm 90°$ (Fig. 4.6). It should be noted that heading angle were estimated from horizontal swimming directions only, because, as pointed out above, the vertical swimming velocities were much smaller. This suggests that the direction of animal movement with respect to the centroid of the swarm is predominantly tangential. In other words, *Daphnia* swam along circular trajectories within the light beam. With the exception of SW1, the nearly symmetrical bi-modal distribution of heading angles showed that the direction of the circular trajectories was

(a)

(b)
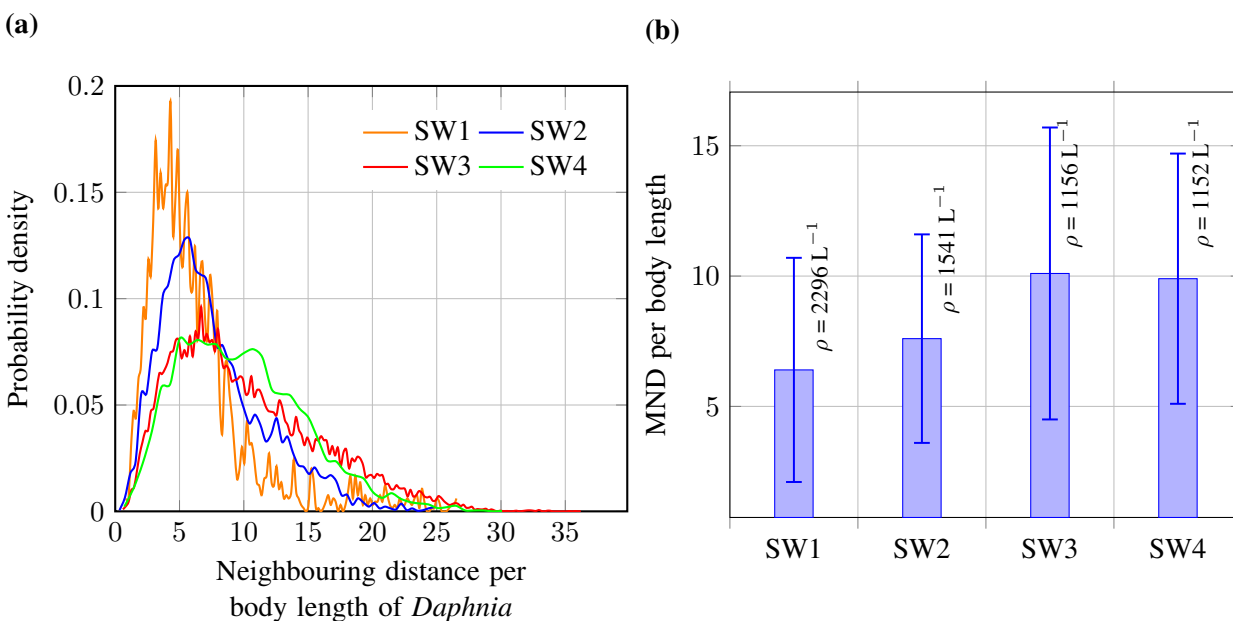
Figure 4.5: *Probability density of neighbouring distance (ND) between swarming* Daphnia. **(a)** *Probability distribution of neighbouring distance for SW1-SW4* **(b)** *Mean neighbouring distance (MND) vs. organism density. Standard deviations are shown by whiskers. Note that both ND and MND are normalized by the mean* Daphnia *body length.*

equally distributed between clockwise and anti-clockwise motions. Nevertheless, SW3 showed the highest probabilities at $\pm 90°$, which indicates that the bimodal circular movement is enhanced when the animals are aligned vertically along the light beam, rather than expanding over larger radial distances.

Unlike the other groups, probability distributions of heading angles for SW1 showed a clear contrast that animals tended to make primarily uni-directional (preferably counter-clockwise) circular movements. This may be due to the fact that the swarm density of SW1 was too high to reverse the swimming direction.

The probability distribution of heading angles of *Daphnia* in the absence of a light stimulus was broadly distributed over the entire angular range ($\pm 180°$), indicating that the animals swam in random directions.

The polarization of swimming velocities varied in a range of 0.04-0.17 in SW1-SW4, whereas in the absence of a light stimulus it was in the range of 0.12-0.33. Thus, the average polarization of *Daphnia* without a light stimulus is two-folds higher than that of swarming animals.
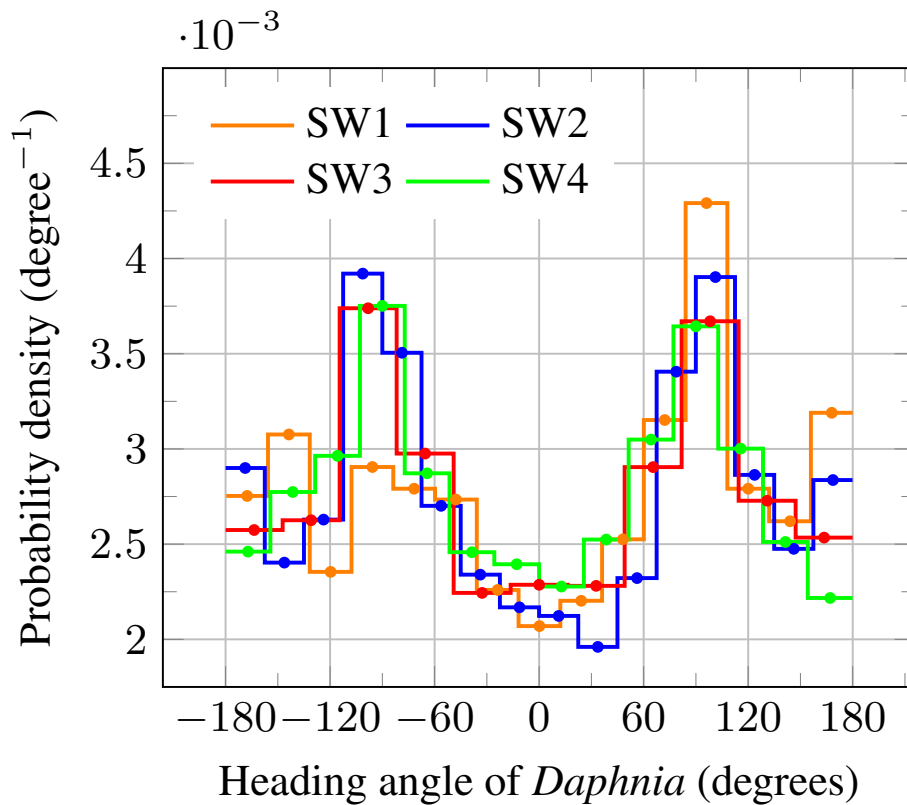
Figure 4.6: *Probability density of heading angles of swarming* Daphnia*. Centres of the bins are shown by colour markers and steps correspond to bin widths.*

4.3.3   Flow perturbation of swarming: energetics

For all swarming groups, the mean horizontal flow speeds in the tank were consistently higher than the vertical flow velocities (Table 4.2) and both were more than one order of magnitude lower than the corresponding swimming speeds of the *Daphnia*. The mean horizontal flow speeds in SW2, SW3, and SW4 were about 15-19% higher than those of SW1, while it was highest in SW3. Differences in vertical flow speeds among the four abundance groups were only marginal. The root mean square (r.m.s) flow velocity derived from all three velocity components were highest along the vertical centreline for SW2-SW4, whereas flow speeds were highest at the outer edge of the tank for SW1 (Fig. 4.7).

The spatially log-averaged rates of viscous dissipation estimated for the different abundance groups within the swarm volumes were very similar for SW2-SW4 ($\approx 1 \times 10^{-6}$ m^{2}s^{-3}), but were about a factor of two lower in SW1 (Fig. 4.8). Despite the swarm volume increased by about 62% from SW2 to SW4, viscous dissipation rates among these groups did not vary for more than about 14%. The mean dissipation rate of the background flow, i.e. without *Daphnia*, was $(3\pm4)\times10^{-8}$ m^{2}s^{-3}. Contour maps of temporal mean dissipation rates were plotted to determine the nature of the

Table 4.2: *Statistics of horizontal and vertical speeds of flow. The horizontal speed corresponds to the magnitude of the mean horizontal velocity vectors, and the speeds averaged over the entire tank. Standard deviations are shown in parentheses.*

Group	Horizontal flow speed (mm s^{-1}) Mean ($\pm$SD)	Vertical flow speed (mm s^{-1}) Mean ($\pm$SD)
SW1	1.48 ($\pm$0.60)	0.56 ($\pm$0.62)
SW2	1.74 ($\pm$0.49)	0.58 ($\pm$0.60)
SW3	1.82 ($\pm$0.48)	0.52 ($\pm$0.66)
SW4	1.77 ($\pm$0.52)	0.58 ($\pm$0.50)

flow induced by different animal groups (Fig. C.3). For SW1, it is apparent that dissipation rates at the core animal occupying region is low in comparison to the near-wall regions of the experimental tank. However, when the number of animals was increased (SW2, SW3), dissipation rates were enhanced at the core region.

4.4 Discussion

4.4.1 Abundance, swarm density, and distribution

By employing previously used experimental approaches for inducing swarming behaviour in zooplankton (Leising and Yen, 1997; Ordemann et al., 2003) we have observed the kinematics of *Daphnia* swarms for variable organism abundance. The organism densities in the experimental tank (2-7 L^{-1}) were within the range of *Daphnia* densities found in natural systems. For instance, the overall median density of *Daphnia* spp. measured over a 4-year period in a lake was 1.59 L^{-1}, while maximum abundances did not exceed 20 L^{-1} (Saunders et al., 1999). Also, in the 8-year seasonal field measurements conducted in three lakes by DeMott and Gulati (1999), the estimated mean annual density of *Daphnia* ranged from 0.7 L^{-1} to 104 L^{-1}. In general, many field surveys have reported maximum *Daphnia* densities below 50 L^{-1} (Searle et al., 2013).

Despite the relatively low organism density in relation to the size of the experimental tank, *Daphnia* aggregated in dense swarms with up to 1000-fold higher densities in the presence of a localized light cue. These densities are clearly beyond the densities observed in the field. This could be attributed to the fact that field sampling is commonly performed by net hauls, which integrate over several cubic meters of water. Also fine-scale acoustic methods average over sampling volumes which are comparable in size to the experimental tank used in our experiments, and did not reveal strongly enhanced *Daphnia* densities in lakes in comparison to net sampling (Lorke et al., 2004; Huber et al., 2011).

In contrast to observation of *Daphnia*, visually guided (diver-supported) small-scale sampling of copepods in marine waters revealed swarm densities of up to 2×10^3 L^{-1} (Udea et al., 1983) and 1.5×10^3 L^{-1} (Hamner and Carlton, 1979). The copepod swarms were observed around light cues similar to those simulated in our experiments. The light gradients were observed above patches
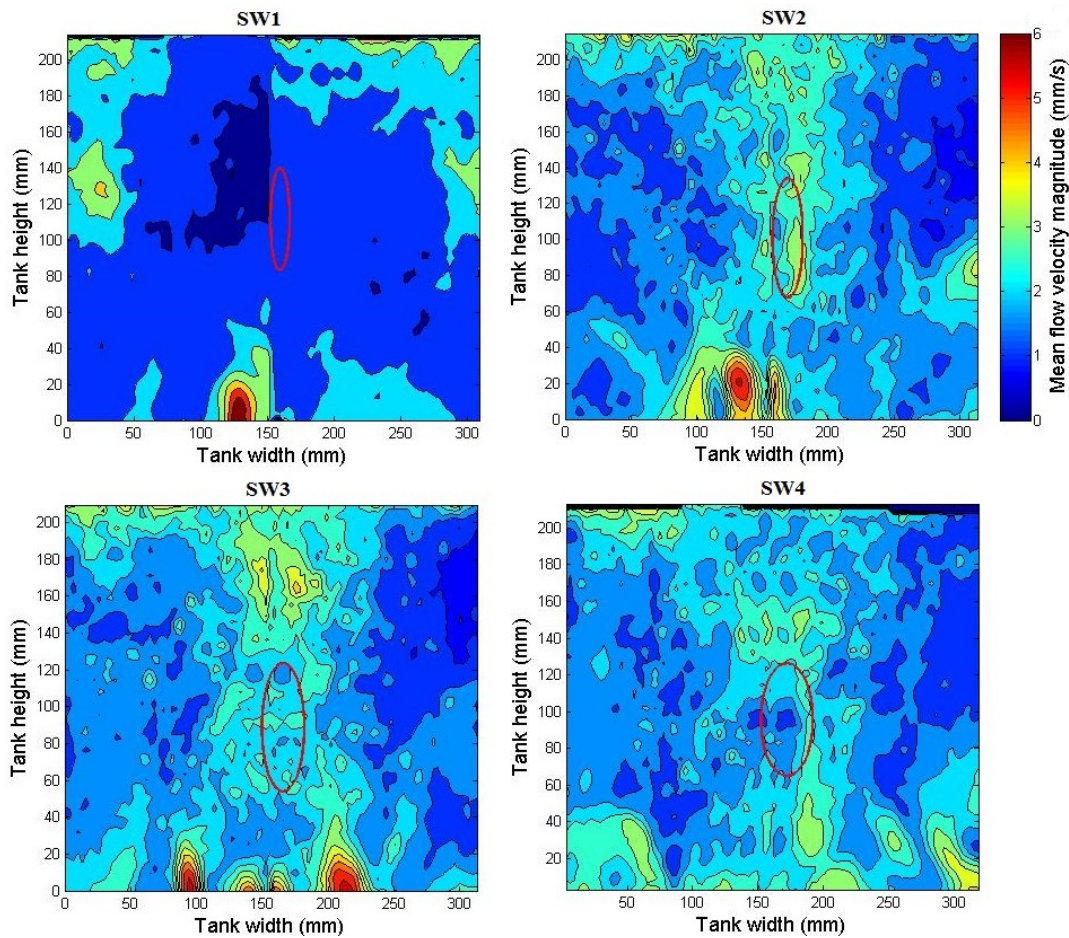
Figure 4.7: *Contour maps of r.m.s. velocities for SW1-SW4. The magnitude of flow velocities were estimated considering all three velocity components. The ellipses marked in red represent the occupying regions of* Daphnia *swarms considering the mean of radial and vertical positions corresponding to each group.*

of pale substrate that reflect more light in comparison to the surrounding substrata (Hamner and Carlton, 1979) or near red mangrove roots (Ambler et al., 1991). Therefore, despite the lack of field measurements of swarm densities in *Daphnia*, the swarm observations of similarly-sized copepod species suggest that the dense swarms observed in our experiments could also be formed under natural conditions, e.g. in the littoral zone of lakes.

The mean neighbouring distance (*MND*) in *Daphnia* swarms was 6.4-10.1 body lengths which is consistent with the values observed in copepod swarms of species Oithona oculata (Hamner and Carlton, 1979), Acartia plumosa (Udea et al., 1983), Dioithona oculata (Ambler et al., 1991), with *MND* values of 14, 9.5, and 7 body lengths respectively.
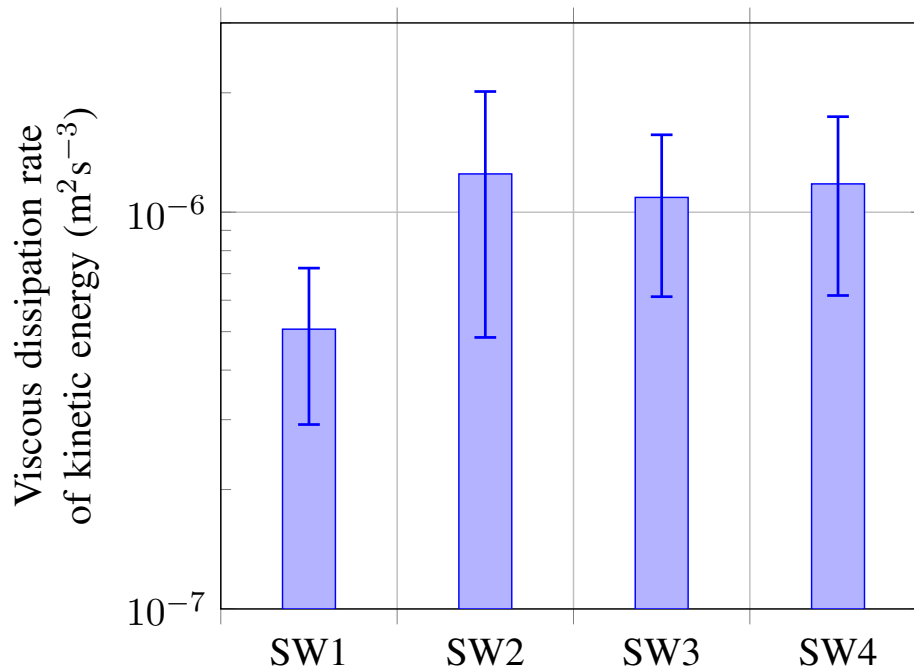
Figure 4.8: *Temporally and spatially log-averaged dissipation rates for different abundance groups (SW1-SW4).*

4.4.2   Swarming kinematics

The mean trajectories of *Daphnia* were mainly horizontal and circular. The predominant heading angles of $\pm 90°$ can be attributed to the phototactic behaviour, by which the swimming direction is controlled by light gradients (Lampert, 2011; Ringelberg, 1999). It is also noteworthy that both horizontal and vertical swimming speeds decreased for increasing swarm density. This can be explained as the swarm density is low it leaves more space for the animals to swim faster. Moreover, greater *MND*s at low swarm densities also support this argumentation.

The two peaks occurring at $\pm 90°$ suggest that the average motion is resolved into clockwise and counter clockwise directions while the probability of average rotational directions being fairly similar indicates that they occur at equal probabilities. These findings have been predicted by numerical simulations where zooplankton is described as active (self-propelled) Brownian particles without interactions (Mach and Schweitzer, 2007). The simulations further revealed that a symmetry-breaking and predominantly unidirectional circling of zooplankton around a light beam can be triggered at higher swarm densities by introducing short-range hydrodynamic interactions. This collective swimming behaviour was termed vortex-swarming (Ordemann et al., 2003; Mach and Schweitzer, 2007). The predominantly clock-wise circular swimming of *Daphnia* in the lowest abundance group (SW1) suggests, that the organisms were performing vortex swarming in this ex-

periment where the swarm density was highest. The hydrodynamic interaction can be controlled by the flow velocity in the hydrodynamic footprints of the swimming *Daphnia*, which can exceed the size of the animal by up to a factor of 500 (Wickramarathna et al., 2014).

Estimated polarization of the swimming velocities was very low in all experiments with a light stimulus. This indicates that polarization is not an appropriate measure to characterize the degree of *Daphnia* swarming or vortex swarming along circular trajectories. Polarization may be an appropriate parameter to express the extent of swarming in the cases where aligned synchronization is following more straight trajectories, having a radius of curvature which is small in comparison to the size of the swarm, such as a flock of birds or a school of fishes (Cavagna et al., 2010). In a circular swarm, the opposing swimming directions at opposite locations on the circle will ultimately lead to a low polarization.

4.4.3 Flow fields and environmental relevance

The flow fields produced by the swarming *Daphnia* differed considerably between vortex swarming (SW1) and the bidirectional swimming at higher abundances (SW2-SW4). In the latter case, the flow velocity and dissipation rates of kinetic energy were enhanced in the centre of the experimental tank, both within the swarm, as well as above and below. The irregular pattern of flow velocities in the core region indicates a strongly variable flow field, which was caused by superposition of hydrodynamic trails of the more randomly swimming *Daphnia*. During vortex swarming, in contrast, the flow velocity and energy dissipation rates were highest along the side walls of the tank, indicating that the unidirectional circular swimming generated a horizontal fluid vortex with the dimensions of the experimental tank, i.e. a large-scale flow field. It can be expected, that once it is established, the inertia of this large-scale vortex stabilises the vortex swarm against random fluctuations in the swimming direction of individual organisms.

It has been speculated, that the existence of large-scale flow field generated by synchronously swimming zooplankton can increase the contribution of small swimmers to vertical mixing in density-stratified waters (Kunze, 2011; Noss and Lorke, 2014). Because the size of the large-scale vortex was determined by the size of the experimental tank in our observations, its potential spatial extent could not be estimated. Although the actual environmental conditions which caused the vortex swarming in one of our experiments could not fully be explained, the existence of potential triggers, e.g. small-scale stationary gradients in light intensity, can only expected to be found in very shallow aquatic systems or in the littoral zone of lakes. Particularly small and shallow ponds, where wind-driven flow velocities are typically small, and where *Daphnia* can appear in high abundances (Steiner, 2004), vortex swarming can be considered to be a potentially relevant process for the resuspension of food particles from the sediment surface. The relatively easy access to such systems provide the opportunity to assess the environmental relevance of *Daphnia* swarming and vortex swarming using high-resolution optical observation techniques, similar to those applied in our laboratory observations.

Acknowledgements

Chapter 5

Major findings and concluding remarks

THIS study was set out to explore interactions of selected biophysical processes that may well affect the zooplankton ecology at smaller scales and quantify the extent of changes in swimming behaviour and fluid disturbances produced by swimming *Daphnia* in response to changing physical environments. As presented in Chapter 1, the existing literature on biophysical interactions of zooplankton within the context of flow and swimming behaviour are inconclusive. Thus, the study sought to answer the following questions:

1. Are *Daphnia* swimming in calm water capable of producing large scale flow structures and how the size and energetics of these hydrodynamic trails are affected by the organism age (size) and swimming patterns?

2. Are zooplankton, *Daphnia* in particular resilient enough to overcome turbulence or do they avoid turbulence ? Is there a threshold of turbulence intensity that they make a transition from overcoming to avoidance?

3. Do *Daphnia* swarms instigate large scale flow structures ? How abundance and swarm densities in aggregations affect their behaviour and induced flow ? Can hydrodynamic interactions cause an alignment of swimming directions in dense swarms?

5.1   Major findings and synthesis

Biophysical processes explored in this thesis included *Daphnia* swimming in calm water, *Daphnia* swimming in turbulence, and *Daphnia* swarming induced by a light source, and age or size of *Daphnia* was used as a morphological parameter only in the case of *Daphnia* swimming in calm water (Fig. 5.1). Behaviour and the induced flow, which may affect zooplankton ecology at smaller scales were characterized using kinematics and energetics indices respectively (Fig. 5.1).
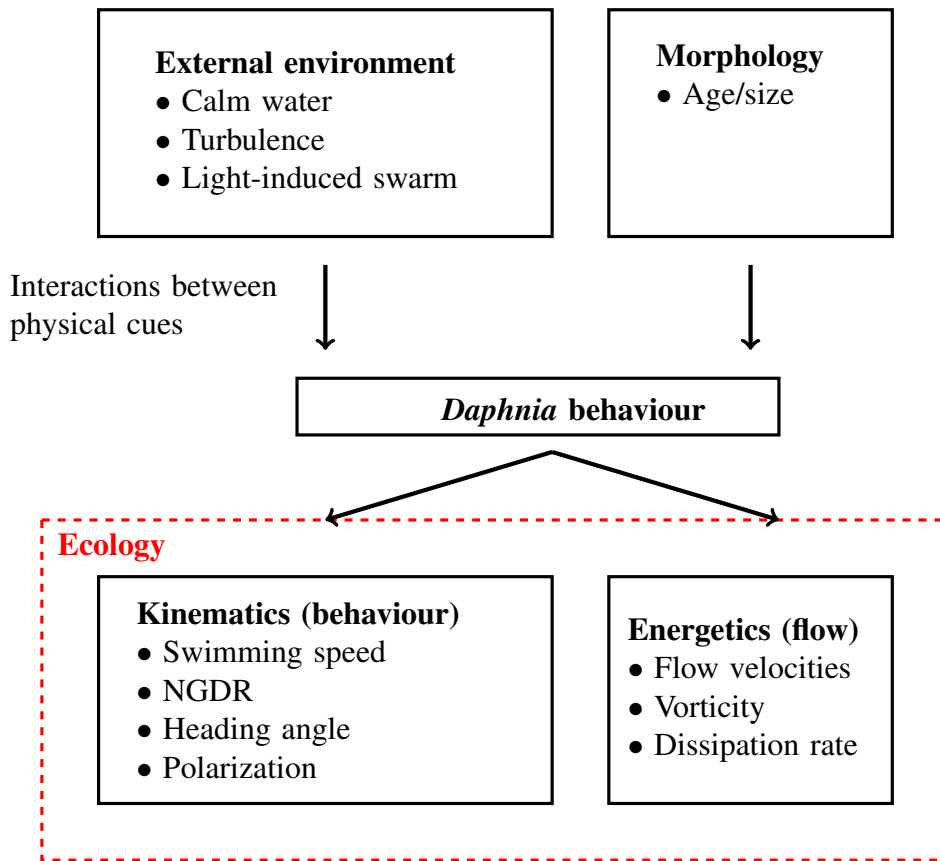
Figure 5.1: *A conceptual diagram depicting kinematic and energetic indices considered in this study to characterize behaviour and induced flow field produced by Daphnia in response to physical environment and organism age. Behavioural responses of organisms and changes in flow fields may affect zooplankton ecology as indicated by red dashed lines.*

The first goal of this work presented in Chapter 2, I investigated the swimming behaviour and flow signature produced by *Daphnia* in calm water. Induced flow signatures were characterized as a function of organisms' swimming pattern and the stage of *Daphnia* development (i.e. age). It was found that *Daphnia* size and the linearity or convolutedness of its swimming trajectory do not influence the width of induced trails or dissipation rates, however, trail volume increased with increasing size of the organisms and its swimming velocity. Trail volume was increased in proportional to the cubic power of Reynolds number, and the biggest trail volume was about 500 times the body volume of the largest daphnids. This finding bears a significant ecological consequence with regard to the risk of predation because a bigger volume means a larger volume of fluid disturbance and consequently a longer time to decay. This finding further demonstrates that the increase of trail volume yielded significantly enhanced total dissipated power at higher Reynolds number. The observed magnitudes of total dissipated power varied in the range of $(1.3\text{-}10)\times10^{-9}$ W. A comparison with other zooplankton species provided conclusive evidence that daphnids possessed the highest swimming speed and total dissipated power in their trails.

Inspired by relatively higher swimming speeds of *Daphnia* in comparison to the other zooplankton species, I explored the notion that *Daphnia* can be more resilient to turbulence. Thus, the second objective of this thesis highlighted above and presented in Chapter 3 showed that within the range of turbulent intensities to which the *Daphnia* are likely to be exposed in their natural habitats, increasing turbulence compelled the organisms to enhance their swimming activity and swimming speed. Upon further increasing of turbulence to rather unrealistically high values, they began to withdraw from active propulsion. Findings of this work further demonstrate that the threshold level of turbulence at which animals start to alleviate from largely active swimming is about 10^{-6} m^2s^{-3}. It was also shown in this study that during the intermediate range of turbulence; 10^{-7} - 10^{-6} m^2s^{-3}, kinetic energy dissipation rates in the vicinity of the organisms is consistently one order of magnitude higher than that of the background turbulent flow.

The work presented in Chapter 2 led to the conclusion that trails produced by individual *Daphnia* are several folds bigger than the organism size, which provoked the notion that *Daphnia* swarms may instigate large scale flow structures. Thus, in the third objective indicated in (3) above, I investigated behaviour and flow induced by groups of *Daphnia* swarms formed by a light source at varied abundance and swarm densities. The results showed that *Daphnia* aggregated in swarms with swarm densities of $(1.1\text{-}2.3) \times 10^3$ L^{-1}, which exceeded the abundance densities by two orders of magnitude (i.e. 1.7 - 6.7 L^{-1}). The estimated swarm volume decreased from 52 cm^3 to 6.5 cm^3, and the mean neighbouring distance dropped from 9.9 to 6.4 body lengths. The findings of this work also showed that mean swimming trajectories were primarily horizontal concentric circles around the light source. Mean flow speeds found to be one order of magnitude lower than the corresponding swimming speeds of *Daphnia*. Furthermore, this study provided evidences that the flow fields produced by swarming *Daphnia* differed considerably between unidirectional vortex swarming and bidirectional swimming at low and high abundances respectively.

The flow signatures observed in turbulent flows were much smaller than those observed in still water, because flow signatures produced by *Daphnia* in turbulent flows are offset by high temporal fluctuations of the flow. Thus, the enhanced risk of predation as concluded in Chapter 2 is somewhat negated in turbulent flows making life easier in their natural habitats. In addition, large trail volumes estimated in still water experiments also implied development of large scale flows in *Daphnia* swarms, and a combination of high abundance in swarms and large trail volumes of individual animals as indicated in still water experiments may have thought to provide an easy access for the predators. However, super-positioning of *Daphnia* trails at lower swarm densities did not permit producing large scale flows, which might again reduce the risk of predation. Moreover, in contrast to the enhanced encounter rates with predators suggested in turbulent flows, *Daphnia* aggregations formed at the appropriate density can increase their foraging success by means of vortex swarming. Also, individual observations of *Daphnia* in turbulent flows indicated that they withdrew from active swimming at high turbulence intensities, which would influence their choice of habitat. However, swimming in search of lower turbulent zones (thereby keeping their fitness) would generally lead to compromise their ingestion. Therefore, in these situations, the loss of ingestion can be restored by aggregating at the right swarm density because vortex swarming leads to transport suspended food particles to upper layers of a water column. This could be the case in small ponds with high *Daphnia*

abundance, where small-scale turbulence is avoided to keep their fitness level yet enhancing their foraging by forming swarms.

Findings of this work observed at organism scale can be expected to affect processes at population scale. Large trail volumes or fluid perturbation induced by swimming zooplankton at smaller scale may play a vital role in particle fragmentation (Steinberg et al., 1997). Specially marine zooplaton have been reported to fragment snow particles to finer size, which reduces the sinking rate. This could affect biological pump as finer particles retaining on surface enhances re-mineralization. Also, aggregation of organisms may increase zooplankton growth and enhanced survival (Woodson et al., 2012). Increased encounter rates caused by turbulence and vortex swarming observed among aggregated organisms could enhance vertical flux of particulate material as it was observed by Kiørboe (1997). Therefore, zooplankton response to physical cues at smaller scales may have important ramifications from particle fragmentation, growth and enhanced survival to enhanced vertical flux of particulate matter.

5.2 Significance and implications

Planktonic organisms had been suggested to affect fluid motion on much larger scales than the organisms themselves (Prairie et al., 2012). Wakes of these organisms may produce kinetic energy comparable to environmental sources (Huntley and Zhou, 2004), however, this was challenged by (Visser, 2007) that it occurs at small length scales and generated energy is dissipated as heat. However, analysis of individual *Daphnia* in this study revealed that *Daphnia* trails can be as bigger as 500 times the size of the organism and the trail volume was proportional to the third power of Reynolds number. This is consistent with some of previous observations. A significant contribution to energy production (Dewar et al., 2006) and fluid mixing (Katija and Dabiri, 2009) was predicted by biophysical modelling while these findings are based on the assumption that hydrodynamic footprints produced is comparable to the organism size which is true for low Reynolds number. Huntley and Zhou (2004) used the turbulent drag law in their estimations of flow disturbance, and the approach holds true for high Reynolds number. Given the fact that the swimming of zooplankton occurs at intermediate range of Reynolds number ($1 < \text{Re} < 100$) which makes both of the above argumentations questionable. Therefore, this study has not only shed the light on these inconclusive former findings concerning the volume of fluid disturbance caused by biophysical interactions of zooplankton within the context of flow and swimming behaviour but also they provide a justification for the *Daphnia* swimming in their natural habitats. Furthermore, the findings suggested that the dissipation rates were enhanced over a spatial extent of 10 times larger than the organism, which leads to enhance small-scale gradients of dissolved substances. Given the quadratic dependence of eddy diffusivity on fluid disturbances (Kunze, 2011), rates of diffusivity and scalar mixing would increase by 100-folds if the fluid disturbance is considered instead of the organism size (Visser, 2007). The size of the daphnids trail estimated in terms of dissipation rates of concentration variance found to vary between $1\text{-}13\times10^{-5}$ m^2s^{-3} (Noss and Lorke, 2014), which is about 100 times bigger than the estimates of this study and consequently justifies the results.

As it was previously reported that presence of turbulence may have far reaching ecological

consequences from the choice of habitats (Pringle, 2007) to increased encounter rates (Rothschild and Osborn, 1988). Findings of this study may help to fathom the significance of turbulence and its intensity on the choice of habitat. The findings that *Daphnia* could withstand turbulence intensity up to 10^{-6} m^{2}s^{-3} demonstrates that they are equally resilient as some of other zooplankton such as copepods. Marine copepods exposed to a small-scale range of turbulence showed that they avoided high turbulence regions by swimming towards calmer waters (Incze et al., 2001; Visser et al., 2001). The dispersive effect of turbulence can increase the average depth of organism distribution (Haury et al., 1990). Turbulence did not affect vertical distribution of zooplankton no matter the water column was stratified or not (Lagadeuc et al., 1997).

As it was shown in still-water experiments, the fluid volume affected or hydrodynamic traces produced by swimming *Daphnia* could be as bigger as 500 times the organism size. As the diffusivities of fluid momentum are several orders of magnitude higher than those of solutes, traces of concentration fluctuations can be even bigger providing chemical cues for predators or enhancing the risk of predation. As this study shows when the turbulence intensity is high enough background flow tends to smear the hydrodynamic traces produced by swimming *Daphnia*. As momentum and solute diffusivities are of equal magnitudes in turbulence flow, smearing of concentration fluctuations can also be expected. Though it is widely accepted notion that turbulence enhances predator-prey encounter rates leading to increase the predation risk of *Daphnia*, this study reveals that *Daphnia* swimming in highly turbulent flows may work in their favour by reducing the risk of predation. Reduced risk of predation in turbulent flow is also supported by other studies (Mackenzie et al., 1994; Prairie et al., 2012), however, the underlined mechanisms are different.

In the case of light-induced *Daphnia* swarms, animal trajectories were primarily concentric circles with similar probabilities for both clock-wise and counter clock-wise directions. This is in agreement with the results predicted by numerical simulations considering zooplankton as self-propelling particles without interactions (Mach and Schweitzer, 2007). The simulations have also predicted a shift from bidirectional to unidirectional at higher swarm densities, which is known as vortex-swarming (Ordemann et al., 2003; Mach and Schweitzer, 2007). This is also consistent with the present study as a predominantly clockwise circling of organisms at the highest swarm density, and the flow velocity and energy dissipation rates being the highest along the side walls of the tank suggesting a horizontal vortex having a spatial extent equalling to the tank dimensions. However, it should be noted that the spatial extent is dependent on the tank size, therefore, the actual spatial extent could not be determined. The large-scale vortex-swarming also affirms a previously suggested notion that the contribution of zooplankton to vertical mixing in stratified waters can enhance by large-scale flow produced by organized swimming (Kunze, 2011; Noss and Lorke, 2014).

Vortex-swarming can be expected in environmental conditions such as in shallow ponds or in the littoral zone of lakes where small-scale stationary gradients in light intensity can be present and the wind-driven flow velocities are small. These are typically the aquatic environments that high abundances of *Daphnia* can be found (Steiner, 2004). One of direct implications of vortex-swarming in the case of shallow waters is that it will enhance the disturbance of nutrient particles located on the bottom and subsequently transport them towards the surface. Furthermore, vortex-swarming

could potentially homogenize a sharp density gradient.

5.3 Recommendation for future research and limitations

This Ph.D. thesis is an attempt to elucidate kinematics and energetics of freshwater zooplankton, *Daphnia* swimming in calm and non-stratified waters, and how they respond to changing physical and environmental conditions individually and as aggregated groups. While the work has contributed to better understand the interaction between biological and physical processes of *Daphnia* swimming in different environments, there are several inevitable constraints of this work, which should be covered by future research addressing similar context.

The most of these are related to experimental limitations. For instance, the calm water experiments presented in Chapter 2, should consider stratification in future work. Because, freshwater lakes in which *Daphnia* abundance is high are supposed to be stratified (Boehrer and Schultze, 2008; Stocker, 2012). The fluid displacement and induced trail volume have been suggested to depend on the strength of density stratification (Noss and Lorke, 2014). However, the influence of density-stratified waters on swimming behaviour and induced flow has so far led to contradictory results. (Gries et al., 1999) observed a negligible influence of density-stratified waters whereas (Ardekani and Stocker, 2010) indicated an influence of stratification on the flow fields generated by swimming *Daphnia*.

In experiments of *Daphnia* swimming in turbulent flows discussed in Chapter 2, a relatively low number of animals used in a large experimental tank. Because, using a very high number of animals would lead to fail the tracking algorithm with overlapping organisms in camera perspectives. Furthermore, having the tracking light source right below the investigated volume would trigger a *Daphnia* swarm (based on the work presented in Chapter 4, *Daphnia* aggregate as a swarm to a light source). Thus, using a large number of organisms would lead to investigate more of a swarm in turbulence, however, this work strictly intended to observe swimming of individual animals. Although it is a challenging task to capture a high number of trajectories of swimming animals in a laboratory induced turbulence without interfering with organisms' behaviour, the work presented in Chapter 3 may benefit from including more organism trajectories.

There exists a strong inter-individual variability in the behaviour of zooplankton. For instance, it has been reported that copepods swarms would need to maintain a mean neighbouring distance (ND) of about 10-15 body lengths (Hamner and Carlton, 1979; Udea et al., 1983). Putting a very high number of animals in a confined enclosure would compromise individuals' nearest neighbouring distance of freely swimming. In a recent work conducted to investigated copepods behaviour in turbulence (Michalec et al., 2015), hundreds of animals were inserted to a tank with a maximum side of 27 cm, which would artificially affect their behaviour (i.e compromising their NDs of freely swimming). Furthermore, considering the mean neighbouring distance of copepods swarms mentioned above, the set-up described in Michalec et al. (2015) presents merely the spatial extent that copepods may utilize to form a swarm. In swarm experiments described in Chapter 4 (30 cm x 25 cm: approximately the same width of our large tank in turbulence experiments), a mean neigh-

bouring distance of about 10 body lengths for an abundance size of 80 organisms was observed. Therefore, inserting a higher number of *Daphnia* would compromise the inter-individual spatial extent required to swim freely in turbulence. Also, high temporal variability in turbulent flows, specially at the highest turbulence level in this work, would require high resolution cameras to capture small-scale changes in flow signature. At least an order of magnitude higher resolution of PIV cameras would provide much closer insight of the flow signature induced by organisms swimming in high turbulent flows.

Swarm experiments presented in Chapter 4, the swarm formation was induced by a light source, however, other cues such as odour of predators may also be an interesting investigation in future research. Similar laboratory experiments could be conducted not only to determine effects of changing swarm cues but also the implications of changing swarm demographics such as species, age, size, and density. Thus, combined effects of swarm triggering cues and demographics on swarm geometry (e.g. size, density, distribution), on swimming behaviour (e.g. orientation, velocity, acceleration) as well as on swarm induced flow field, underline the breadth of possible directions that could be further investigated. Notwithstandingly, it is also significant to verify findings of laboratory experiments by performing in situ measurements in natural environments. Recent technological developments have provided an increased analytical power allowing to investigate aggregations at high temporal and spatial resolutions particularly in situ. In addition to video and motion analysis used in this work, optical plankton counters, acoustic and electronic tagging are some of other technological advancements (Ritz et al., 2011). Each of these technologies has advantageous over the other, for instance, holographic imaging systems can resolve small particles like zooplankton over a larger sample volume. Planar imaging system at a given wavelength can resolve an object of 20micro meters over a depth of field 0.6 mm whereas a holographic system may resolve the same object with a depth of field 100 times larger (Malkiel et al., 1999). Also, global warming has been suggested to form zooplankton aggregations at smaller spatial scales (Ritz, 2000). Rise in temperature significantly reduces the water viscosity, thus, an increase by 5°C would decrease the viscosity of seawater by 15% (Ritz et al., 2011). Therefore, how swarm size, behaviour or flow of freshwater zooplankton such as *Daphnia* are affected by temperature could be a timely investigation. Changes of kinematic and energetics in zooplankton aggregations may have large scale consequences for larger organisms in the ecosystem.

As it was shown throughout this thesis that at millimetre scales *Daphnia* behaviour and flow are shaped by their physical environment from high turbulence reducing the risk of predation to concentric circling of organisms in swarms. The biophysical interactions taking place at one scale may affect processes at another scale. For instance, smaller-scale interactions between a light source and *Daphnia* may affect *Daphnia* distributions in the community or global carbon cycling whereas large-scale changes in temperature driven by global climate change mediate background conditions for processes at smaller-scales. Hence, while this study has drawn some significant advancement and insights concerning biophysical interactions of *Daphnia* at smaller scales and their significance to aquatic environments, future research should also orient on cross-scale research that may provide a more complete understanding of plankton ecology.

5.4 Conclusion

This work identifies relationships between environmental conditions and *Daphnia* responses in terms of resultant *Daphnia* behaviour and flow. The outcome of this study may be of great interest and relevance to biophysical modellers who may seek to parametrize biological and physical interactions of zooplankton using biophysical models. In many of these models, zooplankton have been treated as drifting passive particles without taking into account actual propulsion of their swimming. For instance, this work may be used to parametrize swimming patterns, volume of flow disturbance in calm waters, concentric trajectories in collective swimming, insignificant nature of changes in swimming trajectories in response to turbulence over a broader range. The experimental approach used in this study involved with simultaneous observations of the local flow and organism behaviour using particle image velocimetry in conjunction with particle tracking. This method has very recently gathered some interest in quantifying inertial particle motion in turbulence as well as swimming induced currents in zooplankton. This work however marks one of the first few studies which applied this approach to freshwater zooplankton, *Daphnia*, and exemplifies the breadth of scientific questions that can be investigated by means of such an approach.

Bibliography

Adhikari, D., Gemmell, B., Hallberg, M., Longmire, E., and Buskey, E. (2015). Simultaneous measurement of 3D zooplankton trajectories and surrounding fluid velocity field in complex flows. J. Exp. Biol. 218 (22), 3534-3540.

Adrian, R. J., (1991). Particle-imaging techniques for experimental fluid mechanics. Annual Review of Fluid Mechanics. 23, 261-304.

Alcaraz, M., Saiz, E., Marrasé, C., and Vaque, D. (1988). Effects of turbulence on the development of phytoplankton biomass and copepod populations in marine microcosms. Mar. Ecol. Prog. Ser. 49, 117-125.

Alcaraz, M., Sai, E., and Calbet, A. (1994). Small-scale turbulence and zooplankton metabolism: Effects of turbulence on heartbeat rates of planktonic crustaceans. Limnol. Oceanogr. 39(6), 1465-1470.

Ambler, J. W., Ferran, F. D. and Fornshell, J. A. (1991). Population structure and swarm formation of the cyclopoid copepod Dlolthona oculata near mangrove cays. J. Plankton Res. 13, 1257-1272.

Ambler, J. W., Broadwater, S. A., Buskey, E. J. and Peterson, J. O. (1996). Mating behaviour in swarms of Dioithona oculata. In Lenz, P. H., D. K. Hartline, J. E. Purcell and D. L. Macmillan (eds), Zooplankton: Sensory Ecology and Physiology. Gordon and Breach Science Publishers, Amsterdam: 287-299.

Ambler, J. W. (2002). Zooplankton swarms: characteristics, proximal cues and proposed advantages. Hydrobiologia. 480, 155–164.

Arana, D. C. P., Moore, P. A., Feinberg, B. A., DeWall, J., and Strickler, J. R. (2007). Studying Daphnia feeding behavior as a black box: a novel electrochemical approach. Hydrobiologia. 594, 153–163.

Ardekani, A. M., and Stocker, R. (2010). Stratlets: Low Reynolds number point-force solutions in a stratified fluid. Phys. Rev. Lett. 105, 084502.

Baker, M. A., Gibson, C. H. (1987). Sampling turbulence in the stratified ocean: statistical consequences of strong intermittency. J Phys Oceanogr. 17, 1817–1836.

Banas, N. S., Wang, D. P. and Yen, J. (2007). Experimental validation of an individual-based model for zooplankton swarming. In Seuront, L. and P. G. Strutton (eds), Handbook of Scaling Methods in Aquatic Ecology: Measurement, Analysis, Simulation. CRC Press: 171-178.

Bergstedt, M. S., Hondzo, M., and Cotner, J. B. (2004). Effects of small scale fluid motion on bacterial growth and respiration. Freshwater Biol. 49, 28–40.

Bertrand, A., Grados, D., Colas, F., Bertrand, S., Capet, X., Chaigneau, A., Vargas, G., Mousseigne, A. and Fablet, R. (2014). Broad impacts of fine-scale dynamics on seascape structure from zooplankton to seabirds. Nature Communications. 5, 5239.

Boehrer, B. and Schultze, M. (2008). Stratification of lakes. Rev. Geophys, 46(RG2005).

Borazjani, I., Sotiropoulos, F., Malkiel, E., and Katz, J. (2010). On the role of copepod antennae in the production of hydrodynamic force during hopping. J. Exp. Biol. 213, 3019–3035.

Brooks, J. L. (1947). Turbulence as an environmental determinant of relative growth in daphnia. Proc. Natl. Acad. Sci. USA. 33, 141-148.

Brosseau, C. J., Cline, T. J., Cole, J. J., Hodgson, J. R., Pace, M. L. and Weidel, B. C. (2012). Do Daphnia use metalimnetic organic matter in a north temperate lake? An analysis of vertical migration. Inland Waters. 2, 193-198.

Buchanan, C. and Goldberg, B. (1981). The action spectrum of Daphnia magna (Crustacea) phototaxis in a simulated natural environment. Journal of Photochemistry and Photobiology 34, 711–717.

Buskey, E. J., Peterson, J. O. and Ambler, J. W. (1996). The swarming behaviour of the copepod Dioithona oculata: In situ and laboratory studies. Limnology and Oceanography 41, 513-521.

Carrasco, N. K., Perissinotto, R. and Jerling, H. L. (2013). Zooplankton, in: Perissinotto, R., Stretch, D. D. and Taylor, R. H. (Eds.), Ecology and Conservation of Estuarine Ecosystems: Lake St Lucia as a Global Model. Cambridge University Press, pp. 247-267.

Cavagna, A., Cimarelli, A., Giardina, I., Parisi, G., Santagati, R., Stefanini, F. and Viale, M. (2010). Scale-free correlations in starling flocks. PNAS. 107, 11865-11870.

Chenouard, N., Smal, I., de Chaumont, F., Maska, M., Sbalzarini, I. F., Gong, Y., Cardinale, J., Carthel, C., Coraluppi, S., Winter, M., Cohen, A. R., Godinez, W. J., Rohr, K., Kalaidzidis, Y., Liang, L., Duncan, J., Shen, H., Xu, Y., Magnusson, K. E. G., Jalden, J., Blau, H. M., Paul-Gilloteaux, P., Roudot, P., Kervrann, C., Waharte, F., Tinevez, J.-Y., Shorte, S. L., Willemse, J., Celler, K., van Wezel, G. P., Dan, H.-W., Tsai, Y.-S., de Solorzano, C. O., Olivo-Marin, J.-C. and Meijering, E. (2014). Objective comparison of particle tracking methods. Nature Methods. 11(3), 281–289.

Cohen, J. H. and Forward, R. B. (2009). Zooplankton diel vertical migration - a review of proximate control. Oceanogr. Mar. Biol. 47, 77–110.

Crossland, C. J., Baird, D., Ducrotoy, J. P., Lindeboom, H., Buddemeier, R. W., Dennison, W. C., Maxwell, B. A., Smith, S. V. and Swaney, D. P. (2005). Coastal Fluxes in the Anthropocene, in: Crossland,C. J., Kremer, H. H., Lindeboom, H. J., Marshall-Crossland, J. I. and Le Tissier, M. D. A. (Eds.), The Coastal Zone - a Domain of Global Interactions. Springer-Verlag, Berlin Heidelberg, pp. 1-37.

Dabiri, J. O. (2010). The role of vertical migration in biogenic ocean mixing. Res. Lett. 37, L11602.

Dantec Dynamics A/S, Tonsbakken 16-18 - DK-2740 Skovlunde, Denmark (2012) DynamicStudio v3.20: User's Guide.

Davis, C. S., Flierl, G. R., Wiebe, P. H. and Franks, P. J. S. (1991). Micropatchiness, turbulence, and recruitment in plankton. Journal Of Marine Research. 49, 109-151.

Denman, K. L. and Gargett, A. E. (1995). Biological-physical interactions in the upper ocean: The role of vertical and small scale transport processes. Ann. Rev. Fluid Mech. 27, 225–255.

DeMott, W. and Gulati, R. (1999). Phosphorus limitation in Daphnia : Evidence from a long term study of three hypereutrophic Dutch lakes. Limnology and Oceanography. 44, 1557–1564.

De Silva, I. P. D. and Fernando, H. J. S. (1994). Oscillating grids as a source of nearly isotropic turbulence. Phys. Fluids. 6(7), 2455-2464.

Dewar, W. K., Bingham, R. J., Iverson, R. L., Nowacek, D. P., St. Laurent, L. C., and Wiebe, P. H. (2006). Does the marine biosphere mix the ocean? J. Mar. Res., 64, 541–561.

DiBacco, C., Fuchs, H., Pineda, J., and Helfrich, K. (2011). Swimming behaviour and velocities of barnacle cyprids in a downwelling flume. Mar. Ecol. Prog. Ser. 433, 131–148.

Dodson, S. I., Ryan, S., Tollrian, R. and Lampert, W. (1997). Individual swimming behavior of Daphnia: effects of food, light and container size in four clones. J. Plankton Res. 19, 1537-1552.

Doostmohammadi, A., Stocker, R., Ardekani, A. M. (2012). Low-reynolds-number swimming at pycnoclines. Proc Natl Acad Sci U S A 109, 3856–3861.

Duren, L. A., Stamhuis, E. J. and Videler, J. J. (2003). Copepod feeding currents: flow patterns, filtration rates and energetics. J Exp Biol 206, 255–267.

Eames, I., Belcher, S. E. and Hunt, J. C. R. (1994). Drift, partial drift and Darwin's proposition. J Fluid Mech 275, 201–223.

Ebert, D. (2005). Ecology, epidemiology, and evolution of parasitism in Daphnia, in: Bethesda, M. D.(Ed.), Introduction to Daphnia Biology. National Library of Medicine (US), National Center for Biotechnology Information, pp. 5-18.

Ekvall, M. T., Bianco, G., Linse, S., Linke, H., Bäckman, J. and Hansson, L.-A. (2013). Three-dimensional tracking of small aquatic organisms using fluorescent nanoparticles. PLoS ONE 8, e78498.

Elsinga, G. E., Scarano, F., Wieneke, B. and Van Oudheusden, B. W. (2006). Tomographic particle image velocimetry. Exp Fluids 41, 933–947.

Fields, D. M. and Yen, J. (1997). Implications of the feeding current structure of Euchaeta rimana, a carnivorous pelagic copepod, on the spatial orientation of their prey. J. Plankton Res. 19(1), 79–95.

Fields, D. M. and Yen, J. (1997). The escape behavior of marine copepods in response to a quantifiable fluid mechanical disturbance. J. Plankton Res. 19(9), 1289-1304.

Flierl, G., Grunbaum, D., Levin, D. and Olson, D. (1999). From individuals to aggregations: the interplay between behavior and physics. Journal of Theoretical Biology 196, 397-454.

Folt, C. L. and Burns, C. W. (1999). Biological drivers of zooplankton patchiness. Trends in Ecology and Evolution 14, 300-305.

Fuchs, H., Solow, A., and Mullineaux, L. (2010). Larval responses to turbulence and temperature in a tidal inlet: Habitat selection by dispersing gastropods? J Mar. Res. 68(1), 153-188.

Fuchs, H. L., Hunter, E., Schmitt, E. L. and Guazzo, R.A. (2013). Active downward propulsion by oyster larvae in turbulence. J. Exp. Biol. 216, 1458-1469.

Fuchs, H., Gerbi, G., Hunter, E., Christman, A. and Diez, F. (2015). Hydrodynamic sensing and behavior by oyster larvae in turbulence and waves. J. Exp. Biol. 218, 1419-1432.

Gallager, S. M. (1993). Hydrodynamic disturbances produced by small zooplankton: case study for veliger larva of a bivalve mollusc. J. Plankton Res. 15, 1277–1296.

Gallager, S. M., Yamazaki, H. and Davis, C. S. (2004). Contribution of fine-scale vertical structure and swimming behavior to formation of plankton layers on Georges Bank. Mar. Ecol. Prog. Ser. 267, 27–43.

Garcia, R., Moss, F., Nihongi, A., Strickler, J. R., Göller, S., Erdmann, U., Schimansky-Geier, L. and Sokolov, I. M. (2007). Optimal foraging by zooplankton within patches: The case of daphnia. Mathematical Biosciences, 207, 165–188.

Garrett, C. (2003). Internal tides and ocean mixing. Science, 301, 1858–1859.

Gaylord, B., Hodin, J. and Ferner, M. (2013). Turbulent shear spurs settlement in larval sea urchins. PNAS. 110(17), 6901-6906.

Gendron, D. (1992). Population structure of daytime surface swarms of Nyctiphanes simplex (Crustacea: Euphausiacea) in the Gulf of California, Mexico. Marine Ecology Progress Series 87, 1-6.

Genin, A., Jaffe, J. S., Reef, R., Richter, C. and Franks, P. J. S. (2005). Swimming against the flow: a mechanism of zooplankton aggregation. Science. 308, 860–862.

Gerritsen, J. (1980). Sex and parthenogenesis in sparse populations. The American Naturalist 115, 718-742.

Goudsmit, G.-H., Peeters, F., Gloor, M. and Wüest, A. (1997). Boundary versus diapycnal mixing in stratified natural waters. J. Geophys. Res., 102, 27903–27914.

Granata, T. and Dickey, T. (1991). The fluid mechanics of copepod feeding in a turbulent flow: A theoretical approach. Prog. Oceanogr. 26(3), 243-261.

Gregg, M. C. and Horne, J. K. (2009). Turbulence, acoustic backscatter, and pelagic nekton in monterey bay. J. Phys. Oceanogr., 39, 1077–1096.

Gries, T., Jöhnk, K., Fields, D. and Strickler, J. R. (1999). Size and structure of footprints produced by Daphnia: impact of animal size and density gradients. J. Plankton Res. 21, 509–523.

Hamner, W. H. and Carlton, J .H. (1979). Copepod swarms: attributes and role in coral reef ecosystems. Limnology and Oceanography 24, 1-14.

Haury, L. R., Yamazaki, H. and Itsweire, E. C. (1990). Effects of turbulent shear flow on zooplankton distribution. Deep-Sea Res., 37(3), 447-461.

Haury, L. R., Yamazaki, H. and Fey, C. L. (1992). Simultaneous measurements of small-scale physical dynamics and zooplankton distributions. J. Plankton Res. 14 (4), 513-530.

Hebert, P. D. N., Good, A. G. and Mort, M. A. (1980). Induced swarming in the predatory copepod Heterocope septentrionalis. Limnology and Oceanography 25, 747-750.

Heyward, A. and Negri, A. (2012). Turbulence, cleavage, and the naked embryo: a case for coral clones. Science. 335(6072), 1064–1064.

Huber, M. R. A., Peeters, F. and Lorke, A. (2011). Active and passive vertical motion of zooplankton in a lake. Limnology and Oceanography 56, 695-706.

Huntley, M. E. and Zhou, M. (2004). Influence of animals on turbulence in the sea. Mar. Ecol. Prog. Ser., 273, 65–79.

Incze, L.S., Hebert, D., Wolff, N., Oakey, N. and Dye, D. (2001). Changes in copepod distributions associated with increased turbulence from wind stress. Mar. Ecol. Prog. Ser. 213, 229-240.

Ivey, G. N., Winters, K. B. and Koseff, J. R. (2008). Density stratification, turbulence, but how much mixing? Ann. Rev. Fluid Mech., 40,169–184.

Jackson, J. L, Webster, D. R., Rahman, S. and Weissburg, M. J. (2007). Bed-roughness effects on boundary-layer turbulence and consequences for odor-tracking behavior of blue crabs (Callinectes sapidus). Limnol Oceanogr. 52, 1883–1897.

Jiang, H., Osborn, T. R. and Meneveau, C. (2002). The flow field around a freely swimming copepod in steady motion. Part I: Theoretical analysis. J. Plankton Res. 24, 167–189.

Jiang, H., Meneveau, C. and Osborn, T. R. (2002). The flow field around a freely swimming copepod in steady motion. Part II: Numerical simulation. J Plankton Res 24, 191–213.

Jiang, H. S. and Osborn, T. R. (2004). Hydrodynamics of copepods: A review. Surv Geophys 25, 339–370.

Jiang, H. and Strickler, J. R. (2007). Copepod flow modes and modulation: a modelling study of the water currents produced by an unsteadily swimming copepod. Philosophical Transactions of the Royal Society B-Biological Sciences, 362,1959–1971.

Jiang, H. and Kiørboe, T. (2010). Propulsion efficiency and imposed flow fields of a copepod jump. J. Exp. Biol. 214, 476–486.

Katija, K. and Dabiri, J. O. (2009). A viscosity-enhanced mechanism for biogenic ocean mixing. Nature, 460,624–627.

Kiørboe, T. and Mackenzie, B. (1995). Turbulence-enhanced prey encounter rates in larval fish: effects of spatial scale, larval behaviour and size. J. Plankton Res. 17,2319–2331.

Kiørboe, T. (1997). Small-scale turbulence, marine snow formation, and planktivorous feeding. Sci. Mar. 61, 141–158.

Kiørboe, T. (2007). Mate finding, mating, and population dynamics in a planktonic copepod Oithona davisae: There are too few males. Limnol Oceanogr. 52 (4), 1511–1522.

Kiørboe, T., Jiang, H. S. and Colin, S. P. (2010). Danger of zooplankton feeding: the uid signal generated by ambush-feeding copepods. Proc R Soc B-Biol Sci. 277, 3229–3237.

Kiørboe, T. (2011). How zooplankton feed: mechanisms, traits and trade-offs. Biol Rev Camb Philos Soc 86, 311–339.

Kirk, K. L. (1985). Water ows produced by Daphnia and Diaptomus: Implications for prey selection by mechanosensory predators. Limnol Oceanogr. 30(3), 679–686.

Kleiven, O. T., Larsson P. and Hobaek, A. (1996). Direct distributional response in Daphnia pulex to a predator kairomone. J. Plankton Res. 18, 1341-1348.

Kohlhage, K. (1994). The economy of paddle-swimming: The role of added waters and viscosity in the locomotion of Daphnia magna. Zool Beitr. 35, 47–54.

Kundu, P. K. and Cohen, I. M. (2008). Fluid Mechanics. Elsevier Inc., 4 edition.

Kunze, E., Dower, J. F., Beveridge, I., Dewey, R. K., and Bartlett, K. P. (2006). Observations of biologically generated turbulence in a coastal inlet. Science. 313, 1768–1770.

Kunze, E. (2011). Fluid mixing by swimming organisms in the low-reynolds-number limit. Journal of Marine Research 69, 591–601.

Kvam, O. V. and Kleiven, O. T. (1995). Diel horizontal migration and swarm formation in Daphnia in repsonse to Chaoborus. Hydrobiologia. 307, 177-184.

Laforsch, C. and Tollrian, R. (2004). Extreme helmet formation in Daphnia cucullata induced by small-scale turbulence. J. Plankton Res. 26(1), 81-87.

Lagadeuc, Y., Boute, M. and Dodson, J. J. (1997). Effect of vertical mixing on the vertical distribution of copepods in coastal waters. J. Plankton Res. 19, 1183-1204.

Lampert, W., (2011). Daphnia: Development of a Model Organism in Ecology and Evolution. International Ecology Institute, Oldendorf, Germany.

Larsson, P. and Dodson, S. (1993). Chemical communication in planktonic animals. Archiv für Hydrobiologie. 129, 129–155.

Lauga, E. and Powers, T. R. (2009). The hydrodynamics of swimming microorganisms. Rep Prog Phys 72.

Leal, L.G. (1980). Particle motions in a viscous fluid. Ann Rev Fluid Mech. 12, 435–476.

Leising, A. W. and Yen, J. (1997). Spacing mechanisms within light-induced copepod swarms. Marine Ecology Progress Series 155, 127-135.

Leshansky, A. M. and Pismen, L.M. (2010). Do small swimmers mix the ocean? Phys Rev E. 82, 4.

Lombard, F., Koski, M. and Kiørboe, T. (2013). Copepods use chemical trails to find sinking marine snow aggregates. Limnol Oceanogr. 58, 185–192.

Lorke, A., McGinnis, D. F., Spaak P. and Wüest, A. (2004). Acoustic observations of zooplankton in lakes using a Doppler current profiler. Freshwater Biology. 49, 1280-1292.

Lorke, A. and Peeters, F. (2006). Toward a unified scaling relation for interfacial fluxes. J. Phys. Oceanogr. 36,955–961.

Lorke, A., Weber, A., Hofmann, H. and Peeters, F. (2008). Opposing diel migration of fish and zooplankton in the littoral zone of a large lake. Hydrobiologia. 600, 139-146.

Lorke, A. and Probst, W. N. (2010). In situ measurements of turbulence in fish shoals. Limnol. Oceanogr. 55,354–364.

Lovern, S. B., Strickler, J. R. and Klaper, R. (2007). Behavioral and physiological changes in daphnia magna when exposed to nanoparticle suspensions (titanium dioxide, nano-c-60, and c(60)hxc(70)hx). Environ. Sci. Technol. 41, 4465–4470.

Maar, M., Nielsen, T. G., Stips, A. and Visser, A. W. (2003). Microscale distribution of zooplankton in relation to turbulent diffusion. Limnol. Oceanogr. 48(3), 1312-1325.

Mach, R. and Schweitzer, F. (2007). Modeling vortex swarming in Daphnia. Bulletin of Mathematical Biology. 69, 539-562.

Macintyre, S. (1993). Vertical mixing in a shallow, eutrophic lake: Possible consequences for the light climate of phytoplankton. Limnol. Oceanogr. 38, 798–817.

Mackenzie, B. R., Miller, T. J., Cyr, S., and Leggett, W. C. (1994). Evidence for a dome-shaped relationship between turbulence and larval fish ingestion rates. Limnol. Oceanogr. 39(8), 1790-1799.

Malkiel, E., Alquaddoomi, O. and Katz, J. (1999). Measurements of plankton distribution in the ocean using submersible holography. Meas. Sci. Technol. 10, 1142–1152.

Mann, K. H. and Lazier, J. R. N. (2006). Dynamics of Marine Ecosystems: Biological-Physical Interactions in the Oceans, third ed. Blackwell Science Inc., Boston.

Marrasé, C., Costello, J. H., Granata, T. and Strickler, J. R. (1990). Grazing in a turbulent environment: Energy dissipation, encounter rates, and efficacy of feeding currents in Centropages hamatus. Proc. Natl. Acad. Sci. USA. 87, 1653-1657.

Mathews, J. H. and Fink, K. K. (2004). Numerical Methods Using Matlab. Pearson, 4 edition.

McDonald, K. (2012). Earliest ciliary swimming effects vertical transport of planktonic embryos in turbulence and shear flow. J. Exp. Biol. 215(1), 141–151.

Michalec, F. G., Souissi, S. and Holzner, M. (2015). Turbulence triggers vigorous swimming but hinders motion strategy in planktonic copepods. J R Soc Interface. 12(106), pii: 20150158.

Morris, M. J., Gust, G. and Torres, J. J. (1985). Propulsion efficiency and cost of transport for copepods: A hydromechanical model of crustacean swimming. Mar Biol. 86, 283–295.

Morris, M. J., Kohlhage, K. and Gust, G. (1990). Mechanics and energetics of swimming the small copepod Acanthocylops robustus (Cylopoida). Mar Biol. 107, 83–91.

Murphy, D. W. (2012). Planktonic propulsion: the hydrodynamics, kinematics, and design of metachrony. PhD thesis, Georgia Institute of Technology.

Noss, C. and Lorke, A. (2012). Zooplankton induced currents and uxes in stratified waters. Water Qual Res J Can. 47, 276–285.

Noss, C., Lorke, A. and Niehaus, E. (2013). Three-dimensional tracking of multiple aquatic organisms with a two camera system. Limnol Oceanogr Methods. 11, 139–150.

Noss, C., Dabrunz, A., Rosenfeldt, R. R., Lorke, A. and Schulz, R. (2013). Three-dimensional analysis of the swimming behavior of Daphnia magna exposed to nanosized titanium dioxide. PLoS ONE. 8, e80960.

Noss, C. and Lorke, A. (2014). Direct observation of biomixing by vertically migrating zooplankton. Limnol. Oceanogr. 59(3), 724–732.

OECD. (2004). Guideline for testing of chemicals 202. Organisation for Economic Cooperation and Development.

Okubo, A. and Anderson, J. J. (1984). Mathematical models for zooplankton swarms: Their formation and maintenance. EOS. 65, 731-732.

Okubo, A. and Levin, S. A. (2001). Diffusion and Ecological Problems: Modern Perspectives. Springer.

Ordemann, A., Balazsi, G. and Moss, F. (2003). Pattern formation and stochastic motion of the zooplankton Daphnia in a light field. Physica A: Statistical Mechanics and its Applications. 325, 260-266.

Oviatt, C.A. (1981). Effects of different mixing schedules on phytoplankton, zooplankton and nutrients in marine microcosms. Mar. Ecol. Prog. Ser. 4, 57-67.

Parrish, J. K. and Edelstein-Keshet, L. (1999). Complexity, pattern, and evolutionary trade-offs in animal aggregation. Science. 284, 99-101.

Pearce, C. M., Gallager, S. M., Manuel, J. L., Manning, D. A., O'Dor, R. K. and Bourget, E. (1998). Effect of thermoclines and turbulence on depth of larval settlement and spat recruitment of the giant scallop Placopecten magellanicus in 9.5 m deep laboratory mesocosms. Mar. Ecol. Prog. Ser. 165, 195-215.

Peeters, F., Straile, D., Lorke, A., and Ollinger, D. (2007). Turbulent mixing and phytoplankton spring bloom development in a deep lake. Limnol. Oceanogr. 52, 286–298.

Peters, F. and Redondo, J. M. (1997). Turbulence generation and measurement: application to studies on plankton. Sci. Mar. 61 (Suppl. 1), 205–228.

Pijanowska, J. and Kowalczewski, A.(1997). Predators can introduce swarming behaviour and locomotory responses in Daphnia. Freshwater Biology. 37, 649-656.

Pinel-alloul, B. (1995). Spatial heterogeneity as a multiscale characteristic of zooplankton community. Hydrobiologia. 300/301, 17-42.

Pitchford, J. W., James, A., and Brindley, J. (2003). Optimal foraging in patchy turbulent environments. Mar. Ecol. Prog. Ser. 256, 99–110.

Prairie, J. C., Sutherland, K. R., Nickols, K. J. and Kaltenberg, A. M. (2012). Biophysical interactions in the plankton: A cross-scale review. Limnol. Oceanogr. Fluids and Environments. 2, 121-145.

Price, H. J. (1989). Swimming behavior of krill in response to algal patches: A mesocosm study. Limnol Oceanogr. 34, 649–659.

Pringle, J. M. (2007). Turbulence avoidance and the wind-driven transport of plankton in the surface Ekman layer. Cont. Shelf Res. 27, 670-678.

Ranta, E., Bengtsson, J. and McManus, J. (1993). Growth, size and shape of Daphnia longispina, D. magna and D. pulex. Ann Zool Fennici. 30, 299–311.

Ringelberg, J., Flik, B. J. G, Aanen, D. and Van Gool, E. (1997). Amplitude of vertical migration (DVM) is a function of fish biomass, a hypothesis. Archiv für Hydrobiologie/Beihefte Ergebnisse Limnologie. 49, 71–78.

Ringelberg, J. (1999). The photobehaviour of Daphnia spp. as a model to explain diel vertical migration in zooplankton. Biol Rev Camb Philos Soc. 74, 397-423.

Ritz, D. A. (2000). Is social aggregation in aquatic crustaceans a strategy to conserve energy? Can J Fish Aquat Sci. 57, 59 –67.

Ritz, D. A., Hobday, A. J., Montgomery, J. C. and Ward, A. J. (2011). Social aggregation in the pelagic zone with special reference to fish and invertebrates. Advances in Marine Biology. 60, 161-227.

Rothschild, B. and Osborn, T. (1988). Small-scale turbulence and plankton contact rates. J. Plankton Res. 10(3), 465-474.

Roy, A., Metaxas, A. and Ross, T. (2012). Swimming patterns of larval Strongylocentrotus droebachiensis in turbulence in the laboratory. Mar. Ecol. Prog. Ser. 453, 117–127.

Saiz, E. and Alcaraz, M. (1992). Enhanced excretion rates induced by small-scale turbulence in Acartia (Copepoda: Calanoida). J. Plankton Res. 14(5), 681-689.

Saiz, E., Alcaraz, M. and Paffenhöfe, G. A. (1992). Effects of small-scale turbulence on feeding rate and gross-growth efficiency of three Acartia species (Copepoda: Calanoida). J. Plankton Res. 14 (8), 1085-1097.

Saiz, E., Calbet, A. and Broglio, E. (2003). Effects of small-scale turbulence on copepods: The case of Oithona davisae. Limnol. Oceanogr. 48(3), 1304-1311.

Saiz, E. and Kiørboe, T. 1998. Predatory and suspension feeding of the copepod Acartia tonsa in turbulent environments. Mar. Ecol. Prog. Ser. 122, 147-158.

Saunders, P. A., Porter, K. G. and Taylor, B. E. (1999). Population dynamics of Daphnia spp. and implications for trophic interactions in a small, monomictic lake. J. Plankton Res. 21, 1823-1845.

Schlichting, H. (1977). Boundary Layer Theory. McGraw-Hill, New York, 6th edition, 234–235, 599 pp.

Schmoker, C. and Hernández-León, S. (2003). The effect of food on the respiration rates of Daphnia magna using a flow-through system. Sci. Mar. 67(3), 361-365.

Searle, C. L., Mendelson, J. R., Green, L. E. and Duffy, M. A. (2013). Daphnia predation on the amphibian chytrid fungus and its impacts on disease risk in tadpoles. Ecology and Evolution. 3, 4129-4138.

Seuront, L., Yamazaki, H. and Souissi, S. (2004). Hydrodynamic disturbance and zooplankton swimming behavior. Zoological Studies. 43(2), 376-387.

Seuront, L., Brewer, M. and Strickler, J. R. (2004) Quantifying zooplankton swimming behavior, the question of scale. In Seuront, L. and Strutton, P. G. (eds), Handbook of scaling methods in aquatic ecology: measurement, analysis, simulation. CRC Press, Boca Raton, FL, pp. 333–359.

Shimazaki, H. and S. Shinomoto, (2007). A method for selecting the bin size of a time histogram. Neural Computation. 19, 1503–1527.

Spitael, M. S. (2007). The effects of physical variables on zooplankton distributions in stratified lakes. PhD thesis, University of Minnesota.

Stamhuis, E. J., Videler, J. J., Van Duren, L. A. and Muller, U. K. (2002). Applying digital particle image velocimetry to animal-generated flows: Traps, hurdles and cures in mapping steady and unsteady flows in Re regimes between 10^2 and 10^5. Experiments in Fluids. 33, 801–813.

Steinberg, D. K., Silver, M. W. and Pilskaln, C. H. (1997). Role of mesopelagic zooplankton in the community metabolism of giant larvacean house detritus in Monterey Bay, California, USA. Mar. Ecol. Prog. Ser. 147, 167–179.

Steinbuck, J. V., Roberts, P. L. D., Troy, C. D., Horner-Devine, A. R., Simonet, F., Uhlman, A., Jaffe, J. S., Franks, P. J. S. and Monismith, S. G. (2010). An Autonomous Open-Ocean Stereoscopic PIV Profiler. J. Atmos. Ocean. Tech. 27, 1362-1380.

Steiner, C. F. (2004). Daphnia dominance and zooplankton community structure in fishless ponds. J. Plankton Res. 26, 799-810.

Stiansen, J. E. and Sundby, S. (2001). Improved methods for generating and estimating turbulence in tanks suitable for fish larvae experiments. Sci. Mar. 65, 151-167.

Stocker, R. (2012). Marine microbes see a sea of gradients. Science. 338,628–633.

Strutton, P. G. (2007). Handbook of Scaling Methods in Aquatic Ecology: Measurement, Analysis, Simulation. CRC Press, 1st edition, 338–339 pp.

Sutherland, K. R., Dabiri, J. O. and Koehl, M. A. R. (2011). Simultaneous field measurements of ostracod swimming behavior and background flow. Limnol. Oceanogr. Fluids Environ. 1, 135–146.

Sutherland, K. R., Costello, J. H., Colin, S. P. and Dabiri, J. O. (2014). Ambient fluid motions influence swimming and feeding by the ctenophore Mnemiopsis leidyi. J. Plankton Res. 36, 1310–1322.

Taylor, G. I. (1935). Statistical theory of turbulence. Proc. R. Soc. Lond. A. 151, 421-444.

Tennekes, H. and Lumley, J. L. (1973). A first course in turbulence. MIT Press.

Theunissen, R., Scarano, F. and Riethmuller, M. L. (2006). An adaptive sampling and windowing interrogation method in PIV. Meas. Sci. Technol. 18, 275.

Thompson, S. M. and Turner, J. S. (1975). Mixing across an interface due to turbulence generated by an oscillating grid. J. Fluid Mech. 679(2), 349-368.

Thorpe, S. A. (1985). Small-scale processes in the upper ocean boundary layer. Nature. 318, 519-522.

Tiselius, P. (1992). Behavior of Acartia tonsa in patchy food environments. Limnol Oceanogr. 37, 1640–1651.

Tunstrom, K., Katz, Y., Ioannou, C. C., Huepe, C., Lutz, M. J. and Couzin, I. D. (2013). Collective states, multistability and transitional behavior in schooling fish. PLOS Computational Biology. 9, e1002915.

Udea, H., Kuwahara, A., Tanaka, M. and Azeta, M. (1983). Underwater observations on copepod swarms in temperate and subtropical waters. Marine Ecology Progress Series. 11, 165-171.

Van Duren, L. A. and Videler, J. J. (2003). Escape from viscosity: the kinematics and hydrodynamics of copepod foraging and escape swimming. J. Exp. Biol., 206,269–279.

Van Gool, E. and Ringelberg, J. (1997). The effect of accelerations in light increase on the phototactic downward swimming of Daphnia and the relevance to diel vertical migration. J. Plankton Res. 19, 2041-2050.

Videler, J. J., Stamhuis, E. J., Muller, U. K., Van Duren, L. A. (2002). The scaling and structure of aquatic animal wakes. Integrative and Comparative Biology. 42, 988–996.

Visser, A. W. (2001). Hydromechanical signals in the plankton. Mar. Ecol. Prog. Ser. 222, 1–24.

Visser, A., Saito, H., Saiz, E. and Kiørboe, T. (2001). Observations of copepod feeding and vertical distribution under natural turbulent conditions in the North Sea. Mar Biol. 138, 1011-1019.

Visser, A. W. and Stips, A. (2002). Turbulence and zooplankton production: insights from PROVESS. J. Sea Res. 47, 317-329.

Visser, A. (2007). Biomixing of the oceans? Science. 316, 838–839.

Visser, A. W., Mariani, P. and Pigolotti, S. (2009). Swimming in turbulence: zooplankton fitness in terms of foraging efficiency and predation risk. J. Plankton Res. 31, 121–133.

Walker, J. A. (2002). Functional morphology and virtual models: Physical constraints on the design of oscillating wings, fins, legs, and feet at intermediate reynolds numbers. Integrative and Comparative Biology. 42, 232–242.

Webster, D., Young, D. and Yen, J. (2015). Copepods' response to Burgers' vortex: deconstructing interactions of copepods with turbulence. Integr. Comp. Biol. 55(4), 706-18.

Weissburg, M. J., Doall, M. H. and Yen, J. (1998). Following the invisible trail: mechanisms of chomosensory mate tracking by the copepod Temora longicornus. Philosophical Transactions of the Royal Society London B. 353, 701-712.

Welch, J. and Forward, R. (2001). Flood tide transport of blue crab, Callinectes sapidus, postlarvae: behavioral responses to salinity and turbulence. Mar. Biol. 139(5), 911–918.

Westerweel, J. and Scarano, F. (2005). Universal outlier detection for PIV data. Exp. Fluids. 39(6), 1096-1100.

Wheeler, J. D., Helfrich, K. R., Anderson, E. J., McGann, B., Staats, P., Wargula, A. E., Wilt, K. and Mullineaux, L. S. (2013). Upward swimming of competent oyster larvae Crassostrea virginica persists in highly turbulent flow as detected by PIV flow subtraction. Mar. Ecol. Prog. Ser. 488, 171-185.

Wheeler, J. D., Helfrich, K. R., Anderson, E. and Mullineaux, L. (2015). Isolating the hydrodynamic triggers of the dive response in eastern oyster larvae. Limnol. Oceanogr. 60, 1332–1343.

Wickramarathna, L. N., Noss, C. and Lorke, A. (2014). Hydrodynamic trails produced by daphnia: size and energetics. PLoS ONE. 9(3), e92383.

Woodson, C. B. and Mcmanus, M. A. (2007). Foraging behavior can inuence dispersal of marine organisms. Limnol Oceanogr. 52(6), 2701–2709.

Woodson, C. B., McManus, B. A., Tyburczy, J. A., Barth, J. A., Washburn, L., Caselle, J. E., Carr, M. H., Malone, D. P., Raimondi, P. T., Menge, B. A. and Palumbi, S. R. (2012). Coastal fronts set recruitment and connectivity patterns across multiple taxa. Limnol. Oceanogr. 57, 582–596.

Wu, J. S. and Faeth, G. M. (1993). Sphere wakes in still surroundings at intermediate Reynolds numbers. AIAA Journal. 31, 1448–1455.

Wüest, A. and Lorke, A. (2003). Small-scale hydrodynamics in lakes. Ann. Rev. Fluid Mech. 35, 373–412.

Wunsch, C. and Ferrari, R. (2004). Vertical mixing, energy, and the general circulation of the oceans. Ann. Rev. Fluid Mech. 36, 281–314.

Yamazaki, H. and Squires, K. D. (1996). Comparison of oceanic turbulence and copepod swimming. Mar. Ecol. Prog. Ser. 144, 299-301.

Yen, J. and Strickler, J. (1996). Advertisement and concealment in the plankton: what makes a copepod hydrodynamically conspicuous? Invert Biol. 115, 191–205.

Yen, J., Weissburg, M. J. and Doall, M. H. (1998). The fluid physics of signal perception by mate-tracking copepods. Philosophical Transactions of the Royal Society London. 353, 787-804.

Yen, J. (2000). Life in transition: balancing inertial and viscous forces by planktonic copepods. Biol Bull. 198, 213–224.

Yen, J., Rasberry, K. and Webster, D. (2008). Quantifying copepod kinematics in a laboratory turbulence apparatus. J. Mar. Syst. 69, 283-294.

Zhan, C., Sardina, G., Lushi, E. and Brandt, L. (2014). Accumulation of motile elongated micro-organisms in turbulence. J. Fluid Mech. 739, 22-36.

Appendix A

Supporting information for Hydrodynamic trails produced by *Daphnia*: size and energetics
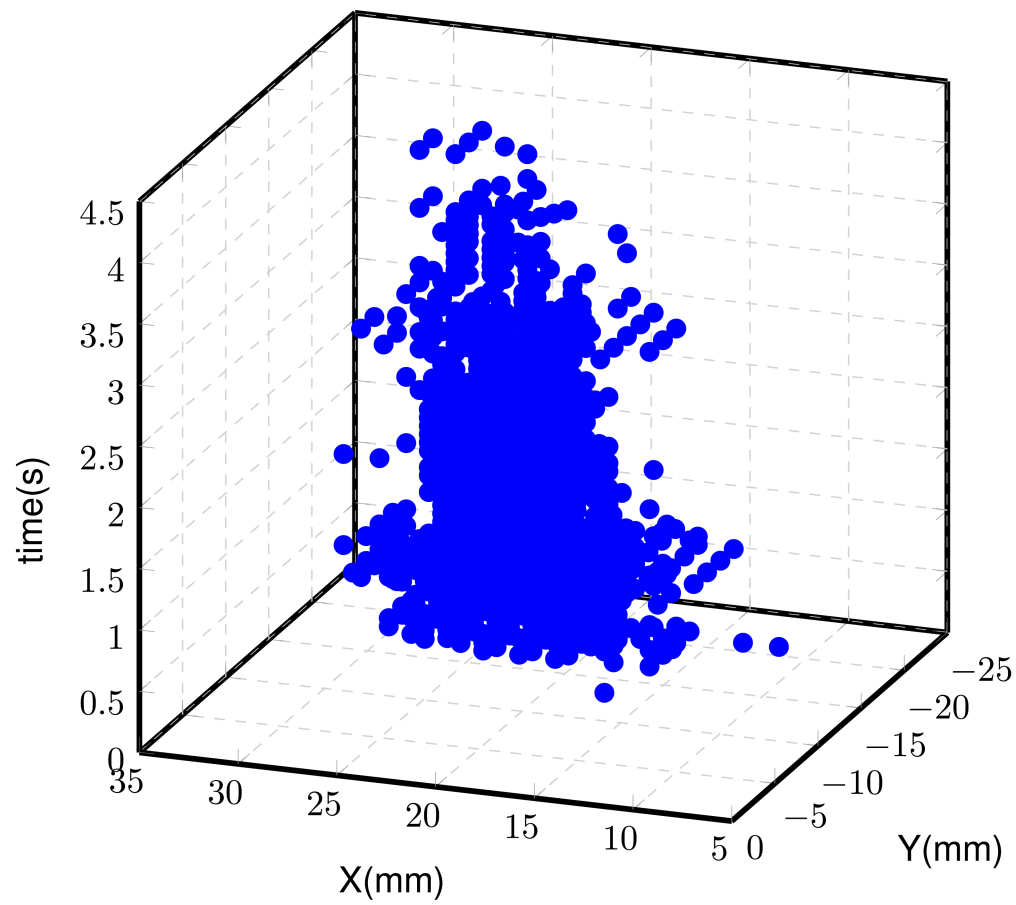
Figure A.1: *An example of a trail produced by a cruising* Daphnia. *The* Daphnia *swims in the negative z-direction, and blue dots indicate locations where dissipation rates exceed the selected threshold. The method illustrated in Figure 2.4 was used in the computation of the trail.*

Table A.1: *Impact of green laser light on organism swimming behavior. Incoming and outgoing angles of the trajectories with respect to the light sheet were estimated for 4 observations per each swimming pattern and age group (i. e., 36 observations in total). The standard deviations of angular differences are shown within parentheses. We found that the difference between these angles remains similar for cruising while the differences of angles for hopping & sinking and looping are within an acceptable range. It should be noted that hopping & sinking and looping are naturally inclined to change the swimming direction. The relatively higher angle for hopping & sinking of 5 days old organisms can be due to switching between hopping and sinking within the width of the light sheet. This implies that the green laser light does not have any major implications that may have lead the organisms to veer from their original pathways. Nevertheless, the presence of the green laser light may affect the organism outside the vicinity of the laser light sheet.*

Age (days)	Incoming-outgoing angle difference ($°$)		
	Cruising	**Hopping & sinking**	**Looping**
5	3.02 ($\pm$3.0)	22.44 ($\pm$15.4)	8.34 ($\pm$5.9)
20	7.45 ($\pm$1.7)	3.36 ($\pm$2.2)	13.14 ($\pm$6.8)
35	1.90 ($\pm$1.3)	8.18 ($\pm$3.0)	11.32 ($\pm$6.8)

Video A.1: *A sample video illustrating the currents induced by* Daphnia *(video file format: avi). Fluid motion is solely caused by swimming* Daphnia. *Frame dimensions are **32** by **32** mm. The video, which was recorded by one of the PIV cameras during our preliminary measurements, shows daphnids of various sizes crossing the laser light sheet. The flow field can be observed visually by following the white seeding particles used for PIV measurements. Judging by the dispersion of seeded particles at each crossing of* Daphnias*, it can be convincingly noted that a sudden leap of induced currents is associated with larger* Daphnias. *The video additionally illustrates that even the passive sinking of larger* Daphnias *can induce much larger trails than those of smaller* Daphnias *swimming at a high speed.*

Video A.2: *Animated three-dimensional vector plot of current velocities illustrating the propulsive jet induced by an upward swimming* Daphnia *(yellow blob) (video file format: avi). The video is based on a single measurement using tomographic PIV conducted at LaVision. The tomographic reconstruction of the volumetric intensity distribution was performed using an implementation of the MART algorithm (Elsinga et al., 2006) and the velocity field was calculated using 3D correlation (*DaVis 8 *by LaVision).*

Links for the videos can be found at 10.1371/journal.pone.0092383

Supporting information for *Daphnia* pushed to the limits: kinematics and energetics of swimming in turbulence

Video B.1: *A sample video illustrating passive tracer particles and Daphnia swimming in turbulence. The video shows a Daphnia being illuminated by the laser light sheet as it crosses the light sheet. The flow field can be observed by following the white seeding particles used for PIV measurements (video file format: mp4).*

Link for the video can be found at https://youtu.be/qmYst5NijFQ

Video B.2: *A video depicting the background and Daphnia (white blob) induced dissipation rates along its pathway shown in Video S1. The colour map indicates the level of dissipation rate while the animals pathway (highlighted in blue) is also shown as it proceeds along its pathway. Note that a contrasting region of the colour map appears as the animal primarily remains within the light sheet. (video file format: mp4).*

Link for the video can be found at https://youtu.be/EHySg8rMXsE

Appendix C

Supporting information for The kinematics and energetics of *Daphnia* swarms
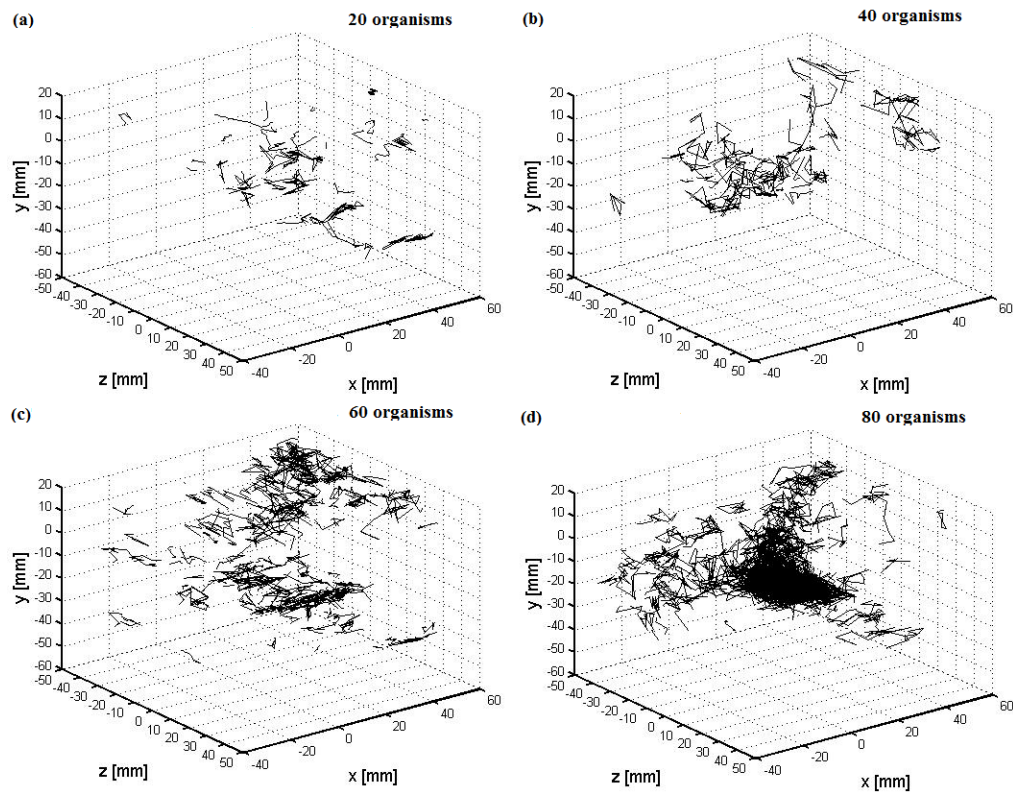
Figure C.1: *Overview of Daphnia tracks without a light stimulus. The tracks of animals for each group are shown in black. Panels* **(a)**-**(d)** *correspond to increasing abundance as indicated in the panels, and the coordinate system in each panel is centred at the centroid coordinate of the corresponding group.*
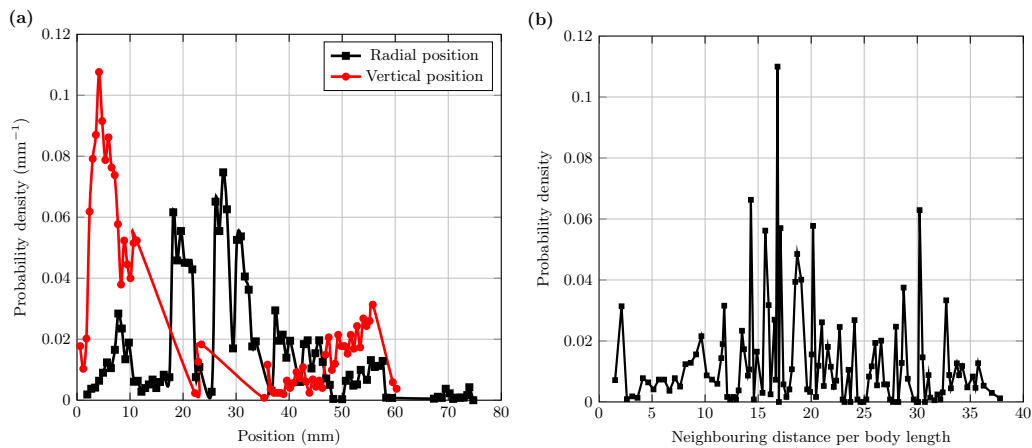
Figure C.2: *Probability density distributions of occupying positions and neighbouring distance of Daphnia in the absence of a light stimulus.* **(a)** *Probability distribution of occupying positions in radial direction on the horizontal plane and vertical direction.* **(b)** *Probability distribution of neighbouring distance. It should be noted that radial positions are given with respect to the centroid coordinates of the groups while the vertical position increasing from the bottom to top of the tank is also presented along the x-axis. All four groups swimming in the absence of a light stimulus are included in estimating each of the probability density distribution.*
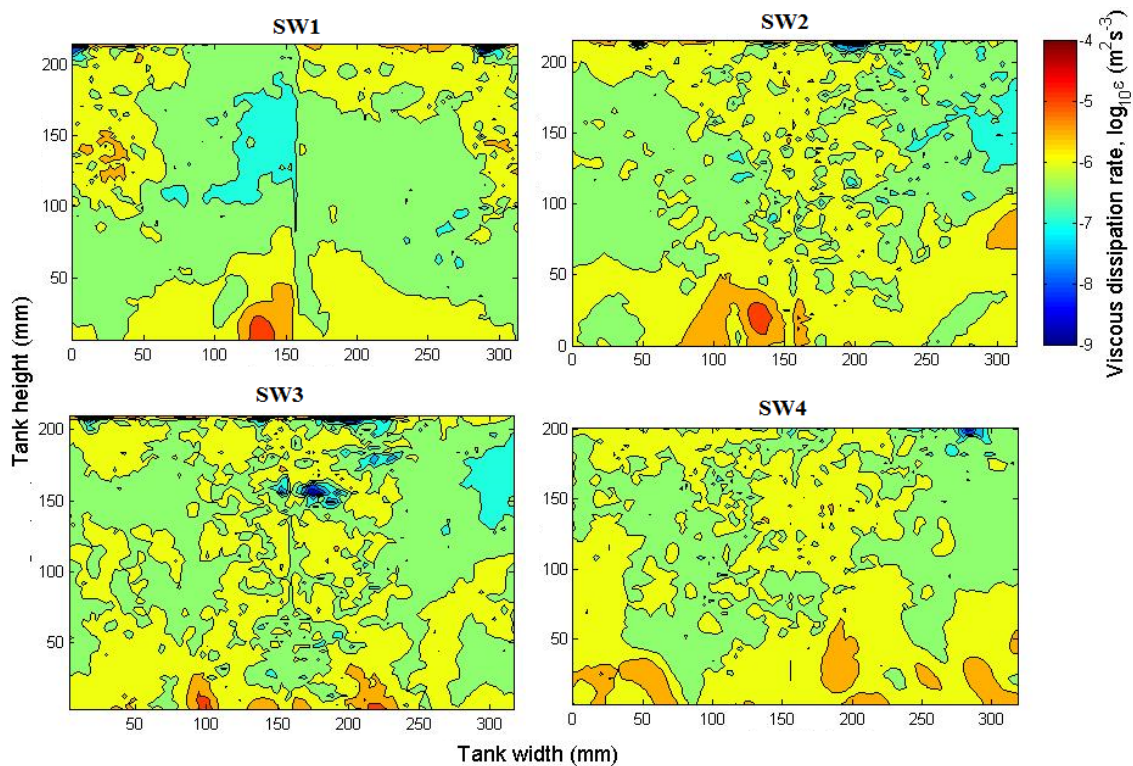
Figure C.3: *Contour maps of temporally averaged viscous dissipation rate of kinetic energy for SW1-SW4. Dissipation rates are given in log-scale.*

Lalith Wickramarathna
Curriculum Vitae

Address: Xylander Straße 15, 76829 Landau, Germany
Phone: (H) +49 (6341) 389 5287
Email: lalith@uni-landau.de
Nationality: Sri Lankan

RESEARCH INTERESTS

Flow visualization, Plankton hydrodynamics, Medical implants, Biomechanics, Energy system modelling, Mechanical Engineering

EDUCATION

2011 May.- Present	**Ph.D. candidate in Environmental Sciences** University of Koblenz-Landau, Germany. *Expected in August 2016.*
2007 Sept.- 2010 Apr.	**M.Sc. in Biomedical Engineering** University of Lübeck and University of Applied Sciences Lübeck, Germany. *Cumulative GPA: 1.9/1.0.*
2002 Jan.- 2003 Aug.	**M. Eng. in Energy Technology** Asian Institute of Technology, Bangkok, Thailand. *Cumulative GPA: 3.65/4.0.*
1995 Dec.- 2000 Jun.	**B.Sc. (Hons.) in Mechanical Engineering** University of Peradeniya, Sri Lanka. *Rank: Second Class.*

EXPERIENCE

2011 May- 2015 Jan.	**Scientist** Institute for Environmental Sciences, University of Koblenz-Landau, Germany.
2009 Sep.- 2010 Mar.	**Guest Researcher** Bern University of Applied Sciences, Biel/Bienne, Switzerland.
2009 Jan.- 2009 Aug.	**Research Assistant** Center for Biomedical and Robotics Technologies, Mahidol Uni., Thailand.
2008 Oct.- 2008 Dec.	**Internship** University of Poitiers, Laboratory of Solid Mechanics, France.
2008 Jun.- 2008 Oct.	**Researcher** Potsdam Institute for Climate Impact Research, Germany.
2005 Jun.- 2007 Aug.	**Instructor** Sirindhorn International Institute of Technology, Thailand.
2003 Aug.- 2005 Apr.	**Research Associate** Asian Institute of Technology Technology, Thailand.
2001 Feb.- 2001 Dec.	**Mechanical engineer** National Engineering Research and Development center, Sri Lanka.

2000 Jul.- 2000 Dec.	**Assistant Lecturer**
	Academy of aeronautical engineering, Lion air group of company, Sri Lanka.
1999 Mar.- 1999 May	**Industrial trainee**
	Skanska International Pvt. (Ltd.), Sri Lanka.

PUBLICATIONS

✎ Wickramarathna, L. N., Noss, C. and Lorke, A. (2016). The kinematics and energetics of *Daphnia* swarms. *Hydrobiologia*. Under review (originally submitted on 24.04.2016).

✎ Wickramarathna, L. N., Noss, C. and Lorke, A. (2016). *Daphnia* pushed to the limits: kinematics and energetics of swimming in turbulence. *Limnologica*. Under review (revised submission on 06.05.2016).

✎ Wickramarathna L. N., Noss, C. and Lorke, A. (2014). Hydrodynamic trails produced by *Daphnia*: size and energetics. *PLoS ONE* 9(3): e92383. Doi: http://dx.doi.org/10.1371/journal.pone.0092383

✎ Pfenniger*, A., Wickramarathna*, L. N., Vogel, R. and Koch, V. M. (2013). Design and realization of an energy harvester using pulsating arterial pressure, *Med Eng Phys*, 35(9), pp. 1256-1265. (*equal first authors). Doi: http://dx.doi.org/10.1016/j.medengphy.2013.01.001

✎ Wickramarathna L. N. (2009). Intracorporeal energy harvesting from windkessel effect of human arterial blood vessels, Master's thesis, University of Applied Sciences, Lübeck, Germany.

✎ Wickramarathna, L. N. and Sensinger, J. W. (2010). Exterior vs. interior rotors in robotic brushless motors, Submitted to 2010 IEEE international conference on robotics and automation.

✎ Wickramarathna, L. N. and Bhattacharya, S. C. (2004). Comparing greenhouse gas emissions and costs of biomass-based power generation and cooking options from a life-cycle perspective, Biomass and Bioenergy.

✎ Wickramarathna, L. N., Bhattacharya, S. C. and Shrestha, R. M. (2005). Energy and environmental implications of biomass energy technologies: Application of AIM/Enduse model for Sri Lanka, International Energy Journal.

✎ Wickramarathna, L. N. (2003). A study of greenhouse gas mitigation potential of modern biomass technologies in Sri Lanka, Master's thesis, Asian Institute of Technology, Thailand.

PROJECTS

⇒ Biomxing: Biologically-induced mixing of stratified waters by swimming zooplankton

⇒ Intracorporeal energy harvesting for medical implants: Design and realization of a prototype of an intracorporeal energy harvester using contraction and expansion of an artery

⇒ Optimization of a robotic upper limb prosthesis: Designing and optimizing a brushless DC motor in a robotic prosthesis

⇒ Asian Regional Research Programme in Energy, Environment, and Climate (ARRPEEC): Life cycle analysis of biomass-based power generation and cooking options

⇒ Research on Innovative Strategic Policy Options (RISPO): Energy system modeling of Bangkok transport sector and developing good practice inventories

⇒ Regional Energy Database (RED): Maintenance of a regional renewable energy database

AWARDS

◆ Awarded a three-term tuition fee fellowship from Asian Institute of Technology, Thailand for M.Eng.in Energy Technology

◆ Awarded the best performance of applied thermodynamics at university of Peradeniya, faculty of engineering in December 2000

◆ Received a special joint award for a development design of paddy threshing machine from Sri Lanka Association for Advancement of Science (SLAAS)

COMPUTER LITERACY

Programming	Matlab, LabVIEW 8.5
Softwares	ANSYS, COMSOL, UGS NX6.0, DynamicStudio (Dantec), HTML development (Adobe Dreamweaver)
Energy System Simulation Models	AIM/End-use, LEAP, GEMIS
Office tools	MS office, LaTeX distributions (MikTeX/TeX Live)

LANGUAGES

English, German (Deutsch test für zuwanderer), Sinhala (Native)

HOBBIES

Cricket, Music, reading, writing

I hereby certify that the particulars given above are true and accurate to the best of my knowledge.

Date: 20/05/2016

Lalith N. Wickramarathna